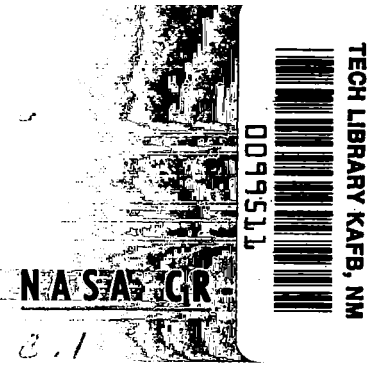

NASA CONTRACTOR REPORT

NASA CR-487

GASEOUS-FUELED CAVITY REACTORS - CRITICALITY CALCULATIONS AND ANALYSIS

Prepared by
GENERAL MOTORS CORPORATION
Indianapolis, Ind.
for Lewis Research Center

NATIONAL AERONAUTICS AND SPACE ADMINISTRATION • WASHINGTON, D. C. • JULY 1966

GASEOUS-FUELED CAVITY REACTORS – CRITICALITY CALCULATIONS AND ANALYSIS

Prepared under Contract No. NAS 3-6073 by
GENERAL MOTORS CORPORATION
Indianapolis, Ind.

for Lewis Research Center

NATIONAL AERONAUTICS AND SPACE ADMINISTRATION

For sale by the Clearinghouse for Federal Scientific and Technical Information
Springfield, Virginia 22151 – Price $5.00

FOREWORD

This report, originally issued as Allison report EDR 3997, represents effort performed under Contract NAS 3-6073 to the National Aeronautics and Space Administration, Lewis Research Center, by the Allison Division, General Motors Corporation.

The individuals performing the principal technical effort include Mr. John A. Eriksen, Mr. Richard M. Kaufman, Dr. William F. Osborn, Mr. E. B. Roth, and Mr. John R. Simmons of the Allison Division. The appendix was written by Dr. Anthony H. Foderaro, Professor of Nuclear Engineering at Pennsylvania State University and a consultant to Allison Division.

The contract was under the technical management of Mr. Robert E. Hyland of the Lewis Research Center.

TABLE OF CONTENTS

LIST OF SYMBOLS

AVR—average velocity ratio

D—diffusion constant

ev—electron volt

E—energy

I—resonance absorption integral

k—Boltzmann's constant

k_{eff}—core multiplication factor

L—slowing-down length or thermal diffusion length

M_c—critical mass

N—material number density

q(u)—slowing-down density

S_n—discrete ordinates

T—temperature

t—absorber thickness

u—lethargy

V—neutron velocity

Δ—indicates an incremental quantity

ϵ—convergence factor

η—fuel multiplication factor = $\nu\sigma_F/\sigma_a$

λ—mean free path = $1/\sigma$

ν—neutrons per fission

ξ—mean log energy decrement

ρ—material density

Σ—macroscopic cross section = $N\sigma$

$\Sigma_a t$—absorption cross section times thickness in centimeters

σ—microscopic cross section

τ—age to thermal

$\phi(E)$—flux per unit energy

$\phi(u)$—flux per unit lethargy

Subscripts

a—absorption

bound—molecular state

f—fast

F—fission

free—molecular state

g—group

g'—new group

R—removal

s—scattering

tr—transport

I, II—groups

1, 2, ... 24—group numbers

I→2—indicates transfer from group I to group 2

I. INTRODUCTION

The calculations to produce the results described herein were performed using the Allison IBM 7094 Mod II computer. The calculations were made to determine the effect of certain material, temperature, and dimensional variables on the criticality and size of a gaseous fueled cavity reactor for nuclear rocket propulsion. The choices of materials, temperatures and dimensions—as well as the choice between one-dimensional or two-dimensional computer runs—were made by the NASA Lewis Research Center. The DTK transport code was used for one-dimensional calculations; the DDK code was used for two-dimensional calculations. All cross sections used were required to have at least three thermal groups. Maximum convergence criteria were specified by the Lewis Research Center where appropriate during the progress of the work.

The discussions in each section of this report specify the choice of variables and explain in more detail how the results were obtained. The computer runs and print-outs, which represent a substantial bulk of material, were furnished to NASA separately.

II. SUMMARY

The following paragraphs summarize the results of the calculations which are given in analytical detail in Sections III, IV, and V.

1. The one-dimensional (spherical) calculations show the following characteristics with regard to reflector materials in the cavity reactors investigated at low temperatures.
   - For a relatively thin (12 in.) reflector, the critical mass is smallest using BeO, somewhat larger using D_2O, and largest by a substantial margin when using carbon.
   - With thicker reflectors (24 in. and 36 in.) the critical mass is nearly the same for BeO and D_2O reflectors. With carbon, however, the critical mass is substantially larger.

2. The one-dimensional calculations show the following characteristics with regard to changes in moderator temperature.
   - The critical mass increases with all materials at temperatures up to 3000°R. The rate of change for D_2O is substantially larger than for the other materials primarily because of the large change in D_2O density with temperature. The percentage change of critical mass with temperature for BeO reflectors is larger than for carbon, although the actual critical mass is always smaller with BeO for equivalent geometries.
   - With a carbon reflector temperature between 3000 and 5000°R (the only material for which 5000°R is applicable), the critical mass levels off or decreases with the increases in temperature.

3. The one-dimensional calculations show the following results with regard to cavity size.
   - In all cavities with a BeO reflector, critical mass increases as cavity size increases. This is also true with the thicker D_2O reflectors (24 and 36 in.) and the thin (12 in.) carbon reflector.
   - With a thin (12 in.) D_2O reflector at 530°R and with thicker (24 and 36 in.) carbon reflectors, there is a shallow minimum critical mass at about 48-in. cavity radius.
   - At elevated D_2O temperatures with a 12-in. reflector, the strong effect of temperature and, hence, density shows a trend giving an increase in critical mass with increase in cavity size.

4. Inserting absorbing material between the cavity fuel and the reflector has the following effects.
   - There is a substantial increase in critical mass with increasing absorber thickness for all materials.
   - The effect of the absorber on critical mass for D_2O and BeO reflector cores is similar in magnitude. The effect on carbon-moderated cores is significantly less than that for the other materials based on percentage increase in critical mass caused by various amounts of absorbing materials.
   - The trend of critical mass with increased temperature, with or without absorber, is essentially unchanged with D_2O reflectors. Conversely, with BeO and carbon reflectors the trend with temperature is changed substantially by the addition of absorbers. This change is accentuated with increasing thickness of absorber and at lower moderator temperatures.

5. Use of a composite reflector by inserting various thicknesses of D_2O between the bulk of the reflector-moderator and the fuel cavity has the following effects.
   - A reduction of as much as 25% in critical mass is obtained from the addition of 12 cm D_2O between the cavity core and BeO reflector.
   - The critical mass with carbon reflector is reduced considerably by the addition of D_2O so that with 4 cm of D_2O the critical mass is reduced by a factor of about five. With 12 cm, the critical mass is reduced by a factor of ten when compared with the 24-in. thick carbon reflector.
   - The variation of critical mass with bulk moderator temperature is changed substantially by the composite reflector including D_2O when compared to the pure BeO or pure carbon reflector. This is true of both the overall trends of the curves of critical mass versus temperature and their general shape.

6. The two-dimensional cylindrical calculation gave critical mass results consistent with the comparative one-dimensional spherical cavity in that the relative critical masses of the two configurations were in proportion to the cavity sizes.

7. In a cylindrical cavity using a composite reflector of D_2O and BeO or carbon, the following are the effects of reducing the radius of the nuclear fuel within the cavity and replacing it with low-density hydrogen.
   - Reducing fuel radius, as a portion of the cavity radius, increases the critical mass much more rapidly for large cavities than for small cavities. This trend is also true for cavities with composite D_2O-BeO reflectors where the L/D ratio is increased from one-third to unity.

8. Neutron balance errors which are primarily due to a relatively large epsilon value are amplified by use of upscattering.

9. The sensitivity of the calculations to epsilon decreases with increased slowing down power—i.e., BeO and D_2O calculations are more insensitive to epsilon variations than carbon.

10. The numerical complexity of a given problem is reduced by increasing fuel concentration and reducing upscattering terms.

11. The results of thermalization theory indicate that temperature effects on critical mass apparently reflect the inverse of the fuel absorption cross section. Therefore, to a major extent, the changes in critical mass with temperature herein are uniquely associated with the plutonium fuel—changing fuel can be expected to markedly change this effect.

12. Within the limits of accuracy in available cross sections, an S_4 specification was sufficient.

III. RESULTS AND DISCUSSIONS

These data are presented in a format which follows the lettering system of Article I of Contract NAS 3-6073. The basic requirements were:

> "Perform analytical services using a computer with a minimum storage core of 8000. The services shall include computation with existing digital nuclear codes, plottings, analysis, and reporting of gaseous fueled cavity reactors for nuclear propulsion. The existing digital nuclear codes shall be TDC or DDK reactor code for two-dimensional transport theory. The existing digital nuclear code shall be DSN or DTK reactor code for one-dimension transport theory. All calculations shall be performed with no less than three thermal groups. Convergence criteria shall be not more than 0.005 for eigenvalue searches and 0.01 for concentration searches. (The convergence criteria for eigenvalue searches were later modified to 0.0001 for paragraphs A, B, and C.) The services shall be performed in accordance with specifications set forth below: . . ."

Those portions of the introductions to the following paragraphs A through G and J which are set off in quotation marks are abstracted from the corresponding paragraphs in the contract.

PARAGRAPH A

"Perform one-dimensional calculations on the following spherical cavity reactors to obtain the critical mass of Pu-239 for a completely filled cavity as a function of reflector-moderator temperature for three cavity radii, three reflector-moderator thicknesses, four reflector-moderator materials, and four temperatures. (Later instructions required running at reduced convergence criteria of 0.0001 at three temperatures and only three materials.)

Cavity radii (in.)	Reflector thickness (in.)	Material	Temperatures (°R)		
			D_2O	BeO	C
24	12	D_2O	530	530	530
48	24	BeO	800	2000	3000
72	36	C	1000	3000	5000

"Calculations shall be performed for all combinations of cavity diameters and reflector thicknesses for each material."

D_2O

The results for the D_2O-moderated reactors are tabulated in Table 3-I and plotted in Figures 3-1, 3-2, and 3-3. The plots present the critical mass as a function of reflector temperature for cavity radii of 24 in., 48 in., and 72 in., respectively, with reflector thicknesses of 12 in., 24 in., and 36 in.

Table 3-I.

Data for D_2O-moderated reactors.

Size (in.) core-reflector	Energy groups	Temp (°R)	$N_{Pu} \times 10^{-24}$ (atoms/cm^3)	$N_{D_2O} \times 10^{-24}$ (atoms/cm^3)	Mass (kg)
24-12	24	530	1.00×10^{-4}	0.0331	37.65
24-12	24	800	2.6×10^{-4}	0.0296	98.0
24-12	24	1000	5.65×10^{-4}	0.024705	212.5
24-24	24	530	5.025×10^{-6}	0.0331	1.88
24-24	24	800	9.10×10^{-6}	0.0296	3.42
24-24	24	1000	2.75×10^{-5}	0.024705	10.35
24-36	24	530	3.18×10^{-6}	0.0331	1.2
24-36	24	800	4.8×10^{-6}	0.0296	1.8
24-36	24	1000	9.4×10^{-6}	0.024705	3.55
48-12	24	530	1.075×10^{-5}	0.0331	32.4
48-12	24	800	4.20×10^{-5}	0.0296	126.5
48-12	24	1000	1.55×10^{-4}	0.024705	467.0
48-24	24	530	1.35×10^{-6}	0.0331	4.07
48-24	24	800	1.975×10^{-6}	0.0296	5.97
48-24	24	1000	3.65×10^{-6}	0.024705	11.00
48-36	24	530	8.25×10^{-7}	0.0331	2.48
48-36	24	800	1.15×10^{-6}	0.0296	3.46
48-36	24	1000	1.80×10^{-6}	0.024705	5.42
72-12	24	530	3.95×10^{-6}	0.0331	39.65
72-12	24	800	1.75×10^{-5}	0.0296	176.0
72-12	24	1000	7.8×10^{-5}	0.024705	785.0
72-24	24	530	6.625×10^{-7}	0.0331	6.65
72-24	24	800	9.8×10^{-7}	0.0296	9.85
72-24	24	1000	1.7×10^{-6}	0.024705	17.2
72-36	24	530	4.5×10^{-7}	0.0331	4.525
72-36	24	800	5.9×10^{-7}	0.0296	5.925
72-36	24	1000	8.6×10^{-7}	0.024705	8.65

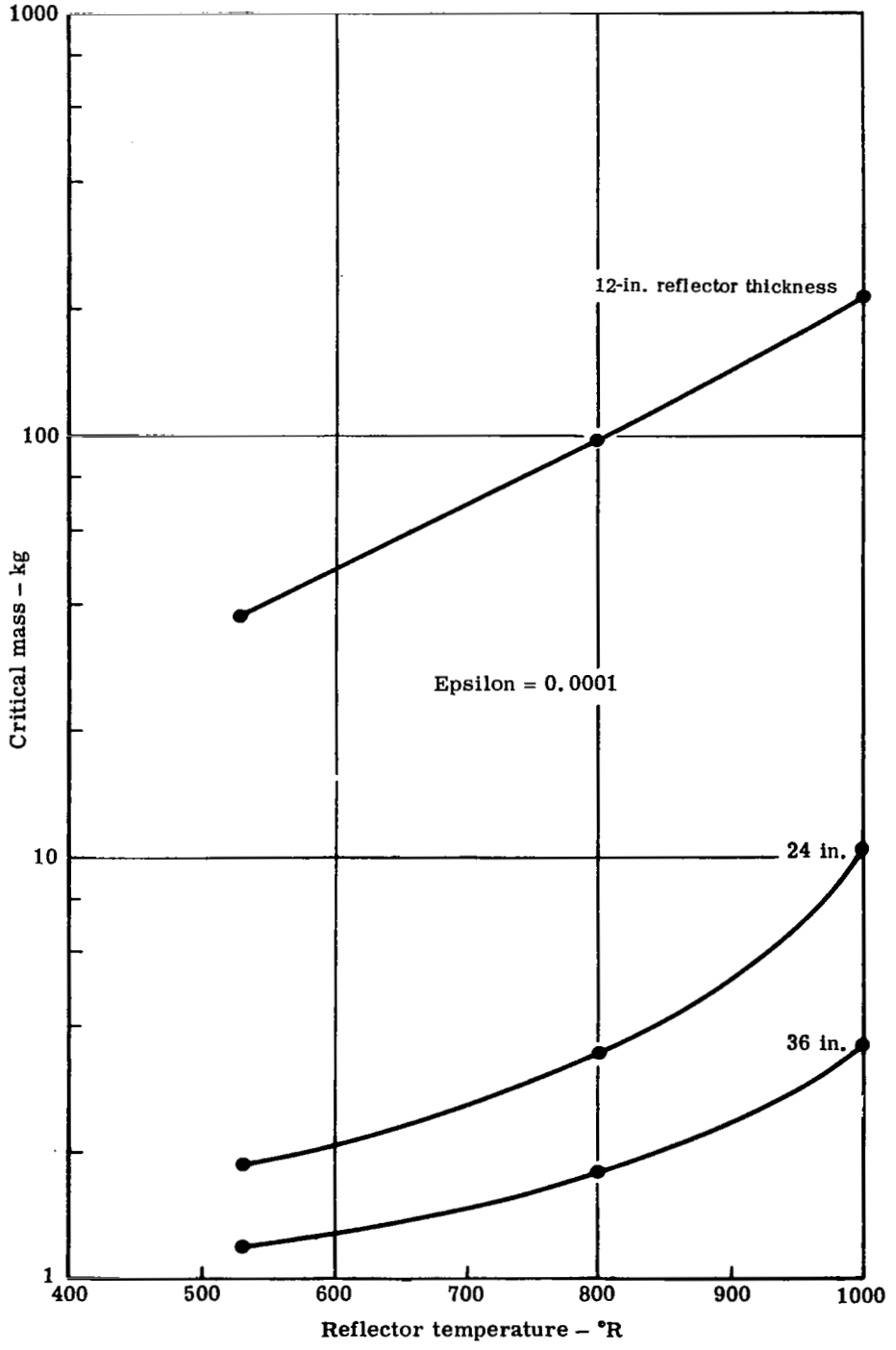

Figure 3-1. Effect of reflector temperature on critical mass – 24 in. spherical cavity radius with D_2O reflector.

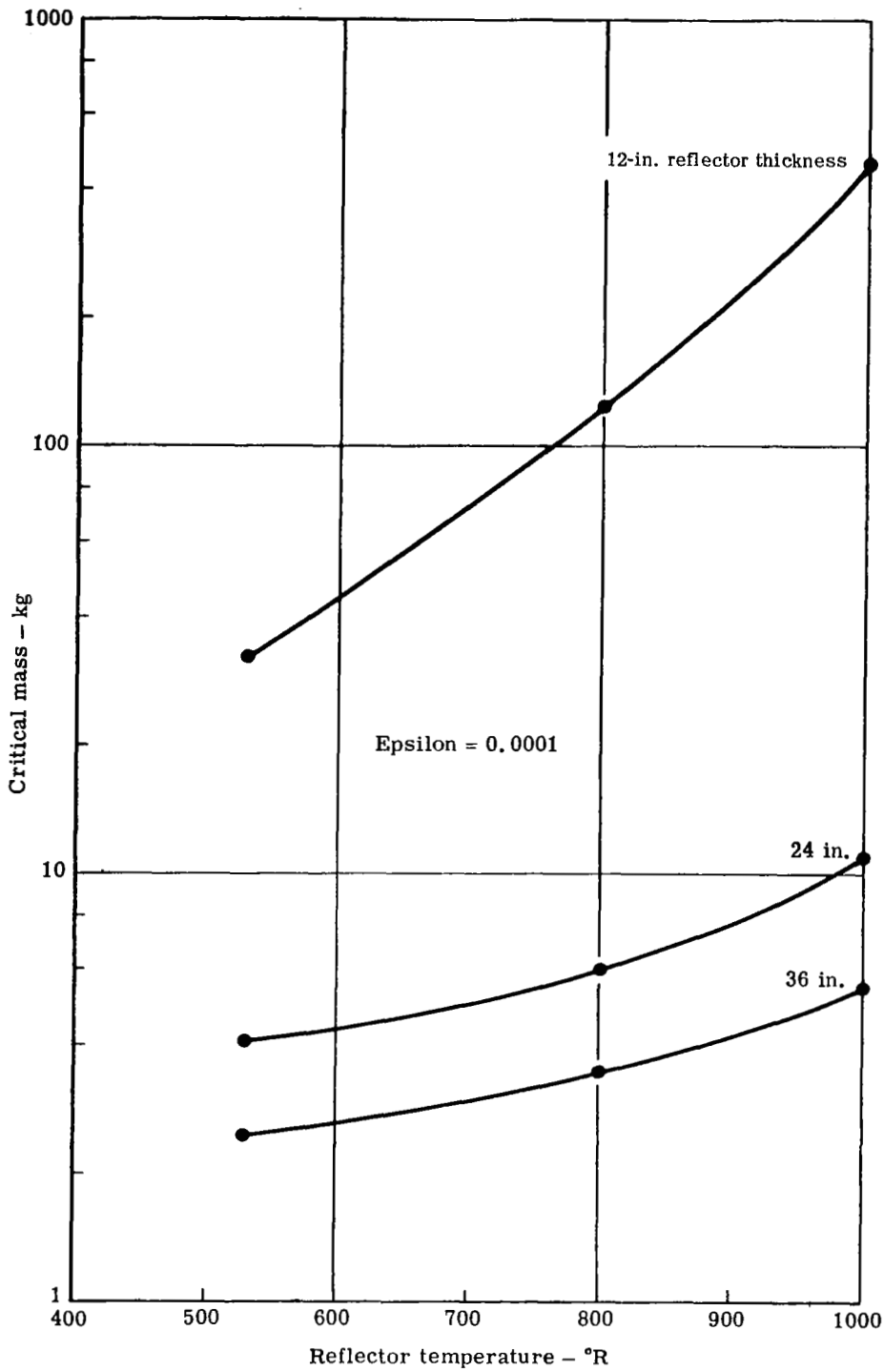

Figure 3-2. Effect of reflector temperature on critical mass – 48-in. spherical cavity radius with D_2O reflector.

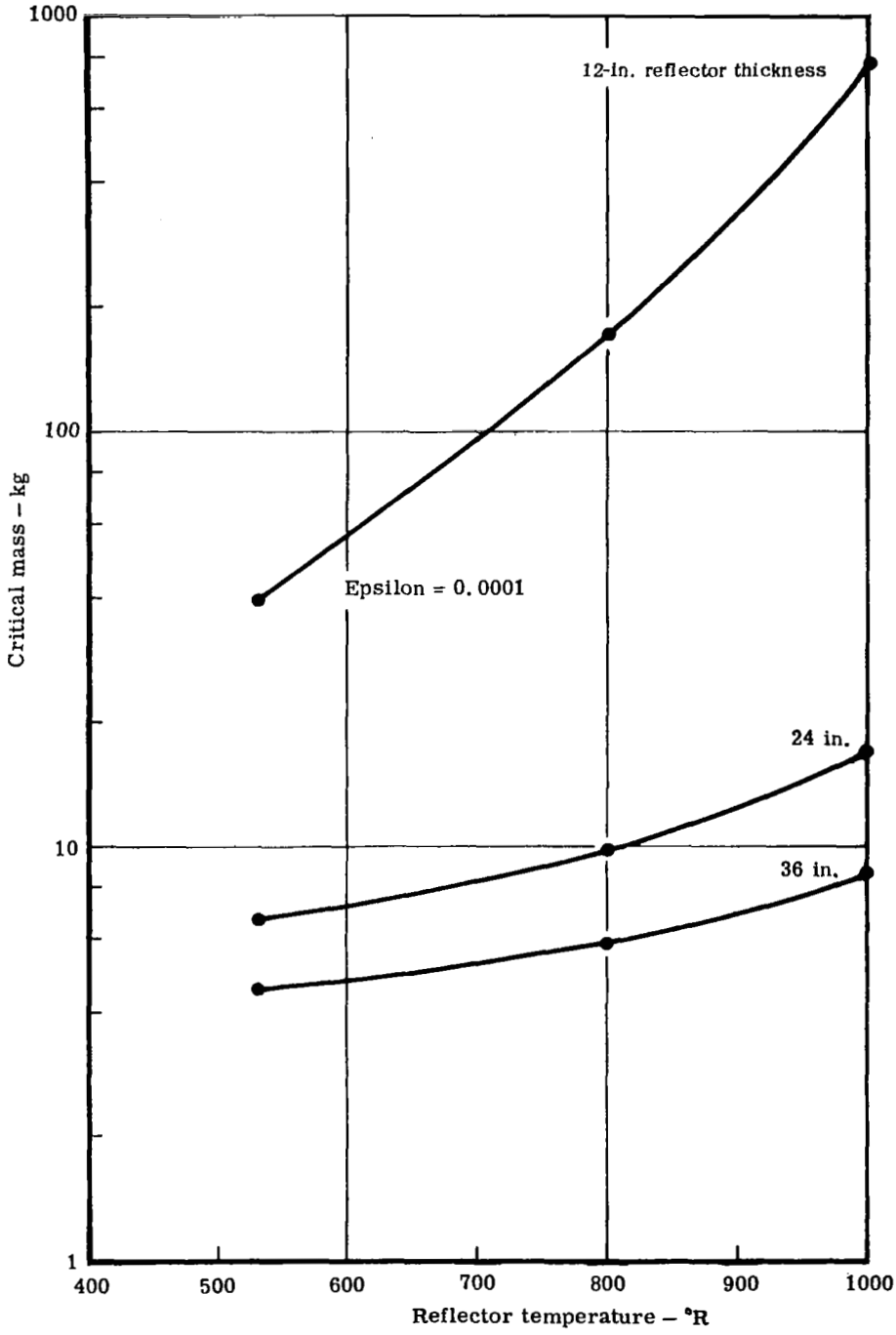

Figure 3-3. Effect of reflector temperature on critical mass – 72-in. spherical cavity radius with D_2O reflector.

The critical number density, i.e., fuel concentration, was obtained by making successive reactivity calculations until two points were obtained within 3% of $k_{eff} = 1.0$. The number density was then plotted versus k_{eff}. The number density desired was obtained from the plot at the intercept with the value $k_{eff} = 1.0$. This method was used with all materials.

The calculations show that with a D_2O reflector the critical mass increases with temperature for all the configurations investigated. This increase is caused by the decrease in moderator density and hardening of the thermal spectrum with temperature. Thus all cavities investigated have a strong negative temperature coefficient with the value varying inversely with reflector thickness.

For a given cavity size, as reflector thickness increases the critical mass decreases as expected. The effect on critical mass is greater between the 12-in. and 24-in. reflectors when compared with that between the 24-in. and 36-in. reflectors. The percent decrease in critical mass with increasing reflector thickness is also greater for the smaller cavities.

The 24-in. radius cavity with 36-in. D_2O at 530°R has the minimum Pu-239 loading of all configurations investigated—1.2 kg. Diffusion theory* gives the same loading. Thus, for highly thermal reactors, transport and diffusion theory coincide if the multigroup cross sections yield the same average values for η (neutrons produced/neutron absorbed in core) and L (diffusion length).

BeO

The results of the BeO-moderated reactors are presented in Table 3-II and in Figures 3-4, 3-5, and 3-6, as plots of critical mass versus reflector temperature.

The critical mass for all reactors increases with temperature to 3000°R (the thermal absorption minimum of Pu-239). This is, however, less apparent than in the graphite-moderated cores. Since the BeO spectrum is the most thermal of the materials considered, the 1/V moderator absorptions have a greater effect in tending to reduce critical mass.

*G. Safonov, "Externally Moderated Reactors," Reactor Physics Second United Nations Int. Conf. on Peaceful uses of Atomic Energy (Geneva), Vol. 12, 1958, pp 705-718.

Table 3-II.

Data for BeO-moderated reactors.

Size (in.) core-reflector	Energy groups	Temp (°R)	$N_{Pu} \times 10^{-24}$ (atoms/cm^3)	$N_{D_2O} \times 10^{-24}$ (atoms/cm^3)	Mass (kg)
24-12	15	530	1.42×10^{-5}	0.1372	5.32
24-12	15	2000	2.65×10^{-5}	0.1372	10.0
24-12	15	3000	3.0×10^{-5}	0.1372	11.6
24-24	15	530	4.48×10^{-6}	0.1372	1.68
24-24	15	2000	5.13×10^{-6}	0.1372	1.93
24-24	15	3000	5.47×10^{-6}	0.1372	2.05
24-36	15	530	4.0×10^{-6}	0.1372	1.51
24-36	15	2000	4.3×10^{-6}	0.1372	1.63
24-36	15	3000	4.5×10^{-6}	0.1372	1.70
48-12	15	530	3.5×10^{-6}	0.1372	9.5
48-12	15	2000	4.5×10^{-6}	0.1372	13.55
48-12	15	3000	5.2×10^{-6}	0.1372	15.65
48-24	15	530	1.32×10^{-6}	0.1372	3.98
48-24	15	2000	1.50×10^{-6}	0.1372	4.52
48-24	15	3000	1.57×10^{-6}	0.1372	4.73
48-36	15	530	1.22×10^{-6}	0.1372	3.673
48-36	15	2000	1.285×10^{-6}	0.1372	3.869
48-36	15	3000	1.41×10^{-6}	0.1372	4.246
72-12	15	530	1.77×10^{-6}	0.1372	18.0
72-12	15	2000	2.48×10^{-6}	0.1372	25.2
72-12	15	3000	2.56×10^{-6}	0.1372	26.0
72-24	15	530	7.13×10^{-7}	0.1372	7.34
72-24	15	2000	8.7×10^{-7}	0.1372	8.30
72-24	15	3000	8.55×10^{-7}	0.1372	8.66
72-36	15	530	6.78×10^{-7}	0.1372	6.87
72-36	15	2000	6.94×10^{-7}	0.1372	7.05
72-36	15	3000	7.16×10^{-7}	0.1372	7.26

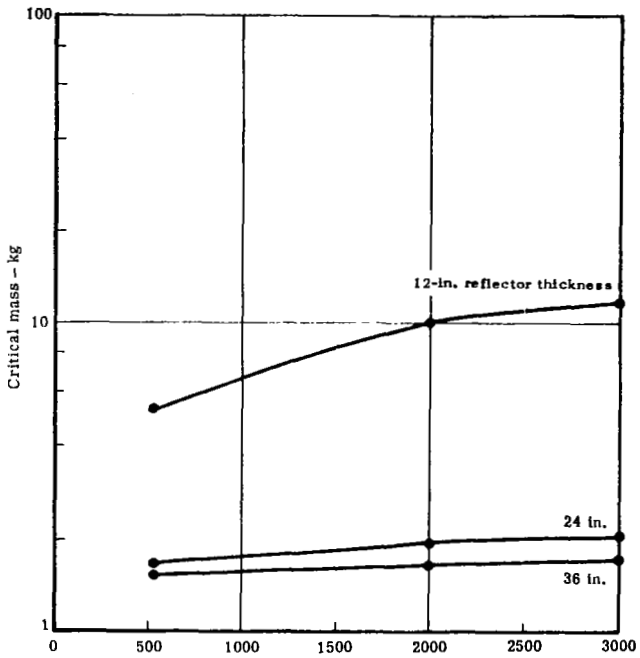

Figure 3-4. Effect of reflector temperature on critical mass – 24-in. spherical cavity radius with BeO reflector.

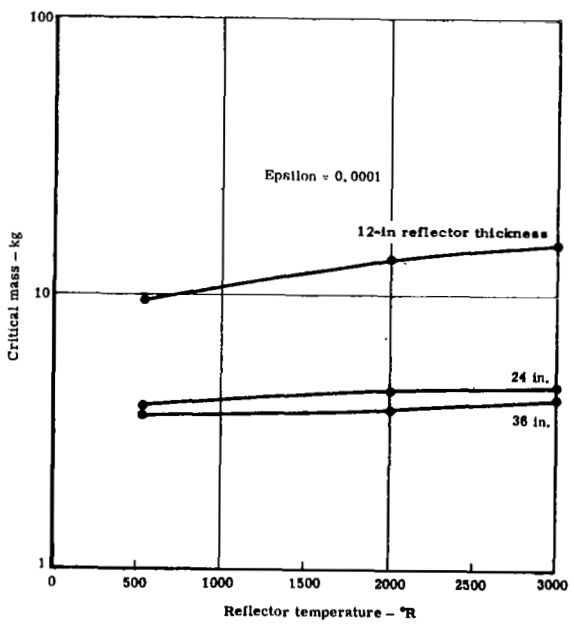

Figure 3-5. Effect of reflector temperature on critical mass – 48-in. spherical cavity radius with BeO reflector.

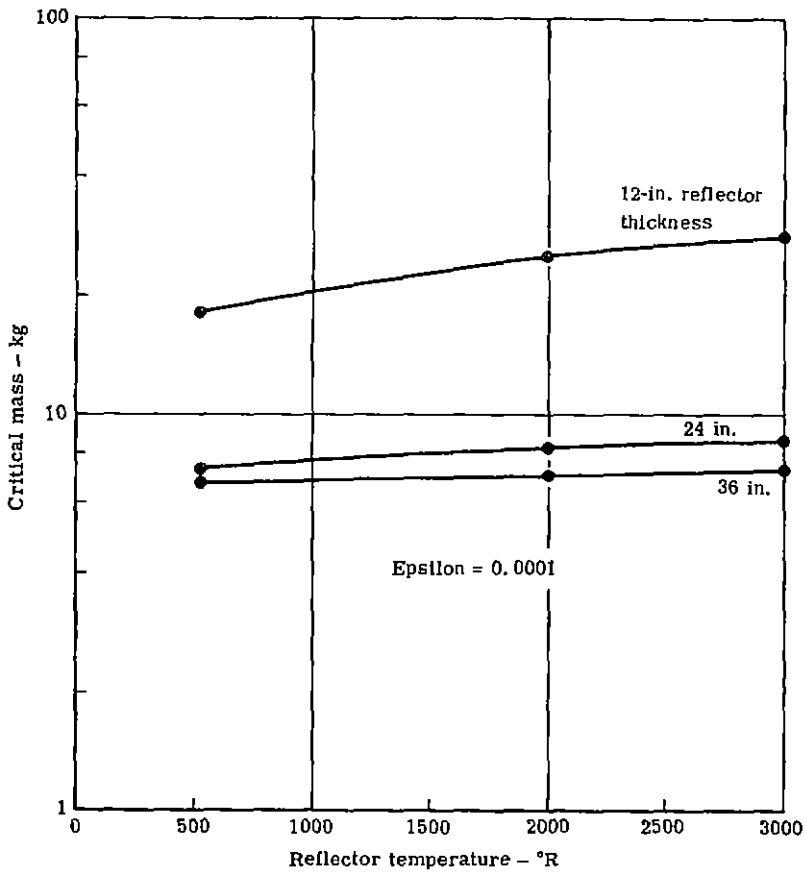

Figure 3-6. Effect of reflector temperature on critical mass – 72-in. spherical cavity radius with BeO reflector.

All of these cavities exhibit a net negative reactivity temperature coefficient from 530 to 3000°R, with the smallest reflector thickness for each cavity showing the largest overall coefficient. The temperature coefficient for the 72-in. cavity reduces in absolute value near 3000°R so that it would probably be positive above this value because of the large fuel resonance. The temperature points, however, are not close enough to determine this.

As with D_2O, for a specific cavity the relative decrease in critical mass for the 12-in. to 24-in. moderated core is much larger than that of the 24-in. to 36-in. moderated core.

Carbon

The results of the carbon-moderated cores are presented in Table 3-III and Figures 3-7, 3-8, and 3-9. The general trend of the curves between 530 and 3000°R is similar to that when D_2O

and BeO are used as moderators. There is, however, a maximum critical mass near 3000°R caused by the plutonium thermal absorption minimum located just before the absorption peak. Beyond that temperature, the decrease in moderator thermal absorption overrides the effect of lower η, resulting in a net decrease in critical mass.

Table 3-III.

Data for carbon-moderated reactors.

Size (in.) core-reflector	Energy groups	Temp (°R)	$N_{Pu} \times 10^{-24}$ (atoms/cm^3)	$N_{carbon} \times 10^{-24}$ (atoms/cm^3)	Mass (kg)
24-12	24	530	6.5×10^{-4}	0.084	245.0
24-12	24	3000	6.6×10^{-4}	0.084	248.5
24-12	24	5000	6.75×10^{-4}	0.084	254.0
24-24	24	530	1.56×10^{-4}	0.084	58.8
24-24	24	3000	1.74×10^{-4}	0.084	66.5
24-24	24	5000	1.64×10^{-4}	0.084	61.6
24-36	24	530	4.725×10^{-5}	0.084	17.8
24-36	24	3000	5.7×10^{-5}	0.084	21.5
24-36	24	5000	5.425×10^{-5}	0.084	20.5
48-12	24	530	2.265×10^{-4}	0.084	680.0
48-12	24	3000	2.42×10^{-4}	0.084	727.0
48-12	24	5000	2.36×10^{-4}	0.084	709.0
48-24	24	530	1.19×10^{-5}	0.084	35.8
48-24	24	3000	1.99×10^{-5}	0.084	59.5
48-24	24	5000	1.80×10^{-5}	0.084	54.0
48-36	24	530	3.9×10^{-6}	0.084	11.7
48-36	24	3000	5.1×10^{-6}	0.084	15.3
48-36	24	5000	4.45×10^{-6}	0.084	13.4
72-12	24	530	1.275×10^{-4}	0.084	1295.0
72-12	24	3000	1.345×10^{-4}	0.084	1369.0
72-12	24	5000	1.335×10^{-4}	0.084	1359.0
72-24	24	530	4.0×10^{-6}	0.084	40.6
72-24	24	3000	6.55×10^{-6}	0.084	66.5
72-24	24	5000	6.625×10^{-6}	0.084	67.0
72-36	24	530	1.575×10^{-6}	0.084	16.0
72-36	24	3000	1.75×10^{-6}	0.084	17.8
72-36	24	5000	1.76×10^{-6}	0.084	17.9

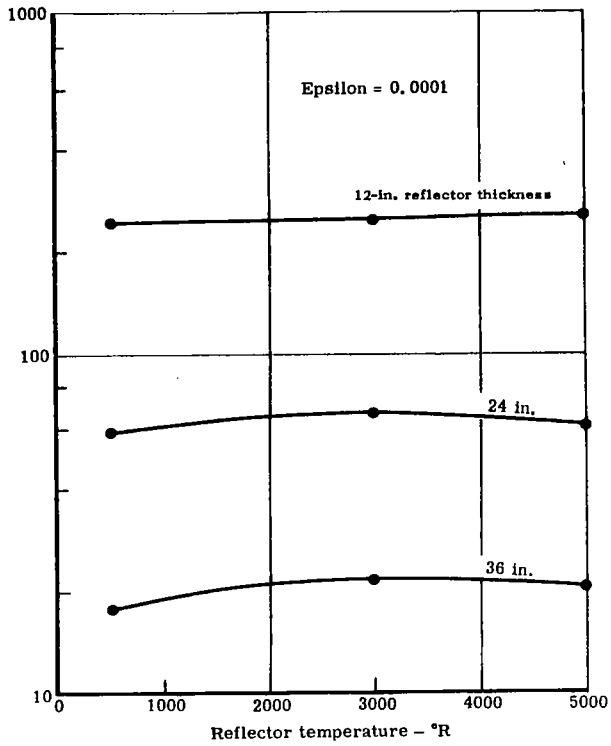

Figure 3-7. Effect of reflector temperature on critical mass – 24-in. spherical cavity radius with carbon reflector.

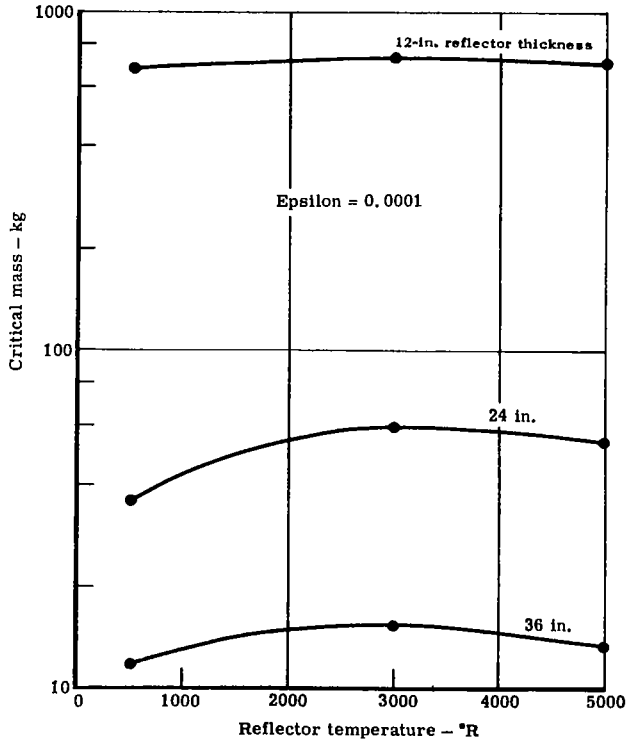

Figure 3-8. Effect of reflector temperature on critical mass – 48-in. spherical cavity radius with carbon reflector.

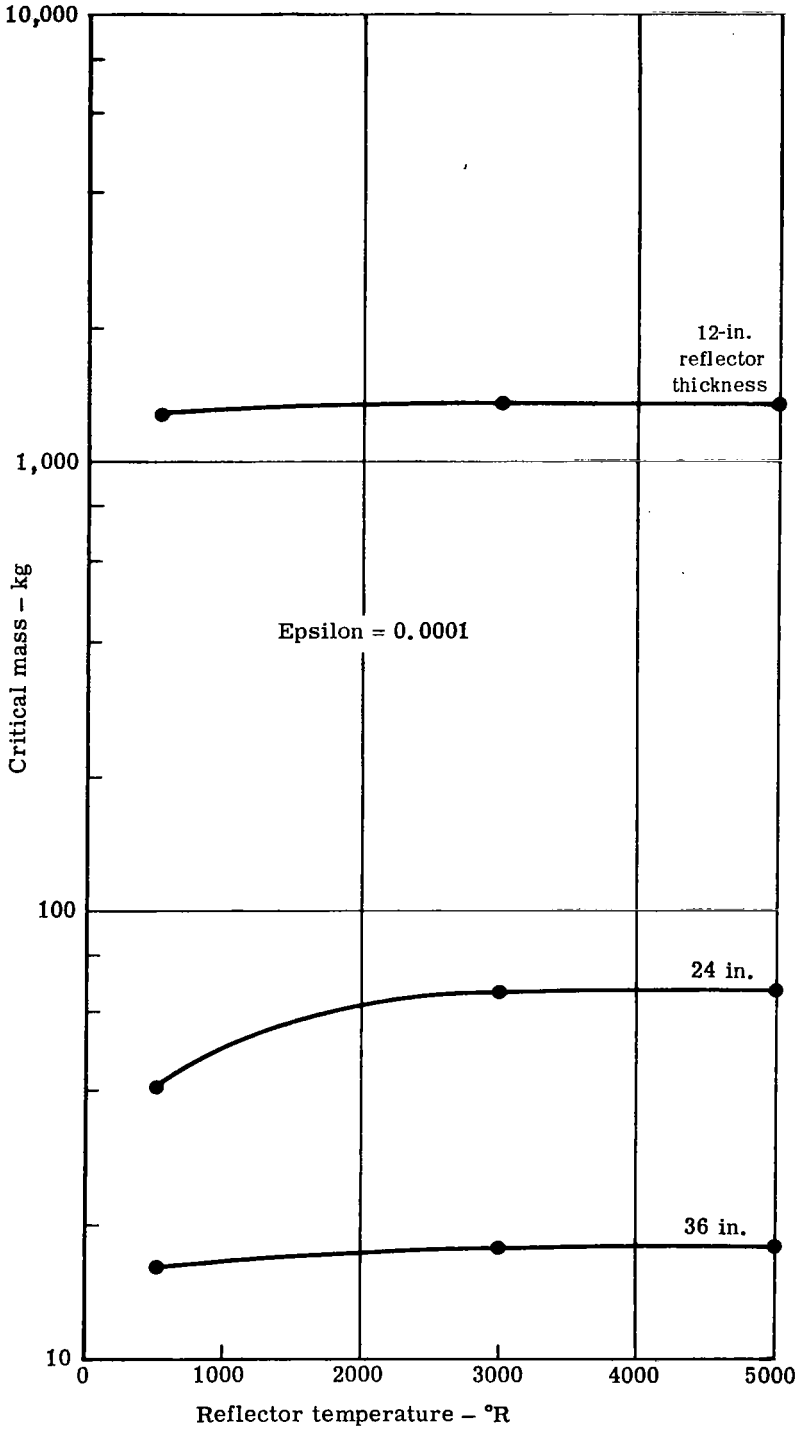

Figure 3-9. Effect of reflector temperature on critical mass – 72-in. spherical cavity radius with carbon reflector.

PARAGRAPH B

"Using a reflector-moderator thickness of 24 in. and a cavity radius of 48 in., as used in paragraph A, insert a region between cavity and reflector so that the thermal macroscopic absorption cross section times the thickness in centimeters ($\Sigma_a t$) is varied between limits of 0.01 and 0.10 for four values. Plot critical mass versus temperature for these reflector-moderator materials."

D_2O

The results of the calculation for D_2O-moderated reactors with the absorber region are plotted in Figure 3-10 and tabulated in Table 3-IV. The plot shows the effect of reflector temperature on critical mass for four $\Sigma_a t$ values of 0.01, 0.033, 0.066, and 0.1. D_2O temperatures 530, 800, and 1000°R were used. As in paragraph A, the critical fuel number density was obtained from a plot of k_{eff} and number density.

These data show that for each $\Sigma_a t$, as the temperature of the reflector is increased, the critical mass is increased. The decrease of moderator density with increasing temperature gives a negative temperature coefficient of reactivity. The spectrum hardening effect is also negative for the D_2O. For each temperature investigated, the expected increase in critical mass is observed with increasing $\Sigma_a t$.

These results show that the change in D_2O moderator density is the major factor affecting the change in critical mass with temperature. However, the constant moderator densities in the BeO and carbon subsequently discussed show more clearly the individual effect of the $\Sigma_a t$ cross section with temperature for each $\Sigma_a t$ value.

BeO

The data for BeO-moderated reactors with absorber region are shown in Figure 3-11 for moderator temperatures of 530, 2000, and 3000°R. These data show a set of reactors completely changing their basic temperature characteristics as a function of $\Sigma_a t$.

The absorber value $\Sigma_a t = 0.1$ gives a positive temperature coefficient of reactivity from 530 to 2000°R. However, as the moderator temperature reaches the Pu-239 absorption minimum near 3000°R, the differential coefficient is reduced almost to zero—this is also true for the 0.066 and

0.033 absorbers. However, for the 0.01 absorber, the reactor follows the same basic characteristics as a reactor with no absorber present—i.e., a negative temperature coefficient of reactivity with the critical mass requirement increasing with increasing moderator temperature to the Pu-239 absorption minimum near 3000°R.

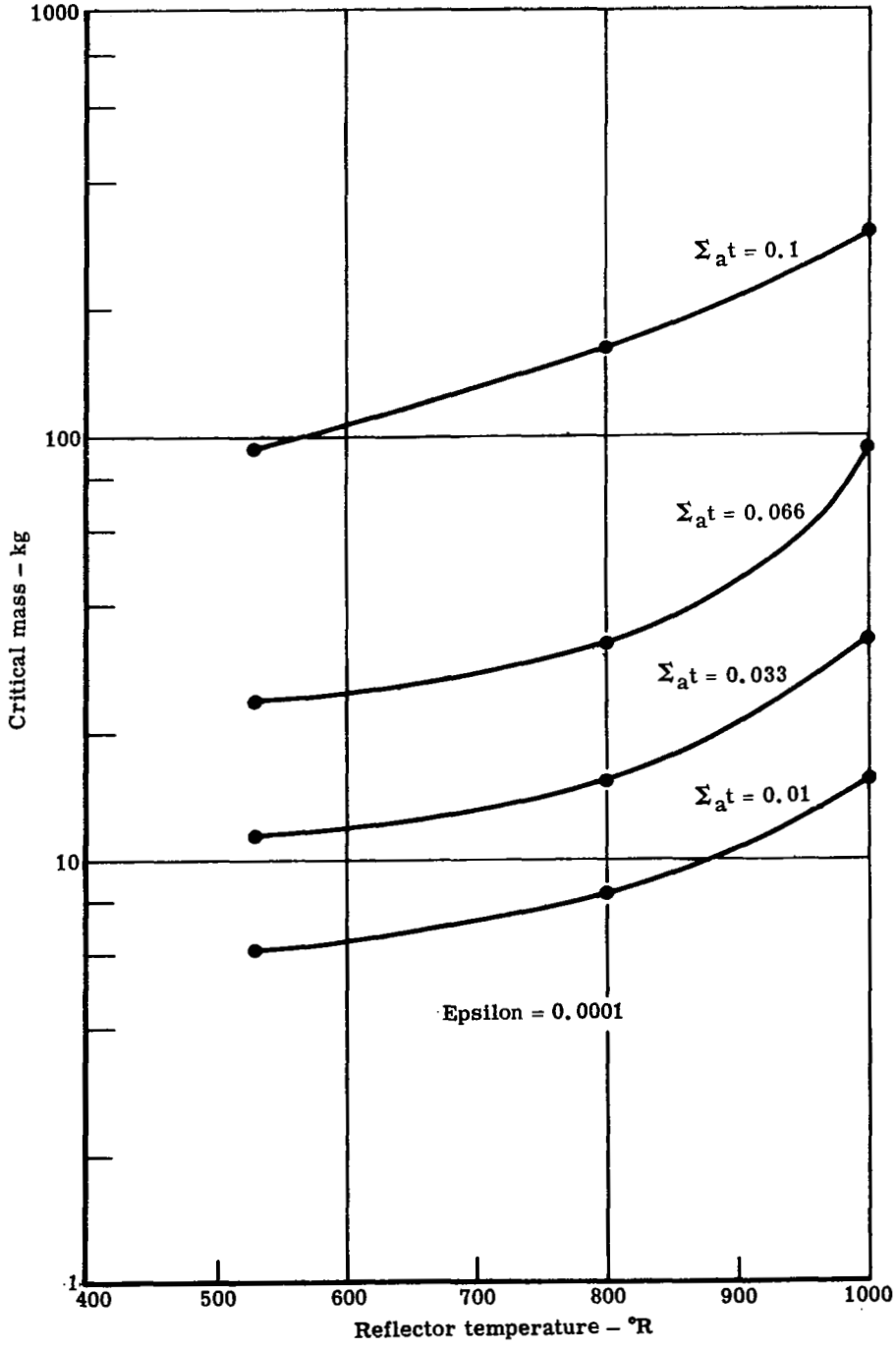

Figure 3-10. Effect of temperature on critical mass with cavity interface absorber – 48-in. spherical cavity radius with 24-in. D_2O outer reflector.

Table 3-IV.

Data for D_2O-, BeO-, or carbon-moderated reactors with absorber region.

Size (in.) core-reflector	Energy groups	Temp (°R)	Absorber thickness $\Sigma_a t$ (cm)	$N_{Pu} \times 10^{-24}$ (atoms/cm^3)	$N_{Nb} \times 10^{-24}$ (atoms/cm^3)	$N_{reflector} \times 10^{-24}$ (atoms/cm^3)	Mass (kg)
				Deuterium oxide			
48-24	24	530	0.1	3.075×10^{-5}	0.0545	0.0331	92.5
48-24	24	800	0.1	5.325×10^{-5}	0.0545	0.0296	160.0
48-24	24	1000	0.1	9.7×10^{-5}	0.0545	0.024705	292.0
48-24	24	530	0.066	7.925×10^{-6}	0.03597	0.0331	23.9
48-24	24	800	0.066	1.075×10^{-5}	0.03597	0.0296	32.3
48-24	24	1000	0.066	3.12×10^{-5}	0.03597	0.024705	93.7
48-24	24	530	0.033	3.75×10^{-6}	0.017985	0.0331	11.3
48-24	24	800	0.033	5.05×10^{-6}	0.017985	0.0296	15.2
48-24	24	1000	0.033	1.083×10^{-5}	0.017985	0.024705	32.6
48-24	24	530	0.01	2.0×10^{-6}	0.00545	0.0331	6.1
48-24	24	800	0.01	2.725×10^{-6}	0.00545	0.0296	8.2
48-24	24	1000	0.01	5.05×10^{-6}	0.00545	0.024705	15.2
				Beryllium oxide			
48-24	15	530	0.1	2.705×10^{-5}	0.0545	0.1372	82.0
48-24	15	2000	0.1	1.7×10^{-5}	0.0545	0.1372	51.2
48-24	15	3000	0.1	1.66×10^{-5}	0.0545	0.1372	50.0
48-24	15	530	0.066	9.26×10^{-6}	0.03597	0.1372	27.9
48-24	15	2000	0.066	8.08×10^{-6}	0.03597	0.1372	24.3
48-24	15	3000	0.066	7.94×10^{-6}	0.03597	0.1372	23.8
48-24	15	530	0.033	4.05×10^{-6}	0.017985	0.1372	12.2
48-24	15	2000	0.033	3.95×10^{-6}	0.017985	0.1372	11.9
48-24	15	3000	0.033	3.85×10^{-6}	0.017985	0.1372	11.6
48-24	15	530	0.01	2.0×10^{-6}	0.00545	0.1372	6.02
48-24	15	2000	0.01	2.08×10^{-6}	0.00545	0.1372	6.26
48-24	15	3000	0.01	2.16×10^{-6}	0.00545	0.1372	6.50
				Carbon			
48-24	24	530	0.1	1.52×10^{-4}	0.0545	0.084	458.0
48-24	24	3000	0.1	1.28×10^{-4}	0.0545	0.084	386.0
48-24	24	5000	0.1	1.19×10^{-4}	0.0545	0.084	360.0
48-24	24	530	0.066	1.025×10^{-4}	0.03597	0.084	309.0
48-24	24	3000	0.066	8.7×10^{-5}	0.03597	0.084	262.0
48-24	24	5000	0.066	8.65×10^{-5}	0.03597	0.084	260.0
48-24	24	530	0.033	5.535×10^{-5}	0.017985	0.084	166.0
48-24	24	3000	0.033	5.56×10^{-5}	0.017985	0.084	167.5
48-24	24	5000	0.033	5.46×10^{-5}	0.017985	0.084	165.0
48-24	24	530	0.01	2.1×10^{-5}	0.00545	0.084	63.25
48-24	24	3000	0.01	3.15×10^{-5}	0.00545	0.084	95.0
48-24	24	5000	0.01	2.99×10^{-5}	0.00545	0.084	90.5

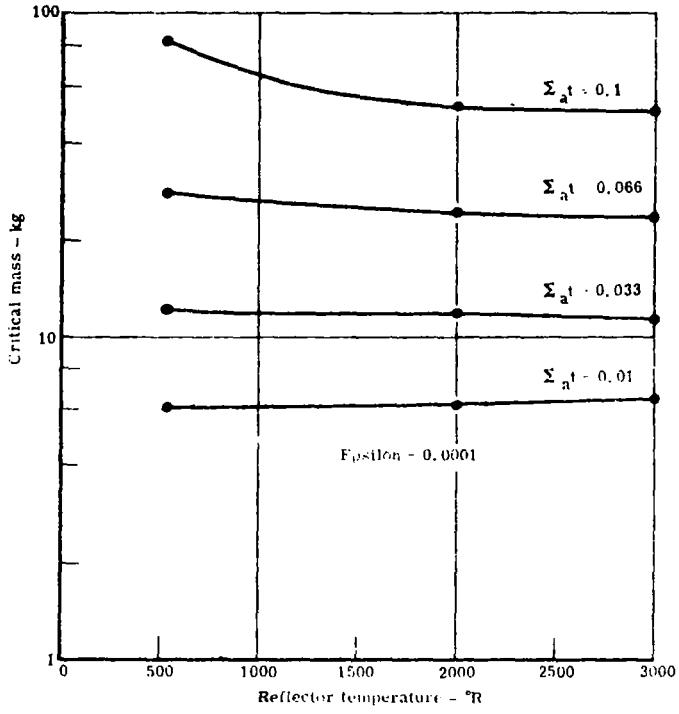

Figure 3-11. Effect of temperature on critical mass with cavity interface absorber – 48-in. spherical cavity radius with 24-in. BeO outer reflector.

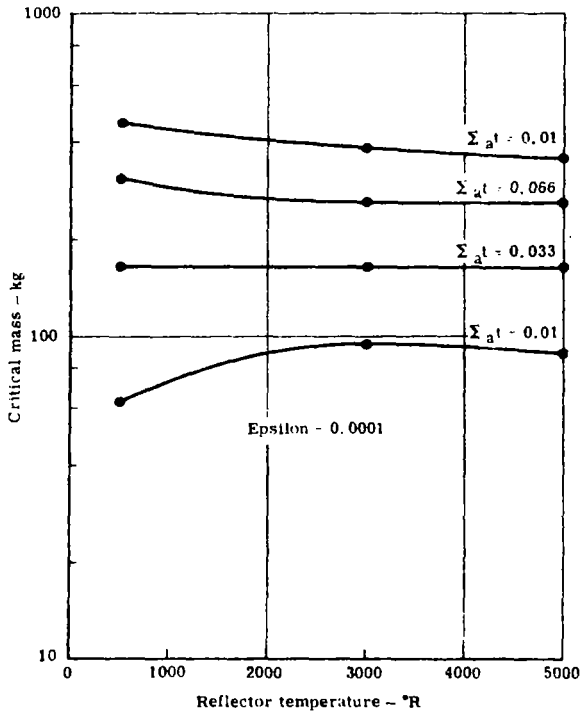

Figure 3-12. Effect of temperature on critical mass with cavity interface absorber – 48-in. spherical cavity radius with 24-in. carbon outer reflector.

Carbon

The results for carbon-moderated reactors with inner absorbers are shown in Figure 3-12 for moderator temperatures of 530, 3000, and 5000°R. As with BeO, the carbon data indicate a set of thermal reactors. The temperature coefficient of reactivity changes from a negative value with no absorber to a positive value at the maximum absorber thickness. A zero overall coefficient exists at $\Sigma_a t = 0.033$.

In the reactors with $\Sigma_a t = 0.01$, the overall temperature coefficient is negative from 530 to 5000°R with a maximum critical mass at 3000°R. The 0.033-in. thickness shows an interesting combination of effects. The changes in η and leakage with temperature are compensated for by reduced 1/V type absorptions. However, when the nominal absorption is increased to give $\Sigma_a t = 0.066$ or 0.10, the 1/V absorptions amplify the positive reactivity effect. Thus, Figure 3-12 shows a uniformly positive temperature coefficient.

In general, BeO and carbon appear to produce reactors with similar temperature characteristics.

PARAGRAPH C

"With the same reflector-moderator thickness and cavity radius, place varying thicknesses of D_2O between cavity and reflector-moderator. Use thicknesses of 4 cm, 8 cm, and 12 cm. The D_2O shall have a temperature of 1000°R. The reactor calculations shall again be performed in a one-dimensional spherical analysis and the critical mass (Pu-239) plotted as a function of reflector-moderator temperature."

BeO

The critical mass for this configuration was calculated for three BeO reflector-moderator temperatures—530, 2000, and 3000°R—and for each thickness of D_2O insert. A fixed cavity radius of 48 in. and a BeO reflector thickness of 24 in. were used.

The critical number density of fuel and, hence, critical mass was obtained as described in paragraph A. The results of these calculations are shown in Table 3-V and Figure 3-13.

In all cases these configurations have a positive temperature coefficient. The basic reason appears to be associated with the thermal character of the neutron spectrum and the reduction of absorption in the reflector materials at the higher neutron temperatures. Since the D_2O was kept at the uniform temperature of 1000°R, the density change with temperature as in paragraph A is eliminated.

Table 3-V.

Data for BeO- or carbon-moderated reactors with inner D_2O reflector.

Size core-inner reflector-outer reflector (in.) (cm) (in.)	Energy group	Temp (°R)	D_2O thickness (cm)	$N_{Pu} \times 10^{-24}$ (atoms/cm^3)	$N_{D_2O} \times 10^{-24}$ (atoms/cm^3)	$N_{reflector} \times 10^{-24}$ (atoms/cm^3)	Mass (kg)
				Beryllium oxide			
48-4-24	15	530	4	1.2×10^{-6}	0.024705	0.1372	3.61
48-4-24	15	2000	4	1.0×10^{-6}	0.024705	0.1372	3.01
48-4-24	15	3000	4	9.5×10^{-7}	0.024705	0.1372	2.86
48-8-24	15	530	8	1.13×10^{-6}	0.024705	0.1372	3.40
48-8-24	15	2000	8	9.2×10^{-7}	0.024705	0.1372	2.76
48-8-24	15	3000	8	8.75×10^{-7}	0.024705	0.1372	2.63
48-12-24	15	530	12	1.120×10^{-6}	0.024705	0.1372	3.36
48-12-24	15	2000	12	8.55×10^{-7}	0.024705	0.1372	2.57
48-12-24	15	3000	12	8.25×10^{-7}	0.024705	0.1372	2.48
				Carbon			
48-4-24	24	530	4	2.525×10^{-6}	0.024705	0.084	7.60
48-4-24	24	3000	4	2.3×10^{-6}	0.024705	0.084	6.925
48-4-24	24	5000	4	2.175×10^{-6}	0.024705	0.084	6.55
48-8-24	24	530	8	1.75×10^{-6}	0.024705	0.084	5.26
48-8-24	24	3000	8	1.40×10^{-6}	0.024705	0.084	4.22
48-8-24	24	5000	8	1.26×10^{-6}	0.024705	0.084	3.80
48-12-24	24	530	12	1.55×10^{-6}	0.024705	0.084	4.66
48-12-24	24	3000	12	1.195×10^{-6}	0.024705	0.084	3.60
48-12-24	24	5000	12	1.07×10^{-6}	0.024705	0.084	3.22

Carbon

The critical mass for this configuration was calculated for three carbon reflector-moderator temperatures of 530, 3000, and 5000°R and for each thickness of D_2O insert. A fixed cavity radius of 48 in. and carbon reflector-moderator thickness of 24 in. were used.

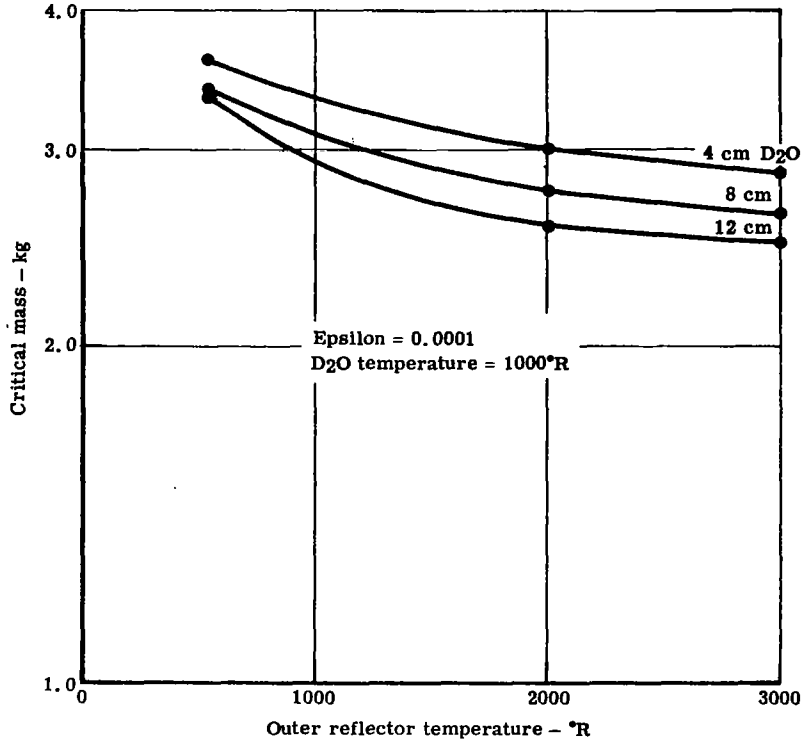

Figure 3-13. Effect of temperature on critical mass with 48-in. spherical cavity radius – inner D_2O reflector and outer 24-in. BeO reflector.

The results of these calculations are shown in Table 3-V and Figure 3-14. In all cases, as with BeO, this arrangement results in a positive temperature coefficient if the D_2O temperature is fixed at 1000°R. Thus, as in the case of BeO, reduced absorptions in the moderator occur with increased temperatures.

The insertion of a thin, 4-cm layer of D_2O between the cavity and carbon reflector-moderator reduces the critical mass, at room temperature, from about 36 kg to less than 8 kg. For higher temperatures, a greater change is observed. Thus, a carbon D_2O composite reflector is almost as effective in reducing critical mass as a BeO reflector.

PARAGRAPH D

"From the results obtained under paragraphs A, B, and C, a spherical cavity with a region representing structural material ($\Sigma_a t$), a D_2O region, and a reflector-moderator region will be selected by the NASA Lewis Research Center.

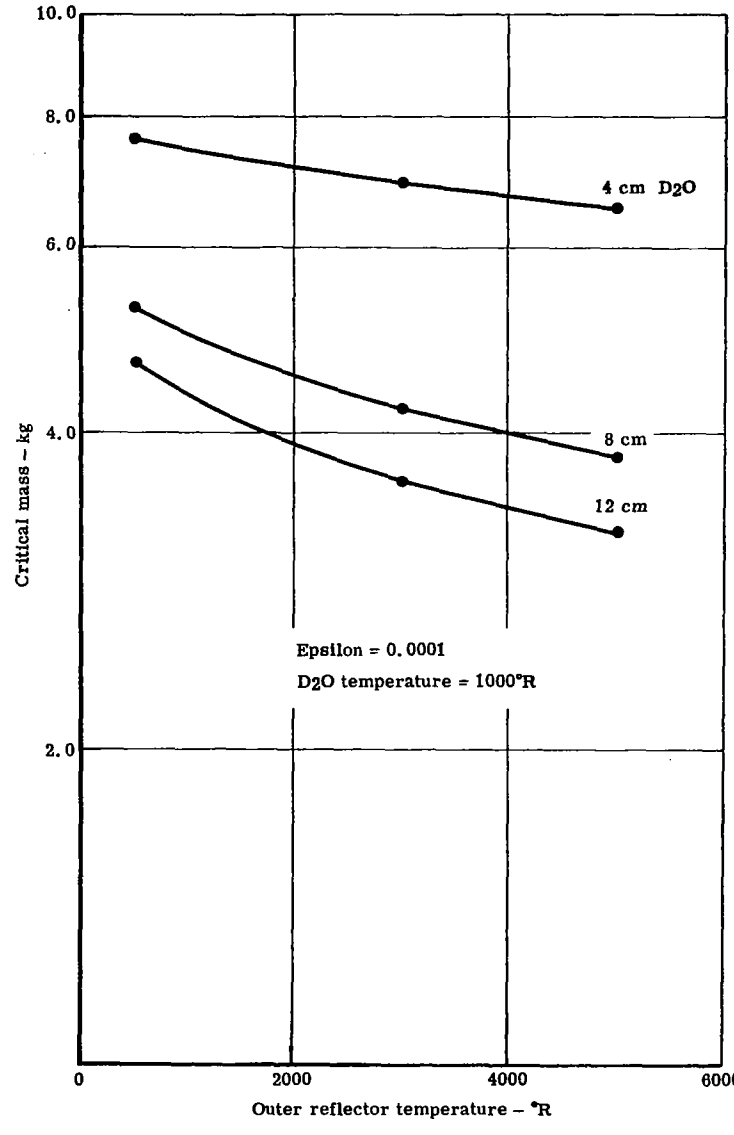

Figure 3-14.
Effect of temperature on critical mass with 48-in. spherical cavity radius – inner D_2 O reflector and outer 24-in. C reflector.

The critical mass of Pu-239 in the spherical cavity in paragraph D shall be determined and compared to a two-dimensional calculation of a cylindrical reactor with a cavity of the same diameter and a length-to-diameter ratio of 1:1. The regions selected by NASA shall completely enclose the cylindrical cavity. Comparison shall be made at 530°R only. A two-dimensional transport analysis shall be used."

A cavity radius of 60 in. with a 24-in. outer BeO reflector was specified. An absorber (structural material) of niobium, 1.58 cm thick at 66% normal density (to allow for cooling), was also selected. An additional 8-cm thickness of D_2O was used.

The results of these runs (see Table 3-VI) were calculated using 5-group cross sections and the k_{eff} calculation mode of the DTK and DDK codes. The number of space intervals in each material was as shown.

Table 3-VI.
Comparison of one- and two-dimensional calculations.

	One-dimensional sphere	Two-dimensional cylinder
Intervals		
Pu (60 in.)	7	7
Nb (1.58 cm)	3	3
D_2O (8 cm)	8	8
BeO (24 in.)	7	7
Atomic density		
$N_{Pu} \times 10^{-24}$ =	3.94×10^{-6}	3.8×10^{-6}
$N_{Nb} \times 10^{-24}$ =	3.597×10^{-2}	3.597×10^{-2}
$N_{D_2O} \times 10^{-24}$ =	3.31×10^{-2}	3.31×10^{-2}
$N_{BeO} \times 10^{-24}$ =	1.372×10^{-1}	1.372×10^{-1}
Epsilon	0.001	0.001
Reactivity	0.991	0.9913
Mass (kg)	23.2	33.6
Neutrons generated per neutron absorbed in fuel	2.00	2.02
Total net leakage	0.144	0.129
Neutrons absorbed in niobium	0.163	0.181
Total neutron absorption in niobium and leakage	0.307	0.310

The results showed that for essentially equivalent values of k_{eff}—0.991 for the sphere and 0.9913 for the cylinder—the concentrations of fuel were almost equal—3.94×10^{-6} and 3.8×10^{-6}, respectively. This meant that the critical masses varied in almost direct proportion to the volumes in the two geometries—(23.2/33.6) ≅ (1/1.5).

In Table 3-VI, the value of (η) differs by less than 1%. Thus, the fuel worths in these geometries are essentially the same. At the same time, the surface-to-volume ratios of both the sphere and cylinder are equivalent and this would normally result in equal leakage. In Table 3-VI, however, the sphere has over 10% more leakage than the cylinder. At the same time, there are approximately 10% more absorptions in the niobium in the cylinder. These differences

balance so that the sum of leakage plus absorptions in niobium for both sphere and cylinder are about equal. (Table 3-VI shows these effects.)

For estimates of fuel concentration for later two-dimensional runs in paragraphs E and F, it was possible to make good "first guesses" by using one-dimensional spheres with surface-to-volume ratios equal to those of the cylinders being calculated. This technique was valid only for the full cavity cases, however.

PARAGRAPH E

"From the results obtained under paragraphs A, B, and C, a thickness of D_2O for the inner region, a thickness for the reflector-moderator region of BeO, and a fuel region temperature will be selected by the NASA Lewis Research Center. This selection provided by NASA shall be used in three series of two-dimensional calculations using the two-dimensional code selected for paragraph D."

This was the first of a series of two-dimensional calculations made to determine the effect of fuel diameter on critical mass. Three cavity radii and three length-to-diameter ratios were used. Each cavity radius (36, 60, and 86 in.) was run with all three length-to-diameter ratios (1:3, 2:3, and 1:1). In each of the nine combinations of cavity radius and length-to-diameter ratio, the critical mass was determined and the fuel radius was then varied to obtain a 1.5 and 5.0 increase in critical mass. The void between the fuel and reflector was considered filled with hydrogen with a number density of 7.0×10^{20} atoms/cm^3.

A 12-cm D_2O inner reflector thickness and a 24-in. BeO outer reflector thickness were selected by NASA for these calculations and held constant for all two-dimensional runs. 1000°R D_2O and 3000°R BeO cross sections were used for these calculations.

Prior to making the two-dimensional runs with the cavity completely filled, a series of one-dimensional calculations was made using spheres having fuel surface-to-volume ratios equivalent to those of the cylinders. The critical fuel number densities from the one-dimensional calculations were then used as first guesses in the two-dimensional calculations in full cavities. This approximation gave results for k_{eff} within ± 3% for a length-to-diameter ratio of 1:3. In the other length-to-diameter ratios the reactivity was closer to ± 1.5% using this method. The number density of the cavities varied by an approximation of $1/r^n$, where n is between 1 and 2.

The final results are presented in Table 3-VII. These results were obtained by performing reactivity calculations, plotting reactivity versus number density, and selecting the number density at which $k_{eff} = 1$. The dimensions, materials, temperatures, and calculational details are also presented in Table 3-VII. The number of axial and radial intervals was held to a minimum and was based on the one-dimensional flux shapes—ten intervals in the cavity, five intervals in the D_2O, and ten intervals in the BeO. Occasionally, a negative flux appeared in the outer portion of the reflector using these intervals. The five-group cross sections with one fast, one intermediate, and three thermal groups based on the multigroup results were used for all paragraph E runs. The convergence criteria were based on a value of $\epsilon = 0.001$ which was smaller (more precise) than the $\epsilon = 0.005$ specified initially in the contract, but larger (less precise) than the $\epsilon = 0.0001$ used in later calculations to verify the reduced number of cross sections. The final answer, k_{eff}, is sensitive to the value of ϵ used.

It was noted from the normalized balance tables for the two-dimensional runs that although the net balance for the entire core was unity (considering at least five significant figures), the sum of the leakage plus absorptions was not unity, varying as much as ± 10%. It was further noted that when $|1.0 - AVR|$, which was printed out on-line, was an order of magnitude below the convergence criteria (ϵ), the sum of the leakage and absorptions more nearly approximated unity. This is an indication of the need for a lower (more precise) convergence criteria when the effects being calculated are small—such as those for temperature coefficient—or when detailed core design is involved. For the substantial geometry effects of these two-dimensional calculations in the interests of reasonable computer running time, $\epsilon = 0.001$ appears adequately small—1% k_{eff}, 10% critical mass, and only 3% in radius for 1% k_{eff}.

To determine the geometry effects, the full cavity critical mass was calculated and the radius of the fuel region was varied to determine the dimension for a given multiple of the initial critical mass. The number densities of the materials in the reactor are presented in Table 3-VII for all configurations with the critical mass. The dimensionless symbol β is used to represent the ratio of fuel radius to cavity radius. Runs 245 through 253 were made with the cavity completely filled with fuel. In runs 254 through 262, the critical mass was increased by a factor of five by decreasing fuel diameter. In runs 263 through 371, the critical mass is 1.5 times greater than the completely filled cavity.

Fluxes which had been previously obtained were used to the fullest possible extent at the beginning of each problem. After obtaining the first set of fluxes for a series of problems, a path through the remaining problems was made using the minimum change in volume as the criteria. In some instances the initial fluxes were found to be influencing the problem. This required a close scrutiny of the results for consistency and required a few reruns where results indicated this was necessary.

Table 3-VII.

Data for two-dimensional BeO-moderated reactor.

Run No.	Cavity radius (in.)	Number of intervals in fuel radially	Number of intervals in fuel axially	$N_{Pu} \times 10^{-24}$ (atoms/cm^3)	Critical mass (kg)	L/D ratio	β
245	36	10	10	1.17×10^{-6}	2.23	1:1	1.0
246	60	10	10	5.0×10^{-7}	4.41	1:1	1.0
247	86	10	10	3.5×10^{-7}	9.08	1:1	1.0
248	36	10	10	1.37×10^{-6}	1.74	2:3	1.0
249	36	10	10	1.90×10^{-6}	1.2	1:3	1.0
250	60	10	10	6.6×10^{-7}	3.88	2:3	1.0
251	60	10	10	1.00×10^{-6}	2.94	1:3	1.0
252	86	10	10	4.23×10^{-7}	7.34	2:3	1.0
253	86	10	10	5.8×10^{-7}	5.02	1:3	1.0
254	36	5	10	1.08×10^{-4}	11.2	1:1	0.23
255	36	5	10	1.03×10^{-4}	8.69	2:3	0.258
256	36	5	10	6.49×10^{-5}	6.03	1:3	0.32
257	60	5	10	3.6×10^{-5}	22.0	1:1	0.264
258	60	5	10	4.49×10^{-5}	19.4	2:3	0.271
259	60	5	10	4.54×10^{-5}	14.7	1:3	0.332
260	86	5	10	1.9×10^{-5}	45.4	1:1	0.30
261	86	5	10	2.31×10^{-5}	36.7	2:3	0.303
262	86	5	10	2.59×10^{-5}	25.1	1:3	0.35
263	36	5	10	7.62×10^{-6}	3.35	1:1	0.48
264	60	5	10	1.51×10^{-6}	6.70	1:1	0.71
265	86	5	10	8.96×10^{-7}	13.6	1:1	0.765
266	36	5	10	7.3×10^{-6}	2.61	2:3	0.53
267	60	5	10	2.84×10^{-6}	5.82	2:3	0.59
268	86	5	10	1.146×10^{-6}	11.0	2:3	0.745
269	36	5	10	1.31×10^{-5}	1.8	1:3	0.465
270	60	5	10	5.55×10^{-5}	4.41	1:3	0.52
271	86	5	10	2.34×10^{-6}	7.53	1:3	0.61

Conditions:

D_2O thickness—12 cm
Reflector thickness—24 in.
D_2O temperature—1000°R
Reflector temperature—3000°R
Number of energy groups—5
Epsilon—0.001
Number of intervals in D_2O in each direction—5
Number of intervals in reflector in each direction—10
Number density of D_2O—2.4705×10^{-2}
Number density of reflector—1.372×10^{-1}

Data for paragraph G were obtained from runs in which fuel did not entirely fill the cavity. By holding mass constant and varying number density and fuel radius, criticality was achieved. Thus, for each mass considered, the effect of β on k_{eff} was found directly.

The sensitivity of the 36-in. cavity to the order of S_n was found by lowering the value of S_n from S_4 to S_2—k_{eff} for the S_2 calculation was 0.9990034 as compared to 1.00367 for the S_4 calculation.

The paragraph E results are presented in Figures 3-15, 3-16, and 3-17. Figure 3-15 gives the results for a 36-in. cavity radius; Figures 3-16 and 3-17 present the 60- and 86-in. cavity radius results. Each plot shows the variation of critical mass with β for the three length-to-diameter ratios.

The trends shown in the plots indicate that the larger cavities have no apparent threshold for critical mass sensitivity with fuel radius as is indicated by the smaller cavities. For the smallest cavity (radius = 36 in., length-to-diameter ratio = 1:3), β = 0.465 for a 50% increase in critical mass; for the largest cavity (radius = 86 in., length-to-diameter ratio = 1:1), β = 0.765 for a 50% increase in critical mass. The remaining sizes fall between these two, increasing with fuel volume.

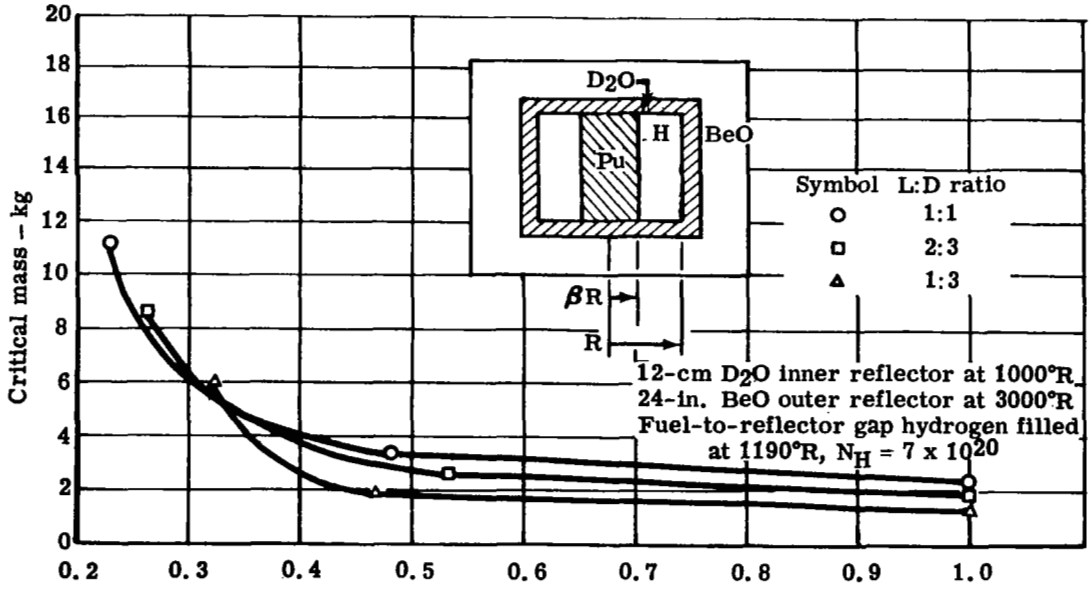

Figure 3-15. Effect of fuel radius-to-cavity radius ratio on critical mass – 36-in. cylindrical cavity radius.

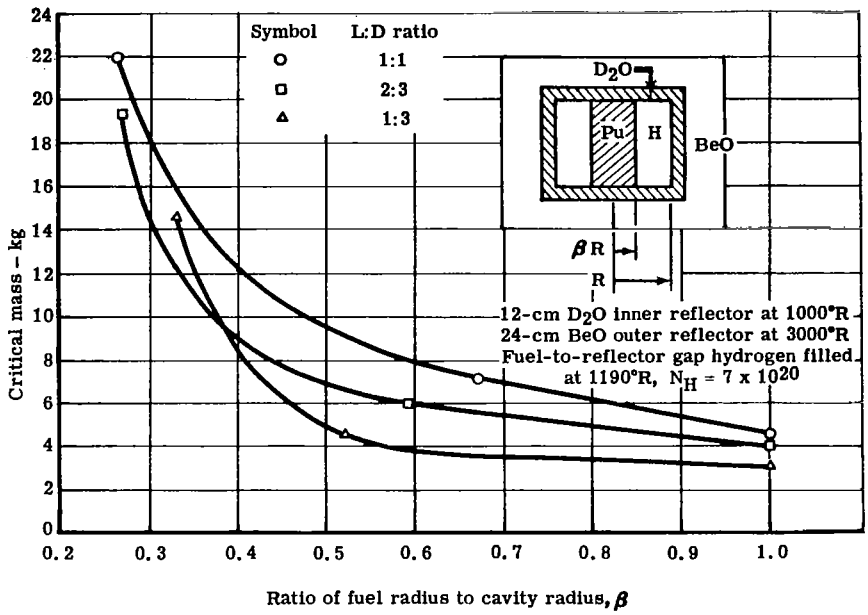

Figure 3-16. Effect of fuel radius-to-cavity radius ratio on critical mass – 60-in. cylindrical cavity radius.

PARAGRAPH F

"Based on paragraph E, one cavity length-to-diameter ratio will be selected by the NASA Lewis Research Center. For the one cavity length-to-diameter ratio, a series of two-dimensional calculations shall be performed as in paragraph E on the same reflector thickness but with 5000°R graphite replacing BeO."

This was a continuation of the two-dimensional runs similar to paragraph E. Three cavity radii of 36, 60, and 86 in. were used with a fixed cavity length-to-diameter ratio of 2:3. The critical mass was determined for the filled cavity. Then, keeping the cavity radius constant, the fuel radius was decreased to increase the critical mass by a factor of 1.5 and 5.0. Hydrogen at a density of 7.0×10^{20} atoms/cm^3 was used to fill the void created between the fuel and inner reflector of D_2O.

The final results, dimensions, materials, temperature, and calculational details are presented in Table 3-VIII. Using a 5-group cross section and $\epsilon = 0.001$, these results were obtained plotting reactivity versus number density and selecting a number density at which $k_{eff} = 1$. The interval spacing used was the same as in paragraph E, and again the total flux prints have shown

negative flux at a few points in the outer reflector. However, the total flux over the core was preserved and the sum of the normalized absorption and leakage was within an average of 3.15% for all runs. Therefore, the total mesh spacing seemed quite adequate.

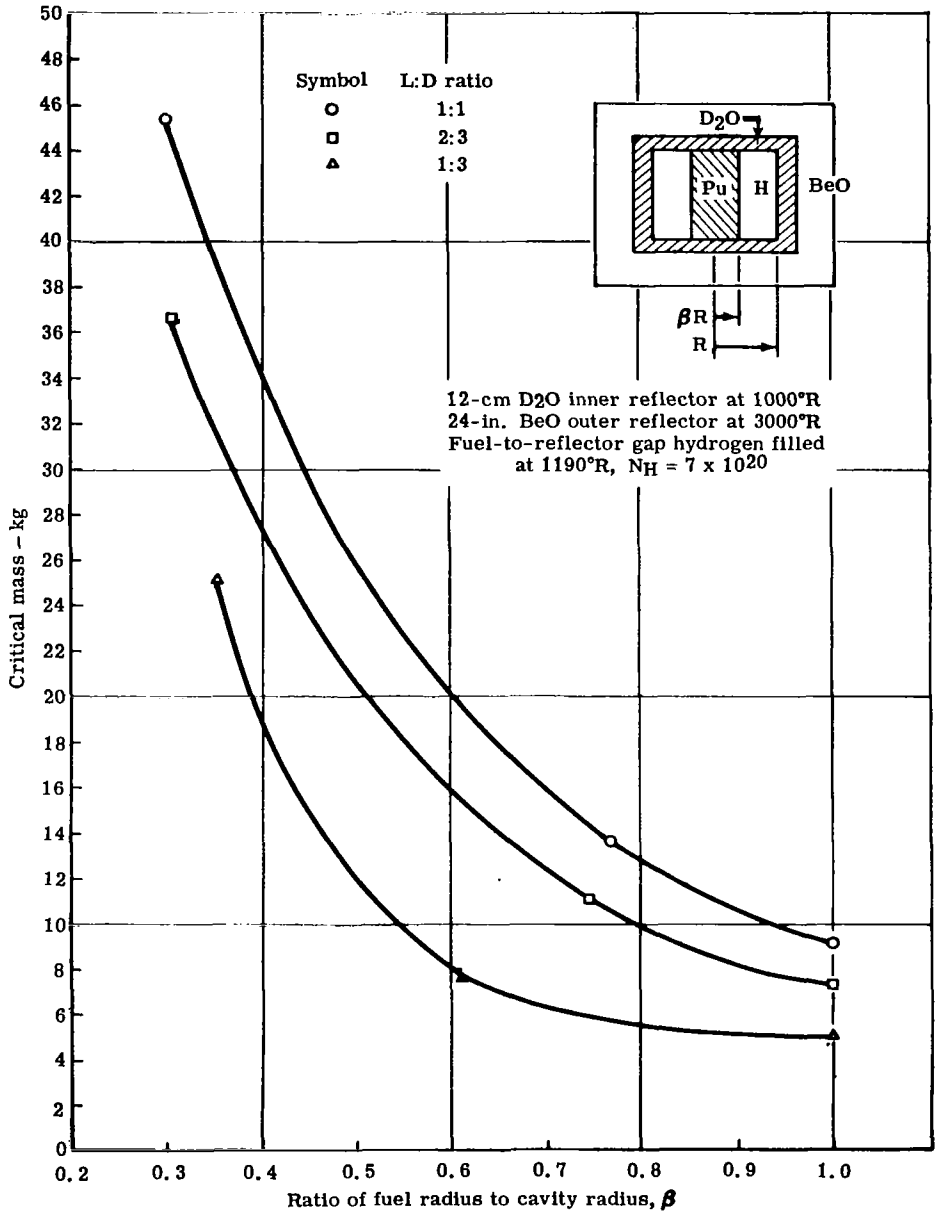

Figure 3-17. Effect of fuel radius-to-cavity radius ratio on critical mass – 86-in. cylindrical cavity radius.

Table 3-VIII.

Data for two-dimensional carbon-moderated reactor.

Cavity radius (in.)	D_2O thickness (cm)	Graphite thickness (in.)	D_2O temp (°R)	Graphite temp (°R)	Number of energy groups	Epsilon	Number density (atoms/cm^3) $N_{Pu} \times 10^{-24}$	$N_{D_2O} \times 10^{-24}$	$N_C \times 10^{-24}$	L/D ratio	β	Critical mass (kg)	$\Delta k_{eff}/\Delta\beta$	Run number
36	8	24	1000	5000	5	0.001	1.95	0.024705	0.084	2:3	1.0	2.48	—	272
60	8	24	1000	5000	5	0.001	0.80	0.024705	0.084	2:3	1.0	4.70	—	273
86	8	24	1000	5000	5	0.001	0.465	0.024705	0.084	2:3	1.0	8.10	—	274
36	8	24	1000	5000	5	0.001	7.1	0.024705	0.084	2:3	0.64	3.72	0.4109	275
60	8	24	1000	5000	5	0.001	2.05	0.024705	0.084	2:3	0.77	6.99	1.040	276
86	8	24	1000	5000	5	0.001	0.99	0.024705	0.084	2:3	0.842	12.15	1.2375	277
36	8	24	1000	5000	5	0.001	73.1	0.024705	0.084	2:3	0.365	12.4	0.88	278
60	8	24	1000	5000	5	0.001	31.25	0.024705	0.084	2:3	0.357	23.3	2.0838	279
86	8	24	1000	5000	5	0.001	18.1	0.024705	0.084	2:3	0.36	40.5	1.246	280

For the full cavity configuration, these reactors have geometry equivalent to paragraph E—i.e., length-to-diameter ratio = 2:3.

From table 3-VIII, runs 272 through 274 were made with the cavity completely filled with fuel. In runs 275 through 277, the critical mass was increased by a factor of 1.5; in runs 278 through 280, the critical mass is 5.0 times greater than with the completely filled cavity.

The final results given in Table 3-VIII are presented graphically in Figure 3-18. The dimensionless symbol β is used to represent the ratio of fuel radius to cavity radius. The plot shows the variation in critical mass with β for the three cavity radii. As in paragraph E, the larger cavity has no apparent threshold for critical mass sensitivity with fuel radius as the smaller cavity seems to indicate.

PARAGRAPH G

"Furnish information showing, in addition to the critical mass, a relationship between reactivity change with change in fuel diameter for given amounts of fuel."

The relationship between change in reactivity and change in fuel diameter was sought by the procedures used in calculating most of the points for paragraphs E and F. Two k_{eff} calculations were usually required to obtain the correct value of k_{eff} for criticality at fuel diameters corresponding to 1.5 and 5 times the "full" cavity value. Thus, with critical mass kept constant, both β (the fuel-to-cavity diameter ratio) and fuel concentration were varied. This yields values of Δk_{eff} and $\Delta\beta$ directly at a constant critical mass. Table 3-IX shows the results, together with related cavity dimensions and critical masses.

A number of plots were made to determine whether the value of $\frac{\Delta k_{eff}}{\Delta \beta}$ had any consistent relationship to critical mass, cavity geometry, or β. Only general trends could be noted. For example, for a given cavity geometry, the ratio $\frac{\Delta k_{eff}}{\Delta \beta}$ increases as the fuel load increases with only one exception (the 60-in. cavity with length-to-diameter ratio of 1:1). The values are close and the anomaly could be attributed to combining errors introduced by the relatively large epsilon of 0.001.

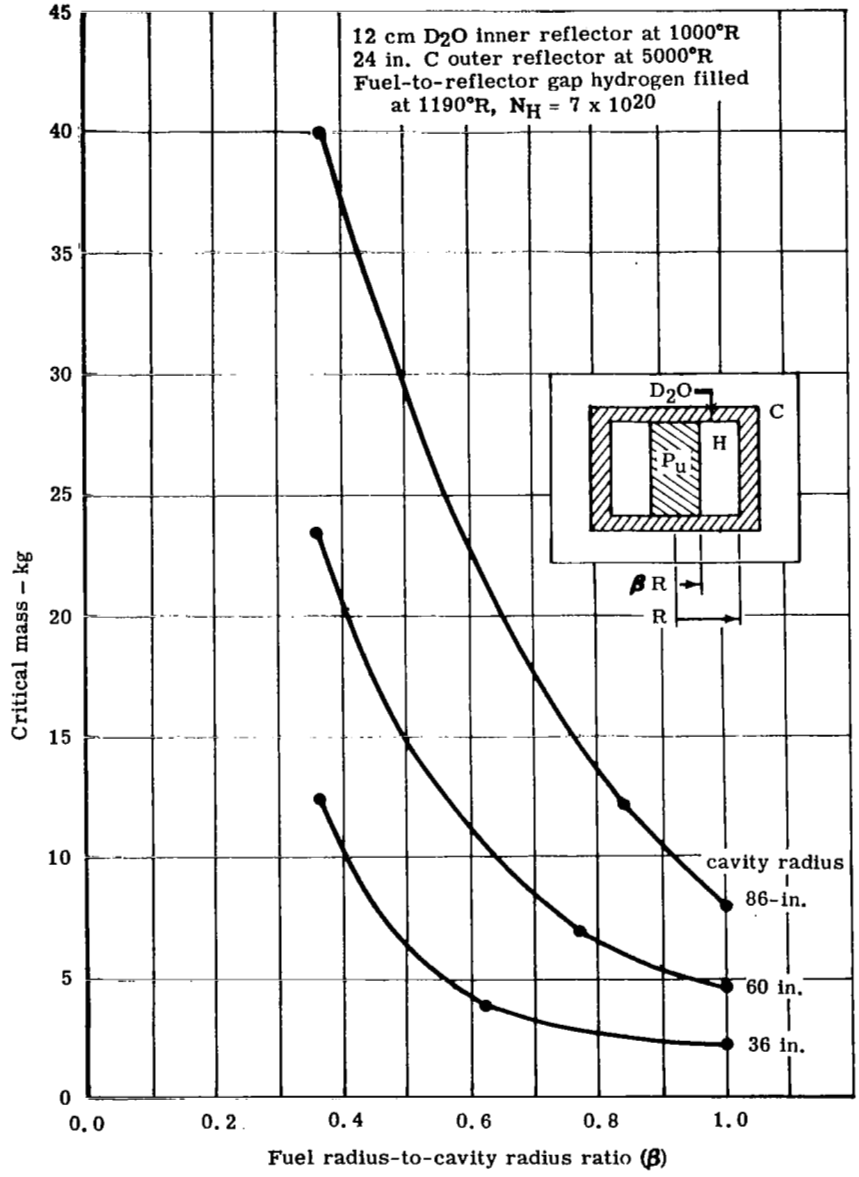

Figure 3-18. Effect of fuel radius-to-cavity radius ratio on critical mass – L:D ratio = 2:3.

The behavior of most of the values of $\frac{\Delta k_{eff}}{\Delta \beta}$ is as would be expected since a much greater geometric effect on reactivity results as the fuel is confined to a smaller proportion of the cavity.

The magnitude of $\frac{\Delta k_{eff}}{\Delta \beta}$ was between 0.4109 and 2.4. This is a relatively small range, considering the extreme ranges of other variables, such as critical mass which varied by a factor of 25, cavity volume which varied by a factor of 40, and changes in reflector materials from BeO to carbon.

Table 3-IX.
Data for paragraph G.

Cavity radius (in.)	L/D ratio	Critical mass (kg)	β	$\frac{\Delta k_{eff}}{\Delta \beta}$
Paragraph E—BeO moderator				
36	1/3	1.8	0.465	0.87
36	1/3	6.03	0.32	—
60	1/3	4.41	0.52	1.4
60	1/3	14.7	0.332	—
86	1/3	7.53	0.61	0.62
86	1/3	25.1	0.35	1.6
36	2/3	2.61	0.53	0.65
36	2/3	8.69	0.258	2.4
60	2/3	5.82	0.59	0.77
60	2/3	19.4	0.271	1.5
86	2/3	11.0	0.745	0.51
86	2/3	36.7	0.303	0.75
36	1	3.35	0.48	0.94
36	1	11.2	0.23	—
60	1	6.7	0.71	1.0
60	1	22.0	0.264	0.69
86	1	13.6	0.765	0.63
86	1	45.4	0.30	1.3
Paragraph F—carbon moderator				
36	2/3	3.72	0.64	0.4109
36	2/3	12.4	0.365	0.88
60	2/3	6.99	0.77	1.040
60	2/3	23.30	0.357	2.08
86	2/3	12.15	0.842	1.237
86	2/3	40.50	0.36	1.246

PARAGRAPH J

"Perform an analysis that shall justify the selection of the order of S_n for the calculation" using the following parameters:

- Geometry—two-dimensional using DDK code
- Material and temperature—D_2O, 1000°R; BeO, 3000°R (same as Paragraph E)
- Reflector thickness—12-cm D_2O, 24-in. BeO (same as Paragraph E)
- Cavity radius—86 in.
- Cavity L/D—2/3
- Fuel material—Pu-239

Five specific calculations of critical mass were called for by this requirement:

1. An initial calculation order S_4 using a set of 13-group cross sections having only one thermal group with a "full cavity, "—i.e., $\beta = 1.0$

2. A calculation order S_4 using the same 13-group cross sections but with β reduced by the addition of hydrogen to a point where the critical mass increased to 1.5 times that of calculation 1

3. A calculation order S_8 using the 13-group cross sections with all other conditions the same as calculation 2

4. A calculation order S_4 using the same set of 15-group cross sections used in the one-dimensional calculations containing up-scattering and multiple thermal groups with all other conditions the same as in calculation 2

5. A calculation order S_4 with a set of 3-group cross sections with all other conditions the same as in calculation 2

The order of S_4 used in calculations for Paragraph A through G was selected initially by comparing a preliminary one-dimensional calculation using S_4 and S_6. As in Paragraph E (page 3-25), S_n value was changed from 4 to 2 in one calculation with a change of less than 0.5% in k_{eff}. The final results are shown in Table 3-X and Figure 3-19. The initial full cavity configuration, $\beta = 1.0$, was run with 13-group cross sections. The number density for $k_{eff} = 1.0$ was obtained from plotting the reactivity versus number density from the specific runs. This number density value was then used as the basis for the critical mass at $\beta = 1.0$. Since the difference between orders S_2 and S_4 should be greater than between orders S_4 and S_6, the accuracy of S_4 was considered adequate. Thus, the scope of the calculations for Paragraph J was substantially more than to verify the selection of S_n. For example, this also provided a basis for comparing results from 3-, 13-, and 15-group cross sections in two-dimensional

Table 3-X

Results of criticality calculations for Paragraph J.

Run No.	Cavity radius (in.)	$N_{PU} \times 10^{-24}$ (atoms/cm^3)	Energy group	Critical mass (kg)	L/D ratio	S_n	β	k_{eff}
252-1	86	3.95×10^{-7}	13	6.84	2/3	4	1.0	1.0
268-1	86	1.28×10^{-6}	13	10.26	2/3	4	0.68	1.002079
268-2	86	1.28×10^{-6}	13	10.26	2/3	8	0.68	1.002125
268-3	86	1.28×10^{-6}	15	10.26	2/3	4	0.68	0.9946824
268-4	86	1.28×10^{-6}	3	10.26	2/3	4	0.68	0.9974802

D_2O thickness—12 cm
Reflector thickness—24 in.
D_2O temperature—1000°R
Reflector temperature—3000°R

Epsilon—0.001
Number density, hydrogen—7.0×10^{-4}
Number density, D_2O—2.4705×10^{-2}
Number density, BeO—1.372×10^{-1}

Verification of S_n Selection

Two-Dimensional Calculation—DDK Code

Two-dimensional calculations were made to verify the previously determined value of S_n using the following parameters—86-in. cavity, L/D = 2/3, and 13-group cross sections. The only variables introduced were the S_4 and S_8 constants. Material density and β were maintained constant.

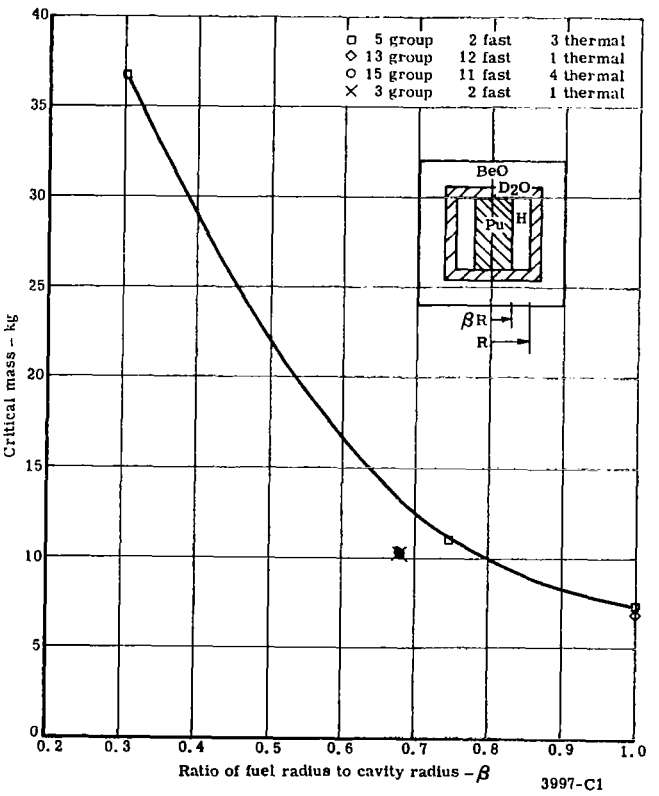

Figure 3-19. Comparison of 15-, 13-, and 3-group two-dimensional criticality calculations with original 5-group set of Paragraph E (86-in. cylindrical cavity radius—L/D = 2/3).

configurations. Since 3- and 13-group cross sections contain no up-scattering terms (i.e., only one thermal group), substantial calculational machine time can be saved if acceptable accuracy can also be obtained.

A slight reduction in critical mass 7.34 to 6.84 kg, was obtained from the 5-group results of Paragraph E. This reduction is a result of the cross section group structure revision as described in Section V.

The next series of runs was made at 1.5 times the critical mass of the $\beta = 1.0$ condition. These calculations used 3-, 13-, and 15-group cross sections, respectively, with no change in critical mass between them but with a slight reduction in critical mass from the previous Paragraph E 5-group runs, as shown in Figure 3-19. The tabulation of these runs and the S_n evaluation is given in Table 3-X. Once criticality was obtained within an acceptable range of $k_{eff} = 1.0$, the present β and number density were considered accurate and no further changes were required. It was found that 15-, 13-, and 3-group cross sections gave consistent results in the two-dimensional DDK calculations as they had in one-dimensional DTK calculations used in checking the cross sections. An advantage was found in using 3-group versus 15-group calculations by the reduction to one-fourth the machine time.

Correlation of Results—3-, 13-, and 15-Group Calculations

To obtain an accurate number density value more rapidly on the initial run, the 3-group cross sections were used in the first run of $\beta = 1.0$. This provided the number density guess for the first of the five required reactivity calculations for this analysis. It also gave a basis for comparison of the 3- and 13-group cross section structures at $\beta = 1.0$. An additional calculation was made at $\beta = 1.0$ with the 15-group cross sections. This resulted in a comparison at $\beta = 1.0$ of the 3-, 13-, and 15-group structures as shown in Table 3-XI. As planned, the 13-group calculation provided the reference point from which the value of critical mass could be increased by a factor of 1.5 through a reduction in β. As shown in Table 3-XI, no significant change in critical mass, 6.84 to 7.03 kg, is observed between the 15-, 13-, and 3-group cross sections.

In determining the β value for the 1.5-times mass configuration, it was found that all calculations using various cross section groups at the same β of 0.68 resulted in similar reactivities. To determine the effect of β, a new value ($\beta = 0.69$) was tried with 15-group cross sections. The results given in Table 3-XII show only a 0.0072 change in reactivity and indicate that β is 0.68 to 0.69 and within the accuracy of the calculational procedures.

Table 3-XI.

Comparison of 15-, 13-, and 3-group calculations at $\beta = 1.0$.

Run No.	Cavity radius (in.)	Energy group	$N_{Pu} \times 10^{-24}$ (atom/cm^3)	k_{eff}	Critical mass (kg)
252-1	86	3	4.23×10^{-7}	1.015175	7.32
252-1	86	3	4.10×10^{-7}	1.004372	7.1
252-1	86	3	4.06×10^{-7}	1.0 (plot)	7.03
252-1	86	13	4.06×10^{-7}	1.01088	7.03
252-1	86	13	3.95×10^{-7}	1.0 (plot)	6.84
252-1	86	15	4.06×10^{-7}	1.009444	7.03
252-1	86	15	3.96×10^{-7}	1.0 (plot)	6.86

Table 3-XII.

Effect of β variation at constant critical mass.

Run No.	Cavity radius (in.)	Energy group	$N_{Pu} \times 10^{-24}$ (atoms/cm^3)		k_{eff}	Critical mass (kg)
268-3	86	15	1.28×10^{-6}	0.68	0.9946824	10.26
268-3	86	15	1.245×10^{-6}	0.69	1.001895	10.26

The results of these calculations gave the same k_{eff} and show no significant change in criticality.

Cavity size (in.)	L/D	Energy group	S_n	β	$N_{Pu} \times 10^{-24}$	$N_H \times 10^{-24}$	$N_{D_2O} \times 10^{-24}$	$N_{BeO} \times 10^{-24}$	k_{eff}
86	2/3	13	4	0.68	1.28×10^{-6}	0.0007	0.024705	0.1372	1.002079
86	2/3	13	8	0.68	1.28×10^{-6}	0.0007	0.024705	0.1372	1.002125

Close agreement is also observed in the neutron balance as shown in Table 3-XIII. This close agreement in criticality and neutron balance for S_4 and S_8 indicates that sufficient accuracy is attained with the S_4 in the two-dimensional calculations.

Since the cross sections of various group structures were developed from the multigroup, it can be concluded that reduction of the twelve fast groups down to two fast groups with an S_4 calculation provides the desired accuracy.

Table 3-XIII.

Neutron balance for 13-group S_4 and S_8.

(NASA, J, L/D = 2/3, 86, W/H, 1.5 M_c, S/N 4 computer data output)

13-GROUP S_4 (268-1)

	1.FXD SOURCE 9.RT LEAK	2.FISS IN 10.HOR LEAK	3.IN-SCATT 11.TOP LEAK	4.SELF-SCATT 12.VERT LEAK	5.OUT-SCATT	6.ABSORPTIONS	7.NET LEAKAGE	8.NET BALANC.
	1	2	3	4	5	6	7	8
1	0.000000+00	2.040000-01	-3.725290-09	4.101895-02	2.142917-01	-1.029442-02	2.444092-06	9.999986-01
2	0.000000+00	3.440000-01	1.543007-01	3.032607-01	5.085864-01	-1.031431-02	2.831303-05	9.999992-01
3	0.000000+00	1.680000-01	3.552298-01	4.923171-01	4.937476-01	7.572557-05	6.245036-06	9.999995-01
4	0.000000+00	1.800000-01	5.960597-01	8.549615-01	7.389710-01	8.361940-05	4.695572-06	9.999995-01
5	0.000000+00	9.000000-02	8.466656-01	2.109182+00	9.364714-01	8.006014-05	1.134399-05	9.999992-01
6	0.000000+00	1.399999-02	9.868451-01	3.205156+00	1.000735+00	8.714487-05	2.228949-05	9.999995-01
7	0.000000+00	0.000000+00	9.907068-01	3.264762+00	9.905617-01	1.292811-04	1.507896-05	9.999992-01
8	0.000000+00	0.000000+00	9.977570-01	3.404762+00	9.975355-01	1.970176-04	2.418107-05	9.999997-01
9	0.000000+00	0.000000+00	9.992313-01	3.564699+00	9.985644-01	6.529149-04	1.334242-05	9.999993-01
10	0.000000+00	0.000000+00	8.833988-01	1.834911+00	8.820528-01	1.340262-03	5.363154-06	9.999995-01
11	0.000000+00	0.000000+00	9.980644-01	8.235219+00	9.936248-01	4.379043-03	5.894520-05	9.999983-01
12	0.000000+00	0.000000+00	1.013386+00	3.694467+00	9.805750-01	3.277105-02	3.931426-05	9.999990-01
13	0.000000+00	0.000000+00	9.805756-01	5.493623+02	2.288818-05	7.877210-01	1.928067-01	9.999745-01
14	0.000000+00	1.000000+00	9.735719+00	5.803670+02	9.735741+00	8.069084-01	1.930382-01	9.999970-01
	9	10	11	12				
1	1.415287-06	1.415287-06	1.030844-06	1.028804-06				
2	1.668271-05	1.668271-05	1.143468-05	1.143031-05				
3	2.733176-06	2.733176-06	2.513799-06	2.511859-06				
4	2.715269-06	2.715269-06	1.983163-06	1.980303-06				
5	6.733066-06	6.733068-06	4.613859-06	4.610924-06				
6	1.323882-05	1.323882-05	8.952784-06	8.950671-06				
7	8.904991-06	8.904991-06	6.173944-06	6.173975-06				
8	1.442167-05	1.442167-05	9.761564-06	9.759398-06				
9	7.941306-06	7.941306-06	5.403152-06	5.401115-06				
10	3.122304-06	3.122304-06	2.231790-06	2.230850-06				
11	3.544317-05	3.544317-05	2.350572-05	2.350202-05				
12	2.410036-05	2.410036-05	1.521564-05	1.521390-05				
13	1.154565-01	1.154565-01	7.730985-02	7.730979-02				
14	1.156357-01	1.156357-01	7.740267-02	7.740258-02				

13-GROUP S_8 (268-2)

	1.FXD SOURCE 9.RT LEAK	2.FISS IN 10.HOR LEAK	3.IN-SCATT 11.TOP LEAK	4.SELF-SCATT 12.VERT LEAK	5.OUT-SCATT	6.ABSORPTIONS	7.NET LEAKAGE	8.NET BALANCE
	1	2	3	4	5	6	7	8
1	0.000000+00	2.040000-01	0.000000+00	4.149738-02	2.143994-01	-1.040274-02	3.082437-06	9.999986-01
2	0.000000+00	3.440000-01	1.544699-01	3.049249-01	5.088111-01	-1.036980-02	2.822004-05	9.999992-01
3	0.000000+00	1.680000-01	3.262831-01	4.979925-01	4.942003-01	7.544872-05	7.053443-06	9.999994-01
4	0.000000+00	1.800000-01	5.595013-01	8.574295-01	7.394237-01	8.314778-05	-5.810732-06	9.999996-01
5	0.000000+00	9.000000-02	8.466822-01	2.114404+00	9.369111-01	7.924638-05	-8.809171-06	9.999993-01
6	0.000000+00	1.400000-02	9.872655-01	3.210252+00	1.001082+00	8.615174-05	3.624624-05	9.999996-01
7	0.000000+00	0.000000+00	9.909529-01	3.268141+00	9.908505-01	1.280116-04	1.375194-05	9.999994-01
8	0.000000+00	0.000000+00	9.979502-01	3.406099+00	9.977089-01	1.959235-04	4.457105-05	9.999991-01
9	0.000000+00	0.000000+00	9.953700-01	3.565852+00	9.987133-01	6.495776-04	6.133853-06	9.999990-01
10	0.000000+00	0.000000+00	8.835245-01	1.835841+00	8.821976-01	1.340351-03	-1.392170-05	9.999995-01
11	0.000000+00	0.000000+00	9.982350-01	8.236774+00	9.937829-01	4.370575-03	7.826561-05	9.999967-01
12	0.000000+00	0.000000+00	1.013569+00	3.695128+00	9.807663-01	3.272350-02	7.831567-05	9.999989-01
13	0.000000+00	0.000000+00	9.807667-01	5.485592+02	0.000000+00	7.875738-01	1.931270-01	9.999328-01
14	0.000000+00	1.000000+00	9.738851+00	5.795895+02	9.738848+00	8.065331-01	1.933941-01	9.999930-01
	9	10	11	12				
1	2.352562-06	2.352562-06	7.360662-07	7.294748-07				
2	1.793625-05	1.793625-05	1.029628-05	1.028379-05				
3	4.582382-06	4.582382-06	2.479255-06	2.471060-06				
4	-3.505409-06	-3.505409-06	-2.254719-06	-2.305323-06				
5	-5.568510-06	-5.568510-06	-3.229503-06	-3.240261-06				
6	2.173624-05	2.173624-05	1.452151-05	1.451000-05				
7	7.666289-06	7.666289-06	6.093810-06	6.085656-06				
8	2.639072-05	2.639072-05	1.818530-05	1.818033-05				
9	3.152504-06	3.152504-06	2.988575-06	2.981348-06				
10	-8.777081-06	-8.777081-06	-5.140886-06	-5.144619-06				
11	4.664044-05	4.664044-05	3.164024-05	3.162516-05				
12	4.814261-05	4.814261-05	3.017909-05	3.017306-05				
13	1.157421-01	1.157421-01	7.738515-02	7.738490-02				
14	1.159029-01	1.159029-01	7.749161-02	7.749124-02				

One-Dimensional Calculation—DTK Code

A one-dimensional evaluation of S_4 and S_8 was made using a Paragraph C-type system (48 in. Pu, 12 cm D_2O—24 in. BeO). These calculations, using 15-group cross sections (11 fast and 4 thermal) also resulted in no significant effect between S_4 and S_8 as shown in the following tabulation and in Table 3-XIV.

Cavity size	Energy group	S_n	$N_{Pu} \times 10^{-24}$	$N_{D_2O} \times 10^{-24}$	$N_{BeO} \times 10^{-24}$	k_{eff}
48 in.-12 cm-24 in.	15	4	8.5×10^{-7}	0.024705	0.1372	1.019082
48 in.-12 cm-24 in.	15	8	8.5×10^{-7}	0.024705	0.1372	1.020153

A further study was made in which an absorber region was used. This comparison was a Paragraph B-type using a $\Sigma_a t$ value of 0.1. The following data also indicate no significant variation between S_4 and S_8.

Cavity size (in.)	Energy group	S_n	$N_{Pu} \times 10^{-24}$	$\Sigma_a t$	$N_{BeO} \times 10^{-24}$	k_{eff}
48-24 (3000°R)	15	4	1.5×10^{-5}	0.1	0.1372	0.9916683
48-24 (3000°R)	15	8	1.5×10^{-5}	0.1	0.1372	1.001271

These data indicate that with the higher fuel concentration caused by the added absorber, the effect of increasing S_n value on criticality is apparent; however, it is of no significant magnitude.

Summary

No significant change in β or fuel concentration was required to maintain the same criticality for the one- or two-dimensional 15-, 13-, and 3-group calculations. It can be concluded therefore, that selection of an S_n of S_4 was adequate for these calculations.

Table 3-XIV.

Neutron balance for 15-group S_4 and S_8.

(NASA, C, 12-cm D_2O, 24-in. BeO, 3000°R computer data output)

15-GROUP S_4

	1.FXD SOURCE 1	2.FISSIONS IN 2	3.IN SCATT. 3	4.SELF SCATT. 4	5.OUT SC ATT. 5	6.ABS.NEUTS 6	7.NET LEAK 7	8.NET BALANCE 8
1	0.000000+00	2.040000-01	1.862645-09	5.262554-02	2.155111-01	-1.152013-02	8.908402-06	9.999995-01
2	0.000000+00	3.440000-01	1.577489-01	3.584541-01	5.133380-01	-1.164343-02	5.405994-05	9.999995-01
3	0.000000+00	1.679999-01	3.382915-01	5.743866-01	5.062314-01	4.812771-05	1.186837-05	9.999997-01
4	0.000000+00	1.800000-01	5.762633-01	9.964771-01	7.561930-01	5.605531-05	1.408186-05	9.999997-01
5	0.000000+00	9.000000-02	8.659786-01	2.454090+00	9.558874-01	6.423332-05	2.673197-05	9.999997-01
6	0.000000+00	1.400000-02	1.008878+00	3.817707+00	1.022759+00	8.729299-05	3.120604-05	9.999996-01
7	0.000000+00	0.000000+00	1.022759+00	3.927602+00	1.022591+00	1.357687-04	3.228704-05	9.999996-01
8	0.000000+00	0.000000+00	1.022591+00	4.087533+00	1.022399+00	1.594828-04	3.160061-05	9.999996-01
9	0.000000+00	0.000000+00	1.022399+00	4.302027+00	1.021781+00	5.822478-04	3.537541-05	9.999996-01
10	0.000000+00	0.000000+00	9.358804-01	3.468648+00	9.356404-01	1.999310-04	3.983405-05	9.999997-01
11	0.000000+00	0.000000+00	1.021542+00	9.497416+00	1.017945+00	3.498674-03	9.736937-05	9.999993-01
12	0.000000+00	0.000000+00	2.111072+01	1.796273+02	2.092539+01	8.657466-02	9.875066-02	9.999996-01
13	0.000000+00	0.000000+00	5.858880+01	1.894099+02	5.817605+01	3.003971-01	1.123512-01	9.999998-01
14	0.000000+00	0.000000+00	5.109942+01	7.333193+01	5.079986+01	2.583300-01	4.122821-02	9.999998-01
15	0.000000+00	0.000000+00	1.313254+01	8.983887+00	1.301961+01	1.082675-01	4.657136-03	9.999999-01
16	0.000000+00	1.000000+00	1.519038+02	4.848900+02	1.519111+02	7.352375-01	2.573705-01	9.999998-01

15-GROUP S_8

	1.FXD SOURCE 1	2.FISSIONS IN 2	3.IN SCATT. 3	4.SELF SCATT. 4	5.OUT SC ATT. 5	6.ABS.NEUTS 6	7.NET LEAK 7	8.NET BALANCE 8
1	0.000000+00	2.040000-01	-1.862645-09	5.290788-02	2.156187-01	-1.162839-02	9.529319-06	9.999994-01
2	0.000000+00	3.440000-01	1.578706-01	3.579117-01	5.134283-01	-1.161014-02	5.214969-05	9.999995-01
3	0.000000+00	1.679999-01	3.382746-01	5.741049-01	5.062152-01	4.760635-05	1.158491-05	9.999996-01
4	0.000000+00	1.800000-01	5.761818-01	9.954606-01	7.561129-01	5.562067-05	1.303526-05	9.999996-01
5	0.000000+00	9.000000-02	8.660204-01	2.453170+00	9.559314-01	6.412598-05	2.455285-05	9.999996-01
6	0.000000+00	1.400000-02	1.008959+00	3.819246+00	1.022839+00	8.753924-05	3.145472-05	9.999996-01
7	0.000000+00	0.000000+00	1.022839+00	3.929972+00	1.022672+00	1.361906-04	3.086443-05	9.999995-01
8	0.000000+00	0.000000+00	1.022672+00	4.089862+00	1.022478+00	1.599733-04	3.384889-05	9.999996-01
9	0.000000+00	0.000000+00	1.022478+00	4.304359+00	1.021861+00	5.836831-04	3.305714-05	9.999996-01
10	0.000000+00	0.000000+00	9.360032-01	2.273696+00	9.357868-01	1.956696-04	2.049641-05	9.999997-01
11	0.000000+00	0.000000+00	1.021644+00	9.574408+00	1.018078+00	3.471277-03	9.452052-05	9.999992-01
12	0.000000+00	0.000000+00	2.111800+01	1.796994+02	2.093368+01	8.586029-02	9.845275-02	9.999994-01
13	0.000000+00	0.000000+00	5.860853+01	1.894764+02	5.819647+01	3.004836-01	1.115616-01	9.999998-01
14	0.000000+00	0.000000+00	5.111283+01	7.334871+01	5.081373+01	2.590343-01	4.006440-02	9.999998-01
15	0.000000+00	0.000000+00	1.313499+01	8.981735+00	1.301973+01	1.087034-01	6.552562-03	9.999998-01
16	0.000000+00	1.000000+00	1.519473+02	4.839313+02	1.519546+02	7.356448-01	2.569864-01	9.999997-01

IV. CODES ANALYSIS

This section describes the computer codes used in the calculations discussed in this report. The code routines discussed are those which contain terms of the transport equation or those in which the convergence criterion is established and tested.

The one-dimensional calculations were done with the DTK code. This one-dimensional transport theory code has evolved from the SNG and DSN codes and is the most recent version of these techniques.

The two-dimensional calculations were done with the use of the DDK code, a two-dimensional transport theory code. DDK is an updated version of TDC.

Both codes are capable of solving inhomogeneous problems with a fixed source, searching for the reactivity, performing a time absorption study, searching for fuel concentration, and determining a zone thickness or a critical radius.

DTK—ONE-DIMENSIONAL TRANSPORT THEORY NEUTRONICS CODE

Transport Equations and Difference Equation used in DTK

The transport equation is linear in the neutron flux and of first order in the variables t, r, and Ω.

If N is the number of neutrons flowing in the direction Ω at position r, per unit time (t) and unit area, and if v is the neutron velocity, the transport equation is given by:

$$S = (1/v)\,(\partial N/\partial t) + \Omega \cdot \text{grad } N + \omega N \qquad (4\text{-}1)$$

where $N = N(t, r, \Omega)$

and where S is the source term and ω is the collision probability per unit length.

Equation (4-1) states that the total derivative of N in the direction Ω equals the rate(s) at which neutrons are introduced (in that direction) less the rate of removal (ωN) by collision.

The DTK code uses multienergy groups. It therefore has an equation for each neutron velocity group and the subscript g is assigned to the terms v, ω, N, and S. The code couples the equation through the source term, S, which is defined as a linear combination of average fluxes, $\bar{N}_g$:

$$S_g = \sigma_{gg} \bar{N}_g + \chi_g F + H_g \qquad (4\text{-}2)$$

where

$\sigma_{gg} \bar{N}_g$ = self-scattering
χ = fission neutron spectrum
H_g = scattering in from other groups

Since the DTK code considers only steady-state neutron transport, then:

$$\partial N/\partial t = 0$$

The transport equation for a spherical geometry takes the form:

$$S = \mu(\partial N/\partial r) + (1/r)(1-\mu^2)(\partial N/\partial \mu) + \omega N \qquad (4\text{-}3)$$

where

r is the radial variable
μ is the direction cosine with respect to r
$N = N(r, \mu)$

The terms r and μ may be represented by sets (r_i) and (μ_m), which form a set of cells $(A_{i,m})$.

It is thus possible to generate a set $(\bar{\mu}_m)$ of discrete directions pertaining to the interval midpoints. This set of discrete directions is the basis of the S_n approximation used in the solution of the transport equation with the DTK code.

Then, proceeding in general terms, the intervals in r may be set so that (r_i) contains the actual boundaries in the problem. At r_i, the flux is denoted as N_i for a particular $\bar{\mu}$. Similarly, N_m is the flux at μ_m for a specific $\bar{r}$. A difference equation can now be formed by averaging the transport equation over the cell, $A_{i,m}$. It is assumed, however, that N is linear over the entire area $A_{i,m}$ in all variables, so that:

$$N_m = 2\bar{N}_{i,m} - N_{m-1} \tag{4-4}$$

and

$$\bar{N}_{i,m} = (N_i + N_{i-1})/2 \tag{4-5}$$

Equations (4-4) and (4-5) are known as the diamond difference condition.

By definition:

$$\bar{r}_i = (r_i + r_{i-1})/2 \tag{4-6}$$

$$\Delta_i = r_i - r_{i-1} \tag{4-7}$$

$$\Delta_m = \mu_m - \mu_{m-1} \tag{4-8}$$

$$s_i = \Delta_i / r_i' \tag{4-9}$$

$$r_i' = 2(r_i^3 - r_{i-1}^3)/3(r_i^2 - r_{i-1}^2) \tag{4-10}$$

The transport equation may now be expressed as a difference equation:

$$S_i = \left[\bar{\mu}_m (N_i - N_{i-1})/r_i - r_{i-1}\right] + \left[(1-\mu^2)(N_m - N_{m-1})/r_i'\right] + \sigma_i \tilde{N}_{i,m} \tag{4-11}$$

where the radial intervals are denoted by the subscript i and the direction cosine (μ) intervals are denoted by the subscript m. Equation (4-11) may now be rewritten:

$$S_i = \left[\bar{\mu}_m (N_i - N_{i-1})/\Delta_i\right] + \left[(1-\mu^2)(N_i + N_{i-1} - N_{m-1})/r_i'\right] - \left[(1-\mu^2) N_{m-1}/r_i'\right] + \sigma_i (N_i + N_{i-1})/2 \tag{4-12}$$

Now, setting $\gamma_m = 1-\mu^2$ and multiplying through by Δ_i,

$$\Delta_i S_i = \bar{\mu}_m (N_i - N_{i-1}) + \gamma_m s_i (N_i + N_{i-1} - N_{m-1}) - \gamma_m s_i N_{m-1} + \sigma_i \Delta_i (N_i + N_{i-1})/2 \tag{4-13}$$

Then collecting terms:*

$$\Delta_i S_i + 2\gamma_m s_i N_{m-1} = \left[\bar{\mu}_m + \gamma_m s_i + (\sigma_i \Delta_i/2)\right] N_i + \left[-\bar{\mu}_m + \gamma_m s_i + (\sigma_i \Delta_i/2)\right] N_{i-1} \quad (4\text{-}14)$$

The difference equation of Equation (4-14) is the equation solved by the DTK code in the reactivity search problems. The DTK solution is obtained by iteration.

Function and Location of Equations in the Code

The following computer subroutines are written in computer language to facilitate interpretation of the results. Where applicable, the appropriate physical notation is also shown for clarity.

Subroutine 804: Computing S_n Constants

$$DC_m W_m = WD_m \quad (4\text{-}15)$$

where

DC_m = direction cosines

W_m = weights

Subroutine 812: Geometric Functions

$$AA_i DC_m = DA_{m,i} \quad (4\text{-}16)$$

where

AA_i represents an area element

If $W_m = 0$, then

$$DB_{m,i} = (DA_{m,i} - DA_{m,i-1})/2 \quad (4\text{-}17)$$

If $W_m \neq 0$, then

$$DB_{m,i} = (W_{m-1}/W_m)\, DB_{m-1,i} + DA_{m,i} - DA_{m,i+1} \quad (4\text{-}18)$$

*C. Lee, Discrete Approximations to Transport Theory, Los Alamos Scientific Laboratories Report No. LA 2595 (1962).

The operation of Equations (4-17) and (4-18) is done S_n times for each space interval, producing sets:

$$DA_{m,i},\ DA_{m,i+1},\ DA_{m,i+2},\ \cdots\ DA_{m,\ i+n}$$
$$DA_{m+1,i},\ DA_{m+1,\ i+1},\ DA_{m+1,\ i+2},\ \cdots\ DA_{m+1,\ i+n} \qquad (4\text{-}19)$$

and

$$DB_{m,i},\ DB_{m,i+1},\ DB_{m,i+2},\ \cdots\ DB_{m,i+n}$$
$$DB_{m+1,i},\ DB_{m+1,\ i+1},\ DB_{m+1,i+2},\ \cdots\ DB_{m+1,\ i+n} \qquad (4\text{-}20)$$

where

$$DA = \mu_m$$
$$DB = \gamma_m s_i$$

Subroutine 821: Calculate the Fission Neutrons

If the theory is regular, then

$$F_i = \nu \sigma_F N_{ig} \qquad (4\text{-}21)$$

where F_i is the neutrons produced from fission events.

Subroutine 822: Calculate Fission Neutron Sums

$$\chi_g F_i = \text{fission neutrons} \qquad (4\text{-}22)$$

where χ_g = the spectrum of the fission neutrons.

The $\chi_g F_i$ portion of the source equation is thus derived.

Subroutine 824: Calculate the Source Term

Since $\chi_g F_i$ was obtained in subroutine 822, it is possible through subroutine 824 to calculate the scattering in from other groups, H_g, and (if applicable) scattering in from an independent source, Q_g, to obtain the total scattering in:

$$ST_i = \chi_g F_i + Q_g + \Sigma_{g\pm4} N_i \sigma_{g \rightarrow g \pm 4} \tag{4-23}$$

Subroutine 832: Preliminary Pass Routine

This subroutine adds the term $\sigma_{gg} N_i$ to the total source term, ST_i, thus defining the new source term, SO_i, as follows:

$$SO_i = \sigma_{gg} N_i + \chi_g F_i + Q_g + \sigma_{g' \rightarrow g} N_i \tag{4-24}$$

This subroutine also determines the transport difference equation to be used in subroutines 843 (inward flow) and 844 (outward flow). A normal calculation would use a connected line segment-based difference equation. However, when the quantity

$$(SO_i/CT\ N_i) - DML \tag{4-25}$$

is negative, the step function-based transport difference equation is to be used.

CT = σ_{tr} at interval i
N_i = total flux at interval i
DML = the tolerance limit (usually 0.5)

Having now determined the source term, the DTK code calculates the inward flow, N_i (in) or the outward flow, N_i (out), depending on the sign of the term $\bar{\mu}_m$.

In subroutines 843 and 844, the DTK code uses the transport difference equation:

$$SO_i + 2\ DB_{i,m}\ NE_m = \left[DA_{i,m} + DB_{i,m} + (CT/2)\right] NI_i + \left[-DA_{i,m} + DB_{i,m} + (CT/2)\right] NI_{i-1} \tag{4-26}$$

where

$DA_{i,m} = \bar{\mu}_m$

$DB_{i,m} = \gamma_m s_i$

$CT = \sigma_{tr}$

NI_i = the angular flux at the cell boundary, i, at the midpoint of the cell surface

SO_i = source

NE_m = the angular flux at the cell midpoint, m

The new flux average is calculated by

$$\overline{NN}_i \text{ (new)} = \overline{NN}_i \text{ (previous pass)} + W_m \bar{N}_i \text{ (new)} \tag{4-27}$$

where

$$\bar{N}_i \text{ (new)} = \left[N_i \text{ (previous pass)} + N_i \text{ (new)} \right] /2 \tag{4-28}$$

Subroutine 843 calculates N_{i-1}; subroutine 844 calculates N_i. The difference equation used in these routines has an alternate equation. If the magnitude of the coefficient of N_i (or N_{i-1}) is equal to or less than unity, since $\gamma_m s_i$ and $\sigma_i \Delta_i$ are inherently positive, oscillations may occur in N_i because the left side of the difference equation is positive. When $\sigma_i \Delta_i$ happens to be large (which often occurs in practice for some velocity groups, in some regions of the reactor), the equation is not satisfactory. The calculated flux, as a function of r_i, may then oscillate between positive and negative values, which is physically unrealistic. To eliminate this difficulty, the DTK code has been equipped with a more rudimentary difference equation, based on step functions rather than connected line segments.

If the alternate, step function-based equation is used in parts of the calculation, the neutron balance will not be complete, but the discrepancy may be used to determine whether finer mesh spacing is called for. Each neutron group is treated separately (usually starting with the highest), with the slowing down of neutrons being the typical process.

The flux for each neutron velocity group is calculated iteratively. Two convergence criteria for the inner iteration are located in subroutine 833.

An error in self-scattering is calculated by:

$$ESC = \Sigma \left[N_i \text{ (new)} - N_i \text{ (previous pass)} \right] \sigma_{gg} \tag{4-29}$$

If

$$\left[\left(\frac{\text{total fission source}}{\text{total number of neutron groups}}\right) \text{epsilon}\right] - \text{ESC} \tag{4-30}$$

is negative, convergence has been achieved. The second test is a test of the "error" in self-scattering by material zone.

After completion of the calculation for a particular group, improved values are obtained for angular flux, N. These values can then be used to calculate the average flux, $\bar{N}_g$, divided by the latest eigenvalue (EV), before proceeding to the next group. A pass through all groups is called an outer iteration or neutron generation. The eigenvalue is estimated after each outer iteration by the equation of subroutine 851:

$$EV = \Sigma_g \text{ (basic } \chi_g) / \Sigma_g \text{ (modified } \chi_g) \tag{4-31}$$

where χ_g is the neutron fission spectrum for a specific group, g.

The DTK code begins the iterative procedure with the assumption that the source term, SO_i, is given in the homogeneous case by a nonzero value of F_i. The next step involves the integration of the S_n difference equations over the radius, r, starting with the highest energy group. After obtaining this first estimate for N_g, the code then proceeds to the next lower energy group, always using the best (most recent) estimate for N_g until all groups have been so treated. At this time, the value of F_i can be recomputed and the iteration procedure performed again (first modifying the eigenvalue if the problem is a homogeneous one) until two final convergence criteria are met.

The entire iteration process is begun from initial guesses for EV and the flux distribution and is terminated when two final convergence criteria are met (subroutine 851).

The first convergence is on lambda (LA):

LA = total fission source/total fission source (previous neutron generation)

The test is:

$$\left[\left|1.0 - LA\right| - \text{epsilon}\right] \tag{4-33}$$

If the result of Equation (4-33) is negative, the first convergence criterion has been met.

For the second criterion, the code defines the average value (AV) as:

$$AV = \Sigma_g \text{ (net leakage}_g + \text{absorptions}_g) \text{ velocity}_g/\text{(total fission source + scattering into group)} \tag{4-34}$$

The average value from the previous outer iteration (neutron generation) is designated AVP. Then

$$AVP/AV = AVR \tag{4-35}$$

The convergence criterion is, therefore:

$$\left[\left|1.0 - AVR\right| - epsilon\right] \tag{4-36}$$

If the result of Equation (4-36) is negative, the problem has converged, where EV is k_{eff}

Table 4-I lists the terms used in the balance table of the DTK code. Figure 4-1 is a flow chart of the DTK code as used herein.

Table 4-I.

DTK balance table terms.

Fission in— $\chi_g F_i$

Inscattering— $SO_i - \chi_g F_i - \sigma_{gg} N_i$

Self-scattering— $\sigma_{gg} N_i$

Outscattering— $\sigma_{tr} N_i - \sigma_{gg} N_i - \sigma_a N_i$

Absorption— $\sigma_a N_i$

Net leakage— $AA_i J_R - AA_i J_L$

Total density— $V_i N_i/VE_g$

Total flux— $V_i N_i$

Right flux— $N_i W_i$

Right flow— $N_i WD_i$

Right current— $N_i WD_i$

Neutron balance— $(\chi_g F_i + SO_i - \chi_g F_i - \sigma_{gg} N_i)/(AA_i J_R - AA_i J_L + \sigma_a N_i + \sigma_{tr} N_i - \sigma_{gg} N_i - \sigma_a N_i)$

= (fission in + inscattering)/(net leakage + absorptions + outscattering)

where V_i = volume at interval i

VE_g = velocity of group g

AA_i = area element

J_R = current density, right

W_i = weights direction

WD_i = direction weight * direction cosines

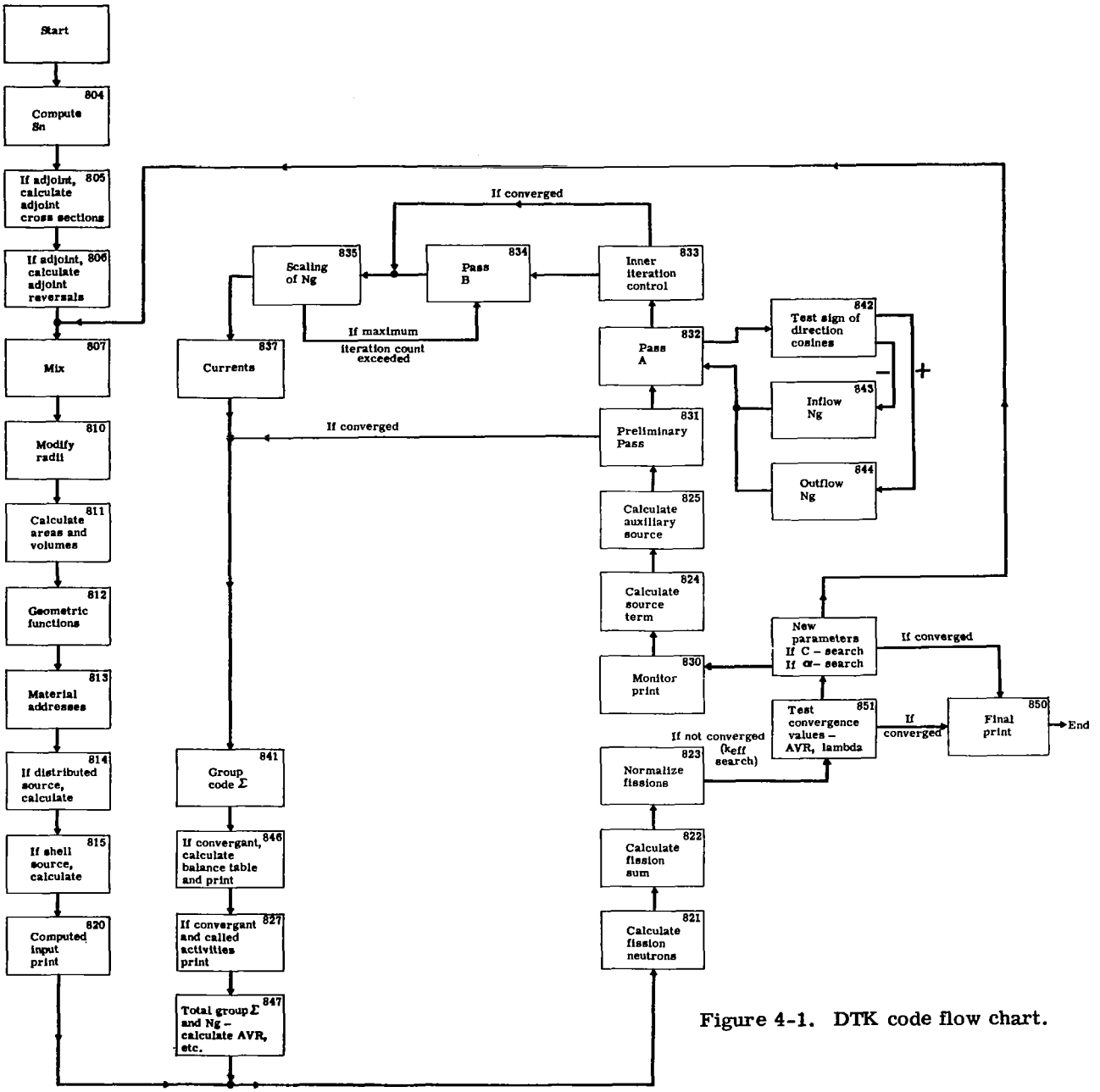

Figure 4-1. DTK code flow chart.

Changes Made to the DTK Code

When running the DTK code with extremely sensitive problems, the second convergence criterion may necessitate running as many as 100 more outer iterations (over and above the iterations needed to converge on lambda), with a change in k_{eff} of approximately 0.5%.

The code has been modified so that when sense switch 5 is depressed, the code is required to converge only on lambda. (See subroutine 851, Figure 4-2.)

DDK—TWO-DIMENSIONAL TRANSPORT THEORY NEUTRONICS CODE

The general comments in the description of the DTK code also apply to the DDK code, with the following exceptions.

The S_n approximation scheme is now two-dimensional in nature; consequently, the calculation of total flux now consists of the following.

If μ is negative and η is negative, the inward flux is:

$$\overleftarrow{N}_i = (G0_i\ N_g^{left} + G2_i N_g^{bottom} + G4_i\ N_g^{angular} + SO_i)/(G0_i + G2_i + G4_i + CT_i) \tag{4-37}$$

If μ is negative and η is positive, the inward flux is:

$$\overleftarrow{N}_i = (G0_i\ N_g^{left} + G2_i N_g^{top} + G4_i N_g^{angular} + SO_i)/(G0_i + G2_i + G4_i + CT_i) \tag{4-38}$$

If μ is positive and η is negative, the outward flux is:

$$\overrightarrow{N}_i = (G0_i\ N_g^{right} + G2_i\ N_g^{bottom} + G4_i\ N_g^{angular} + SO_i)/(G0_i + G2_i + G4_i + CT_i) \tag{4-39}$$

If μ is positive and η is positive, the outward flux is:

$$\overline{N}_i = (G0_i\, N_g^{\text{right}} + G2_i\, N_g^{\text{top}} + G4_i\, N_g^{\text{angular}} + SO_i)/G0_i + G2_i + G4_i + CT_i) \tag{4-40}$$

where

$$G0_i = \Delta z \left| \mu \right| (A0_{i+1} + A0_i) \tag{4-41}$$

$$G2_i = 2 \left| \eta \right| A1_i \tag{4-42}$$

$$G4_i = \Delta z \left| \tilde{\mu} \right| (A0_{i+1} - A0_i) \tag{4-43}$$

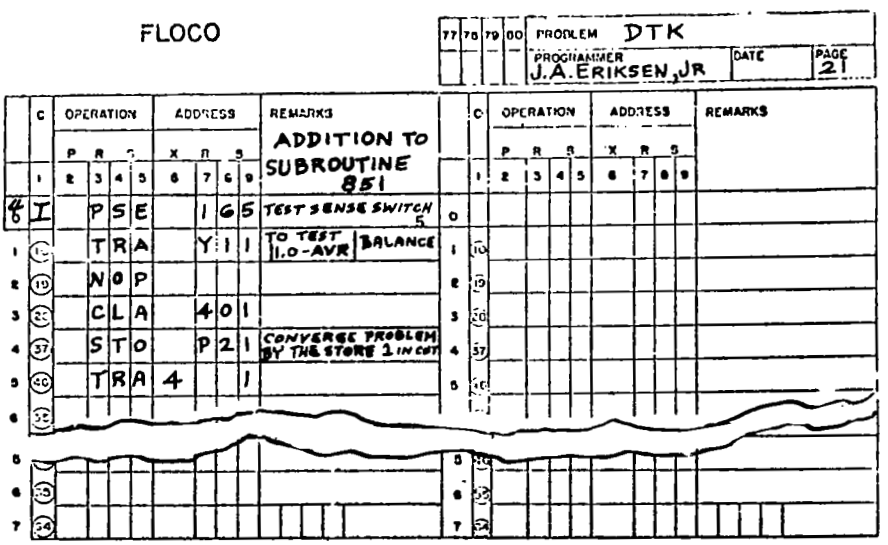

Figure 4-2. Addition to subroutine 851 for DTK.

and

SO_i = total source at interval i
CT_i = σ_{tr} at interval i
$A0_i$ = radial area element at interval i
$A1_i$ = axial area elements at interval i
Δz = axial intervals

The DTK and DDK codes use the same method of iteration to solve the transport difference equations. The codes perform an inner iteration on each neutron velocity group, converging upon an "error" in self-scattering by group and material zone. The final convergence criteria (on lambda and on average velocity ratio) are identical in both codes.

Figure 4-3 is the flow diagram for the DDK code as used herein. The basic difference in this diagram and that of Figure 4-1 is that for the DDK code, the shell source routine has been removed and replaced by a modify-geometry routine rather than a modify-radii routine.

The theory of the codes has been rigorously analyzed by Lee.* The numerical procedures of the codes have been developed by Carlson.†

Changes Made to the DDK Code

The DDK code uses a vast amount of computer time in the first few outer iterations. Considerable computer time is saved by reducing the number of inner iterations during the first outer iterations.

The DDK code was changed so that the maximum number of inner iterations is kept at a relatively low value (e.g., five) until the value of lambda (for an eigenvalue search problem) is within 10¢ of converging. At this point the maximum number of inner iterations is placed at the usual maximum of 50, and the problem continues. (See subroutine 851, Figure 4-4.)

Another function included was an override to print $|1.0 - AVR|$ on-line for reactivity searches. This override works only if sense switches 1 and 5 are depressed. The value of $|1.0-AVR|$ is printed as EQ. (See subroutine 830, Figure 4-4.)

*Lee, op. cit.

†B. Carlson, Numerical Solution of Transient and Steady State Neutron Transport Problems, Los Alamos Scientific Laboratories Report No. LA 2260, 22 January 1959. (Report of work performed under AEC Contract W-7405-ENG. 36.)

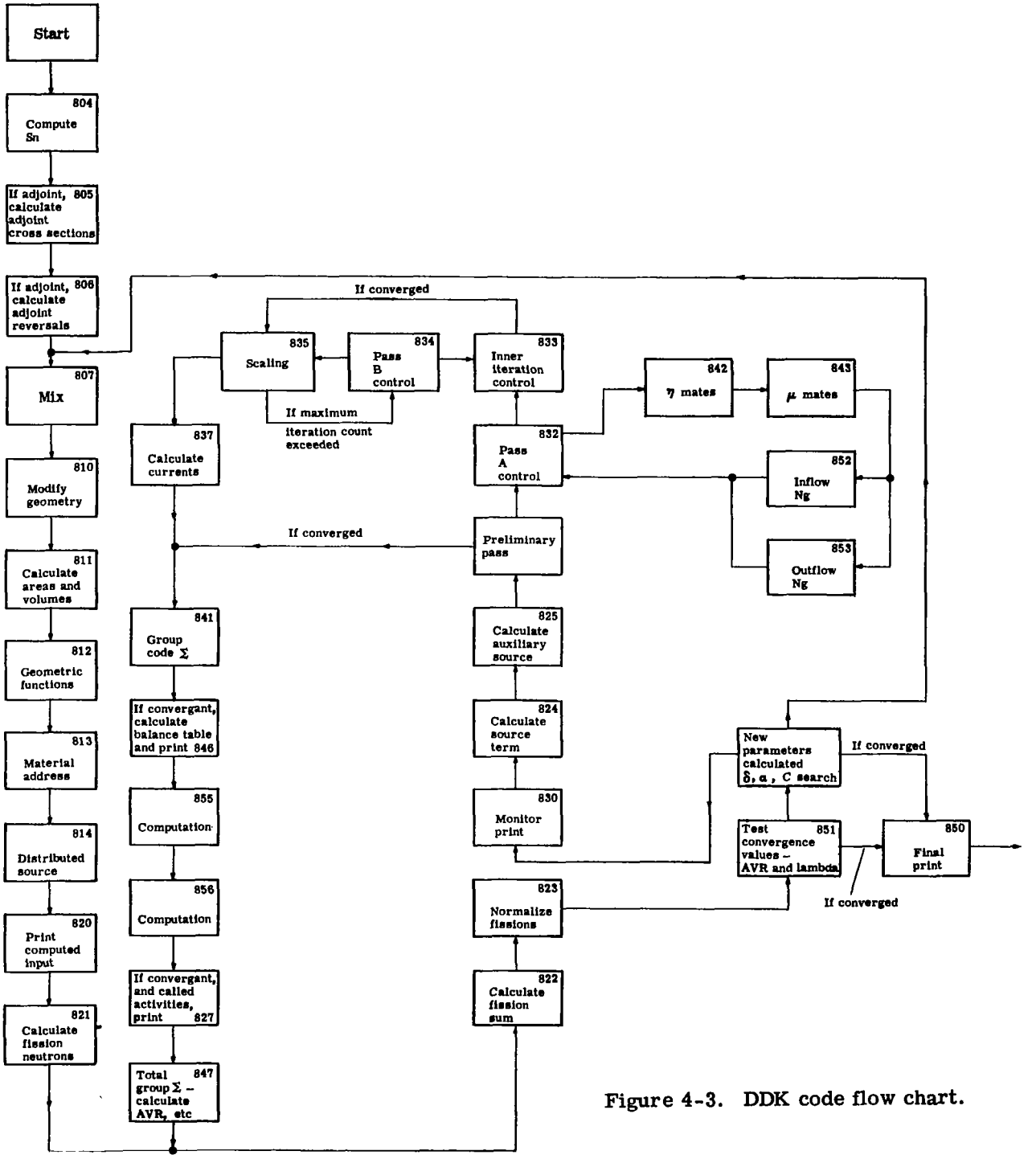

Figure 4-3. DDK code flow chart.

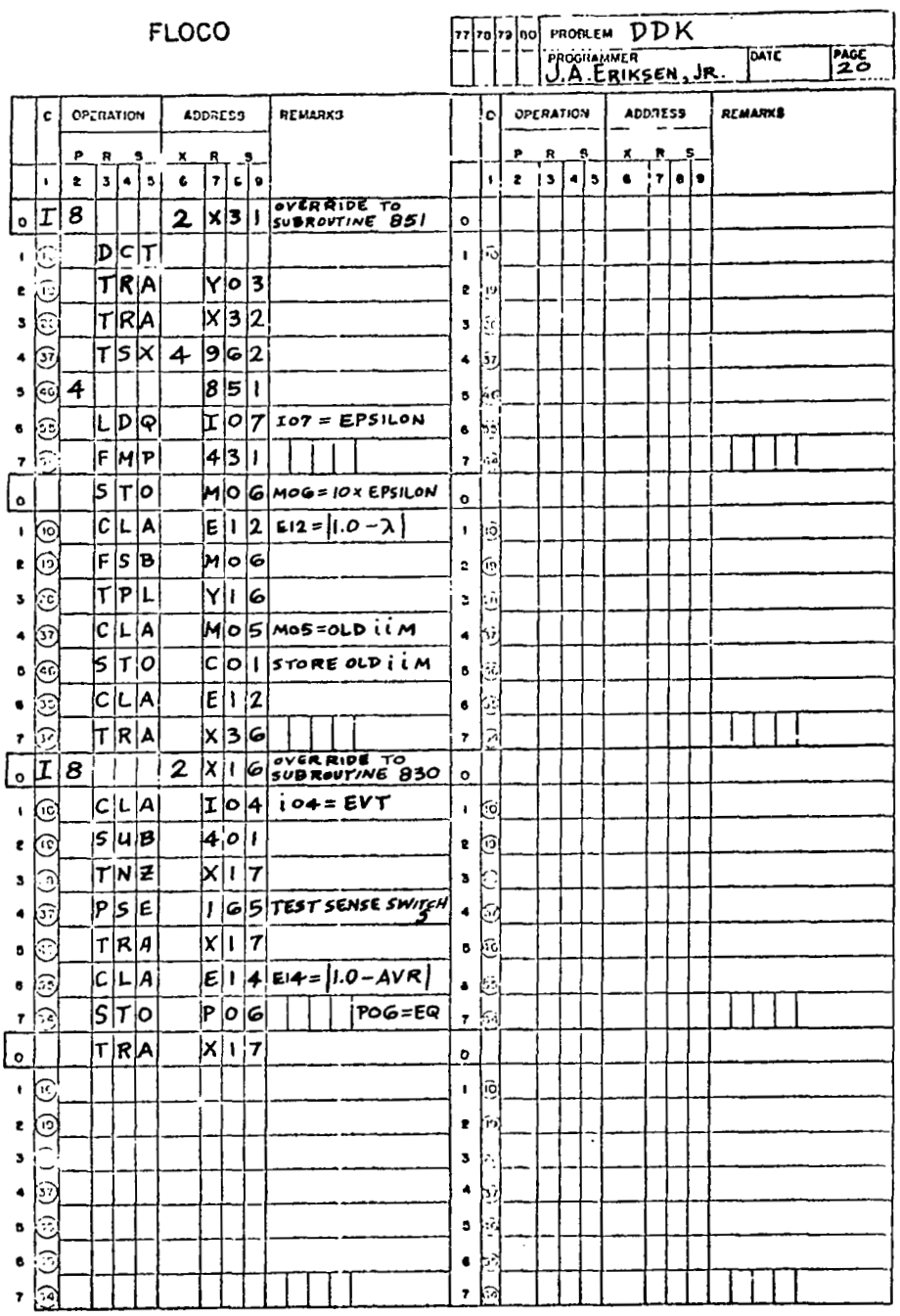

Figure 4-4. Addition to subroutines 851 and 830 for DDK.

CROSS SECTIONS CODE

The appendix to this report contains a mathematical procedure to develop the average group-to-group transfer cross sections of deuterium and oxygen. The following paragraphs describe the computer code evolved to employ the technique discussed in the appendix.

The probability per unit time that a neutron with velocity v' will scatter into a range dv about v is defined as P (v', v) dv. Using the relation of the transfer cross section to this probability as Equation (A-48),

$$\sigma(v',\ v)\ dv = \frac{P\ (v',\ v)\ dv}{v'} \qquad \text{(A-48)}$$

Using the assumptions presented to integrate Equation (A-49), Equations (A-51) and (A-52) were used to calculate the energy decrease by collision ($v' \geq v$) and the energy increase by collision ($v \geq v'$), respectively.

The matrices of numbers according to Equation (A-48) were calculated at five equally spaced velocity intervals within each group. A Simpson's rule numerical integration was used (having calculated the end points and using equally spaced intervals) to integrate $\sigma(v',\ v)$ over the final velocities v.

The code used consists of a main program and three subroutines—COMPTE, ERFUNC, and ERFUN. The COMPTE subroutine is used to evaluate Equations (A-51) and (A-52). These equations required the evaluation of an error function:

$$\text{Erf}\ (x) = (2/\sqrt{\pi}) \int_0^x e^{-y^2}\ dy \qquad \text{(A-53)}$$

Evaluation of this equation was done in subroutine ERFUN. Subroutine ERFUNC is used to ensure that the value of x is positive.

The code calculates the average group-to-group transfer cross section for one specific element. The D_2O transfer cross sections are obtained externally by using Equation (A-47):

$$\sigma_{D_2O}\ (v',\ v) = 2\sigma_D\ (v',\ v) + \sigma_O\ (v',\ v) \qquad \text{(A-47)}$$

Table 4-II is a listing of the nomenclature used in the program. Figure 4-5 is the code for loss or gain of energy in a collision, using the IBM 7094 Mod II computer. Figure 4-6 is a sample output data sheet for oxygen at 556°K.

Table 4-II.
Cross sections machine code.

Name	Definition	Units
A	Scattering junction coefficient	barns/atom
B	Scattering junction coefficient	barns/atom
AK-K	Constant	amu/ev
T	Temperature of element	°Kelvin
N	Number of different temperatures	—
X	Energy of neutrons in specific group	ev
V	Component corresponding to x energy	ev
S	Transfer cross section obtained by Simpson integration	—
V*	The arithmetic average energy for group g, using the lower energy bound for groups g and g-1	ev
V + x ($-4 \leq x \leq 4$)	Specific energy group into which transfer probability P is given for group g	—
AM-M	Mass of element	amu

```
      DIMENSION S(8,25)
      DIMENSION V(10,25,5),P(8,25,5),FMT(8),I(99),X(15),F(10,25,5)
B     FMT(1)=6O6O6O654001
B     FMT(2)=6O6O6O654002
B     FMT(3)=6O6O6O654003
B     FMT(4)=6O6O6O654004
B     FMT(5)=6O6O6O652001
B     FMT(6)=6O6O6O652002
B     FMT(7)=6O6O6O652003
B     FMT(8)=6O6O6O652004
   10 READ INPUT TAPE 7,100,N,A,B,AM,AK
  100 FORMAT(I2,4E8.4)
      DO 110 I=1,8
      READ INPUT TAPE 7,120,M,(X(L),L=1,13)
      DO 109 K=1,5
      F(1,I,K)=M
      F(2,I,K)=X(K+8)
      F(3,I,K)=X(2)
      F(4,I,K)=X(3)
      F(5,I,K)=X(4)
      F(6,I,K)=X(5)
      F(7,I,K)=X(6)
      F(8,I,K)=X(7)
      F(9,I,K)=X(8)
  109 F(10,I,K)=X(9)
  110 F(2,I,1)=X(1)
  120 FORMAT (I2,9E7.4,/2X4E7.4)
      READ INPUT TAPE 7,130,(T(I),I=1,N)
  130 FORMAT(8E9.5)
      DO 200 K=2,10
      DO 199 L=1,25
      DO 198 M=1,5
  198 V(K,L,M)= SQRTF ( 2. * F(K,L,M) )
  199 CONTINUE
  200 CONTINUE
      DO 2001 I=1,N
      Z=T(I)
      DO 400 L=1,5
      CALL COMPTE  (A,B,AM,AK,Z,V(1,1,L),P(1,1,L))
  400 CONTINUE
      DO 403 L=1,8
      DO 402 K=1,8
      DO 401 M=1,5
  401 P(L,K,M)= P(L,K,M)/V(2,K,M)
  402 CONTINUE
  403 CONTINUE
      DO 501 K=1,8
      DO 500 L=1,8
  500 S(L,K)=(V(2,K,1)-V(2,K,5))*(P(L,K,1)+4.*P(L,K,2)+2.*P(L,K,3)+4.*
     1P(L,K,4)+P(L,K,5) )/12.
  501 CONTINUE
      WRITE OUTPUT TAPE 6,1801,A,B,AM,AK,T(I)
      WRITE OUTPUT TAPE 6,1802,(F(1,I,3),I=1,3),(F(2,I,3),I=1,3)
      WRITE OUTPUT TAPE 6,1803,FMT(8),(F(10,L,3),S(8,L),L=1,3)
      WRITE OUTPUT TAPE 6,1803,FMT(7),(F(_9,L,3),S(7,L),L=1,3)
```

Figure 4-5. IBM 7094 code for loss or gain of energy in a collision. (Sheet 1 of 4).

```
      LOSS OR GAIN OF ENERGY IN A COLLISION   (L-77, COLLISI)

      WRITE OUTPUT TAPE 6,1803,FMT(6),(F( 8,L,3),S(6,L),L=1,3)
      WRITE OUTPUT TAPE 6,1803,FMT(5),(F( 7,L,3),S(5,L),L=1,3)
      WRITE OUTPUT TAPE 6,1803,FMT(1),(F( 3,L,3),S(1,L),L=1,3)
      WRITE OUTPUT TAPE 6,1803,FMT(2),(F( 4,L,3),S(2,L),L=1,3)
      WRITE OUTPUT TAPE 6,1803,FMT(3),(F( 5,L,3),S(3,L),L=1,3)
      WRITE OUTPUT TAPE 6,1803,FMT(4),(F( 6,L,3),S(4,L),L=1,3)
      WRITE OUTPUT TAPE 6,1802,(F(1,I,3),I=4,6),(F(2,I,3),I=4,6)
      WRITE OUTPUT TAPE 6,1803,FMT(8),(F(10,L,3),S(8,L),L=4,6)
      WRITE OUTPUT TAPE 6,1803,FMT(7),(F( 9,L,3),S(7,L),L=4,6)
      WRITE OUTPUT TAPE 6,1803,FMT(6),(F( 8,L,3),S(6,L),L=4,6)
      WRITE OUTPUT TAPE 6,1803,FMT(5),(F( 7,L,3),S(5,L),L=4,6)
      WRITE OUTPUT TAPE 6,1803,FMT(1),(F( 3,L,3),S(1,L),L=4,6)
      WRITE OUTPUT TAPE 6,1803,FMT(2),(F( 4,L,3),S(2,L),L=4,6)
      WRITE OUTPUT TAPE 6,1803,FMT(3),(F( 5,L,3),S(3,L),L=4,6)
      WRITE OUTPUT TAPE 6,1803,FMT(4),(F( 6,L,3),S(4,L),L=4,6)
      WRITE OUTPUT TAPE 6,1804,(F(1,I,3),I=7,8),(F(2,I,3),I=7,8)
      WRITE OUTPUT TAPE 6,1803,FMT(8),(F(10,L,3),S(8,L),L=7,8)
      WRITE OUTPUT TAPE 6,1803,FMT(7),(F( 9,L,3),S(7,L),L=7,8)
      WRITE OUTPUT TAPE 6,1803,FMT(6),(F( 8,L,3),S(6,L),L=7,8)
      WRITE OUTPUT TAPE 6,1803,FMT(5),(F( 7,L,3),S(5,L),L=7,8)
      WRITE OUTPUT TAPE 6,1803,FMT(1),(F( 3,L,3),S(1,L),L=7,8)
      WRITE OUTPUT TAPE 6,1803,FMT(2),(F( 4,L,3),S(2,L),L=7,8)
      WRITE OUTPUT TAPE 6,1803,FMT(3),(F( 5,L,3),S(3,L),L=7,8)
      WRITE OUTPUT TAPE 6,1803,FMT(4),(F( 6,L,3),S(4,L),L=7,8)
 2001 CONTINUE
      GO TO 10
 1801 FORMAT(1H110X4HA  =G18.7/11X4HB  =G18.7/11X4HM  =G18.7/11X4HK  =
     1G18.7/11X4HT  =G18.7///)
 1802 FORMAT(1HO///14X5HGROUP F4.0,29X5HGROUP F4.0,29X5HGROUP F4.0,/
     114X4HV* =G18.7,16X4HV* =G18.7,16X4HV* =G18.7//15X1HV17X1HP18X1HV
     217X1HP18X1HV17X1HP//1H )
 1803 FORMAT(A6,6G18.7)
 1804 FORMAT(1HO///14X5HGROUP F4.0,29X5HGROUP F4.0,                  /
     114X4HV* =G18.7,16X4HV* =G18.7,          //15X1HV17X1HP18X1HV
     217X1HP18X          //1H )
      END(1,1,0,0,0,1,1,1,0,0,0,0,0,0,0)
```

Figure 4-5. (Sheet 2 of 4).

```
      SUBROUTINE COMPTE (A,B,AM,AK,T,V,P)

      SUBROUTINE COMPTE (A,B,AM,AK,T,V,P)
      DIMENSION V(10,25),P(8,25)
      C1=(AM+1.)/AM/2.0
      C2=(AM-1.)/AM/2.0
      YSQ=AM/T/.0001724
      Y=SQRTF(YSQ)
      YT=C1*Y
      YQ=C2*Y
      YTP=C1*SQRTF(YSQ+AK)
      YQP=(C2*YSQ-C1*AK)/SQRTF(YSQ+AK)
      C3=C1*C1*AM
  200 C4=YSQ*Y/SQRTF(YSQ+AK)*C3/(YSQ+AK*(AM+1.))
      DO 1713 L=1,8
      DO 1712 M=3,10
      A1 = YQ * V(2,L) + YT  * V(M,L)
      A2 = YT  * V(M,L) - YQ  * V(2,L)
      A4 = YT  * V(2,L) + YQ  * V(M,L)
      A5 = YQP * V(2,L) + YTP * V(M,L)
      A6 = YTP * V(M,L) - YQP * V(2,L)
      A8 = YTP * V(2,L) + YQP * V(M,L)
      CALL ERFUNC (A1,E1)
      CALL ERFUNC (A2,E2)
      CALL ERFUNC (A4,E4)
      CALL ERFUNC (A5,E5)
      CALL ERFUNC (A6,E6)
      CALL ERFUNC (A8,E8)
      IF(V(2,L)-V(M,L)) 1300,1300,1100
 1100 A3 = YT  * V(2,L) - YQ  * V(M,L)
      CALL ERFUNC (A3,E3)
      A7 = YTP * V(2,L) - YQP * V(M,L)
      CALL ERFUNC (A7,E7)
 1110 P(M-2,L) = A * C3 * V(M,L) / V(2,L) * ( E1 + E2  + ( E3 - E4 )
     1          * EXPF( YSQ / AM * ( V(2,L)**2 - V(M,L)**2 ) ) )
     2          + B * C4 * V(M,L) / V(2,L) * ( ( E5 + E6 ) *  EXPF(
     3          - AK * YSQ * V(2,L)**2 / (YSQ + AK) )  + (E7 - E8)
     4          * EXPF( YSQ / AM * ( V(2,L)**2  - ( YSQ + AK * (AM+1.)
     5          * V(M,L)**2 ) / ( YSQ + AK) ) )
      P(M-2,L)=P(M-2,L)*2.
      GO TO 1712
 1300 A9 = YQ  * V(M,L) - YT  * V(2,L)
      CALL ERFUNC (A9,E9)
      A10= YQP * V(M,L) - YTP * V(2,L)
      CALL ERFUNC (A10,E10)
 1310 P(M-2,L) = A * C3 * V(M,L) / V(2,L) * ( E2 - E1  + ( E4 - E9 )
     1          * EXPF( YSQ / AM * ( V(2,L)**2 - V(M,L)**2 ) ) )
     2          + B * C4 * V(M,L) / V(2,L) * ( ( E6 - E5 ) * EXPF(
     3          - AK * YSQ * V(2,L)**2 / (YSQ + AK) )  + (E8 - E10)
     4          * EXPF( YSQ / AM * ( V(2,L)**2  - ( YSQ + AK * (AM+1.)
     5          * V(M,L)**2 ) / ( YSQ + AK) ) )
      P(M-2,L)=P(M-2,L)*2.
 1712 CONTINUE
 1713 CONTINUE
      RETURN
      END(1,1,0,0,0,1,0,1,0,0,0,0,0,0,0)
```

Figure 4-5. (Sheet 3 of 4).

```
      SUBROUTINE ERFUN  (X,ERF)

      SUBROUTINE ERFUN  (X,ERF)
      IF (X+4.) 400,500,500
  400 ERF=-1.
      GO TO 590
  500 IF(X-4.0) 520, 520, 510
  510 ERF=1.0
      GO TO 590
  520 L=0
      ERRC=1.0/X
      ERRF=2.0*X
      AN=1.0
      ANF=1.0
      RP=1.0
      XX=X
      IF(X-3.1) 530, 530, 570
  530 ANF=ANF*AN
      L=L+1
      XX=-XX*X**2
      DEL=XX/(ANF*(AN+0.5))
      ERRF=ERRF+DEL
      IF(ABSF(DEL)-0.00002) 550, 550, 540
  540 AN=AN+1.0
      GO TO 530
  550 ERF=ERRF*0.56418958
      GO TO 590
  570 XX=-XX*X**2
      L=L+1
      IF(L-50) 573, 573, 600
  573 RP=RP*(2.*AN-1.0)
      DEL=RP/(2.0**AN*XX)
      ERRC=ERRC+DEL
      IF(ABSF(DEL)-0.00005) 585, 585, 580
  580 AN=AN+1.0
      GO TO 570
  585 ERF=1.0-ERRC/(1.7724538*EXPF(X**2))
  590 RETURN
  600 WRITE OUTPUT TAPE 6,700
  700 FORMAT(1H05X77HERROR FUNCTION SERIES HAS NOT CONVERGED, STOPPED AT
     1FIFTIETH TERM AND RETURN. )
      GO TO 590
      END(1,1,0,0,0,1,1,0,0,0,0,0,0,0,0)

      SUBROUTINE ERFUNC (A,B)

      SUBROUTINE ERFUNC (A,B)
      IF ( A ) 10, 20, 30
   10 C=-A
      CALL ERFUN (C,B)
      B=-B
      GO TO 40
   20 B=0.
      GO TO 40
   30 CALL ERFUN (A,B)
   40 RETURN
      END(1,1,0,0,0,0,0,1,0,0,0,0,0,0,0)
```

Figure 4-5. (Sheet 4 of 4).

```
A =      3.8000000
B =      0.6000000
M =      17.607000
K =      2.8800000
T =      556.00000
```

GROUP 17. V* = 0.2184000

	V	S
V+4	0	-0
V+3	0	-0
V+2	0	-0
V+1	0	-0
V-1	0.1720000	9.6549362
V-2	0.1222000	2.1465979
V-3	0.7280000E-01	0.1285132
V-4	0.4400000E-01	0.7761450E-02

GROUP 18. V* = 0.1720000

	V	S
V+4	0	-0
V+3	0	-0
V+2	0	-0
V+1	0.2184000	4.1811381
V-1	0.1222000	6.4682946
V-2	0.7280000E-01	0.7075003
V-3	0.4400000E-01	0.6337482E-01
V-4	0.2930000E-01	0.8879581E-02

GROUP 19. V* = 0.1222000

	V	S
V+4	0	-0
V+3	0	-0
V+2	0.2184000	0.4288657
V+1	0.1720000	2.7258037
V-1	0.7280000E-01	3.6044956
V-2	0.4400000E-01	0.5720130
V-3	0.2930000E-01	0.1228705
V-4	0.2300000E-01	0.5021078E-01

GROUP 20. V* = 0.7280000E-01

	V	S
V+4	0	-0
V+3	0.2184000	0.1335140E-01
V+2	0.1720000	0.1543087
V+1	0.1222000	1.6234471
V-1	0.4400000E-01	4.1235248
V-2	0.2930000E-01	1.3695839
V-3	0.2300000E-01	0.7058080
V-4	0.1280000E-01	0.1504841

GROUP 21. V* = 0.4400000E-01

	V	S
V+4	0.2184000	0.6602298E-03
V+3	0.1720000	0.1063116E-01
V+2	0.1222000	0.1964003
V+1	0.7280000E-01	2.4893298
V-1	0.2930000E-01	5.1772950
V-2	0.2300000E-01	3.1031431
V-3	0.1280000E-01	0.9101899
V-4	0	-0

GROUP 22. V* = 0.2930000E-01

	V	S
V+4	0.1720000	0.1400423E-02
V+3	0.1222000	0.3989768E-01
V+2	0.7280000E-01	0.7770221
V+1	0.4400000E-01	3.4245478
V-1	0.2300000E-01	6.6647499
V-2	0.1280000E-01	2.3387764
V-3	0	-0
V-4	0	-0

GROUP 23. V* = 0.2300000E-01

	V	S
V+4	0.1222000	0.1653847E-01
V+3	0.7280000E-01	0.4032790
V+2	0.4400000E-01	2.0632977
V+1	0.2930000E-01	4.1885980
V-1	0.1280000E-01	3.5768856
V-2	0	-0
V-3	0	-0
V-4	0	-0

GROUP 24. V* = 0.1280000E-01

	V	S
V+4	0.7280000E-01	0.9575262E-01
V+3	0.4400000E-01	0.6635953
V+2	0.2930000E-01	1.6022639
V+1	0.2300000E-01	2.2415307
V-1	0	-0
V-2	0	-0
V-3	0	-0
V-4	0	-0

Figure 4-6. Sample data output sheet for oxygen at 556°K.

V. CROSS SECTIONS

The basic reference for cross sections and group structure was LAMS-2941.* Complete sets were obtained from plots of tabulated values. The D_2O and BeO cross sections were generated for the study. Collapsed group sets were calculated empirically. In all cases, the requisite three thermal energy groups were maintained. In this regard the basic checks on use of reduced groups were criticality calculations in representative configurations. No additional cross sections other than the elastic transport values and the S_4 angular weights are used for anisotropic effects.

The various group specifications are listed in Table 5-I. The eleven thermal groups of the LAMS-2941 24-group can be collapsed into four groups by lethargy-weighting the transfer and transport cross sections. The result is a single upscattering and single downscattering number per group. Also, in the lower resonance range where scattering properties are constant per unit lethargy, groups 11, 12, and 13 can be reduced to one group. The result is a 15-group theory with the first ten groups identical with the first ten groups of the 24-group theory. The absorption terms for the five reduced groups should be flux-weighted by means of a 24-group solution. When the multigroup values of σ_a vary as $1/v$, it is sufficient to obtain a simple average value for one of the thermal groups and to scale for the others using the new group velocities. However, when σ_a varies greatly with energy (as in the case of the plutonium resonance at 0.297 ev), it is necessary to obtain a typically "effective" value from a multigroup run.

By defining the maximum thermal energy at 0.25 ev, group 12 can be added to groups 7 through 11 to make a single "slowing-down" region. Groups 1 through 6, which contain the multigroup fission spectrum, result in a single fast group with a one-fission neutron source. This forms the basis of the 5-group. The three thermal groups are the same as groups 13, 14, and 15 of the 15-group, but the constants for the first two must be estimated independently from data on fission energy diffusion coefficients and slowing-down lengths in the different moderating materials.

The 15-group structure is useful in building up a set of BeO cross sections since the fast groups are available from LAMS-2941 (18-group).

Assuming that there are six consecutive energy groups with transfer numbers up to $\sigma_{g \rightarrow g\pm3}$, when the groups are to be collapsed by threes into two groups, only two transfer cross sections remain—one up and one down. Numbering the groups 1 through 6, we assume a value, ϕ_I, for

---

*Los Alamos Group-Averaged Cross Sections, Los Alamos Scientific Laboratory of the University of California, LAMS-2941, July 1963.

Table 5-I.

5-, 15-, and 24-group specifications.

Group No.			Energy range			
5-group	15-group	24-group	from 10 Mev	u	Δu	v (cm/shake)
	1	1	3 Mev	1.204	1.204	28.5
	2	2	1.4	1.966	0.762	19.9
1	3	3	0.9	2.408	0.442	14.7
v = 14.7	4	4	0.4	3.219	0.811	11.0
	5	5	0.1	4.605	1.386	6.7
	6	6	17 kev	6.377	1.772	2.7
	7	7	3.35	8	1.623	1.237
	8	8	0.454	10	2.0	0.5071
	9	9	61.44 ev	12	2.0	0.1866
2	10	10	22.6	13	1.0	0.0854
v = 0.1866		11	8.315	14	1.0	0.0518
	11	12	3.059	15	1.0	0.0314
	v = 0.0314	13	1.1256	16	1.0	0.0191
		14	0.4141	17	1.0	0.0116
	12	15	0.3224	17.25	0.25	0.00799
	v = 0.00799	16	0.2511	17.5	0.25	0.00738
		17	0.1965	17.75	0.25	0.00651
3	13	18	0.1535	18	0.25	0.00575
v = 0.00554	v = 0.00554	19	0.0924	18.5	0.5	0.00477
		20	0.056	19	0.5	0.00372
4	14	21	0.034	19.5	0.5	0.002896
v = 0.00316	v = 0.003166	22	0.0252	19.8	0.3	0.002367
5	15	23	0.0206	20	0.2	0.002088
v = 0.0019	v = 0.0019	24	0.005	—	1.22	0.001756

the resultant flux level in the new group, I, composed of the original groups 1, 2, and 3. $\Sigma_{I\to II}\,\phi_I\,\Delta u_I$ then becomes the total outscattering.

The contribution to the total outscattering (slowing-down density) varies within the new large group by the same probabilities as the original three groups:

$$\Sigma_{I\to II}\phi_I\Delta u_I = \Sigma_{1\to4}\phi_1\Delta u_1 + (\Sigma_{2\to4} + \Sigma_{2\to5})\phi_2\Delta u_2 + (\Sigma_{3\to4} + \Sigma_{3\to5} + \Sigma_{3\to6})\phi_3\Delta u_3 \quad (5\text{-}1a)$$

or, approximately,

$$\Sigma_{I\to II} = \Sigma_{1\to4}(\Delta u_1/\Delta u_I) + (\Sigma_{2\to4} + \Sigma_{2\to5})(\Delta u_2/\Delta u_I) + (\Sigma_{3\to4} + \Sigma_{3\to5} + \Sigma_{3\to6})(\Delta u_3/\Delta u_I) \quad (5\text{-}1b)$$

where

$$\Delta u_I = \Delta u_1 + \Delta u_2 + \Delta u_3 \quad (5\text{-}2)$$

A similar relation can be written for the upscattering term $\Sigma_{II\to I}$. The approximation for few group numbers generated by this method depends on the assumption that both the transport and absorption cross sections are slowly varying among the original three groups. Otherwise the original group numbers should be reweighted by the perturbed flux of the multigroup run before collapsing to fewer groups.

For downscattering alone, it is easily shown that the transfer numbers are slowing-down cross sections, for if the slowing-down density, q(u), is

$$q(u) = \xi\Sigma_s(u)\phi(u) \quad (5\text{-}3)$$

the downscattering per lethargy is

$$\xi\Sigma_s/\Delta u = \Sigma_{g\to g+1} \quad (5\text{-}4)$$

In Equation (5-1), if all the terms except $\Sigma_{3\to4}$ are zero, then

$$\Sigma_{I\to II} = \Sigma_{3\to4}(\Delta u_3/\Delta u_I) \quad (5\text{-}5)$$

The removal terms for the combined group, with constant downscattering per unit lethargy, are simply scaled inversely by the increased width. In this way, groups 11, 12, and 13 in both carbon and BeO were reduced to one group.

In the particular case of groups 14 through 24, which have eight transfers each, the regrouping neglects four numbers—i.e., $\sigma_{16\leftrightarrows 20}$ and $\sigma_{19\leftrightarrows 23}$.

Since a flux lethargy plot peaks at 2kT, it is possible to obtain a fair thermal spectrum for moderator temperatures up to half the upper energy limit of the thermal groups. However, if the highest energy group is too wide, both energy and lethargy spectrums will peak within it and the high energy portion of the spectrum loses shape.

Half the upper limit of group 14 corresponds to 12,000°R. The highest temperature quoted in LAMS 2941 for this thermal group structure is 6000°R (0.280 ev).

However, if reflector properties can be maintained with fewer groups, it is advantageous to do so for some parametric studies. The 15-group specifications accommodate the same temperature range as the 24-group specifications. By including group 12 in the slowing-down range and reducing the groups above thermal to two, the 5-group thermal limit is at 0.251 ev or approximately 5000°R. Thus, the flux lethargy spectrum is halved for this temperature and the flux-energy representation does not exceed the Maxwellian peak. This piles up flux in group 3 but the distortion is not too serious since the carbon thermal diffusion length leakage and fuel absorption are reproduced fairly well. Use of the 5-group, 5000°R carbon set is limited to the D_2O-carbon combination reflectors, and these reflectors exhibit 50% less fuel reactivity worth than in their multigroup versions. It was decided to keep to the conservative (lower k_{eff}) side of the 24-group in this instance since the latter representation with the Maxwellian peak near the 0.297-ev plutonium resonance may give somewhat optimistic results. In any case, the 5000°R carbon-D_2O combination in the 24-group shows phenomenal reflecting power. Also, the effect is insensitive to reasonable variations of the upper thermal group cross sections and therefore appears to be a real effect.

The reason for this power can be rationalized from the neutron balance of the 24-group runs. The fluxes in groups 14, 15, and 16 are high in carbon and are leaking practically the entire original fission neutron. The bulk of this leakage (75%) is back toward the core. At these energy groups, D_2O downscattering is more than twice as effective as at fission energies. Thus, the efficiency of the D_2O is amplified by carbon putting the fast neutrons back into the D_2O at a more effective energy. The value of the average fuel cross section over groups 14, 15, and 16 rises 60% over the value for pure D_2O at 1000°R. Another way of expressing the

phenomenon is to say simply that the 5000°R carbon effectively reduces the transparency (to fast neutrons) of D_2O down to the plutonium resonance. This is an obvious advantage in this fuel.

PLUTONIUM

24-Group

Groups 1 through 14 are the same in σ_a, $\nu\sigma_f$, and σ_{tr} as the 18-group listing in LAMS 2941. These have been used directly since lethargy values are identical with the 24-group over this energy range—i.e., 10 Mev to 0.4141 ev covering a lethargy interval of 17 units.

Groups 1 through 6 have the g→g + 5 transfer term eliminated and the g→g values rebalanced by this difference. Groups 7 through 14 have g→g + 1 terms set equal to $\xi\sigma_s$(σ_s = 8.4 barns) and the σ_{gg} value held at 9.94 barns.

The absorption and fission values (σ_a and $\nu\sigma_f$) for groups 15 through 24 are obtained from BNL 325.* The g→g values are placed at 9.94 barns and the g→g + 1 terms at 0.07 group transport numbers are then derived as total cross sections by summing. The average value of ν used throughout equals 2.92. Absorption cross sections in the resonance range above 1.125 ev and high thermal range (0.25 to 1.125 ev) are assumed to be the infinite dilution values. Thus, the non-1/v shape and the large resonance at 0.297 ev are unmodified by any assumed spectrum.

The representation of plutonium in the 24 intervals is straightforward except for the resonance at 0.297 ev. The 0.25 lethargy intervals (Δu) through this energy range cause the peak to appear unrealistically sharp in group 16. The group values of σ_a for plutonium as obtained from the BNL 325 data yield the averages shown in Table 5-II when used with carbon and D_2O reflectors.

The flat flux average over groups 14, 15, and 16 is

$$\sigma_a = \Sigma\sigma_a(u)\Delta u/(u_2 - u_1) \qquad (5\text{-}6)$$

$$= [(221)(1.0) + (1650)(0.25) + (5060)(0.25)]/1.5$$

$$= 1266 \text{ barns}$$

Therefore, for the light loading required by the D_2O, the thermal flux actually increases near the energy interval of the plutonium resonance, in the opposite sense of self-shielding.

*D. J. Hughes and R. B. Schwartz, Neutron Cross Sections, 2nd Edition, New York, Brookhaven National Laboratory, 1 July 1958.

Table 5-II.

Average σ_a carbon and D_2O reflectors.

Run	15	17	60	62
Reflector material	C	C	D_2O	D_2O
Reflector thickness (in.)	24	24	36	36
Reflector temperature (°R)	530	5000	530	1000
Average of groups 11, 12, and 13	80.5	79.7	82.7	78.5
Average of groups 14, 15, and 16	555	438	1485	1120
	0.0001	0.0001	0.0001	0.0001

The carbon runs do show the large self-shielding expected when the fuel density increases in this geometry. The greater absorption rate produces larger flux depressions in the fuel, especially near resonance.

For the carbon moderator, the maximum fractional energy loss per collision for the neutrons is 0.284, just exceeding the lethargy width (0.25) in this range. Carbon groups 14, 15, 17, and 19 contain several transfer terms (5 up, 5 down) which provide for scattering through the 5060-barn peak of group 16.

Despite the extreme variation in thermal spectrum between 530 and 5000°R, the effective value of the resonance absorption, I, varies by only 27%; therefore, for carbon

$$(\Delta I/I)/\Delta T = -0.27/4470 = -6 \times 10^{-5}/°R \qquad (5\text{-}7)$$

Equation (5-7) indicates that the spectral shift effect due to moderator temperature is an order of magnitude greater than a Doppler coefficient typical of well moderated cores. Therefore, fuel temperature would probably be of relatively small influence.

Since the LAMS 2941 24-group carbon cross section furnishes the most complete data over a wide temperature range, the carbon cores serve as the basis for reducing the 24-group plutonium for use with the smallest group sets of carbon, BeO, 1000°R D_2O, and 1100°R and low-density hydrogen.

Runs 15 and 17 in particular serve as a reference for this modification as well as a check on the reduced carbon cross sections. The group averages derived from these are listed in Tables 5-III and 5-IV, with the flat flux values quoted for comparison in Table 5-V. The fast groups of the 24-group, groups 1 through 6, correspond to group 1 of the 5-group, and groups 1 through 16 are replaced by group 2 of the 5-group.

Table 5-III.

5-group fast and resonance values.

Group	σ_a	$\nu\sigma_f$
1	2.05	5.472
2	1500	2700

Table 5-IV.

5-group plutonium thermal cross sections obtained from 24-group carbon runs.

Group	Equivalent in 24-group	ϵ = 0.0001		ϵ = 0.001	
		σ_a	$\nu\sigma_f$	σ_a	$\nu\sigma_f$
3	17, 18, and 19	923	1630	885	1565
4	20, 21, and 22	756	1580	776	1622
5	23 and 24	1315	2800	1349	2878

Table 5-V.

Flat flux values.

Group	σ_a	$\nu\sigma_f$
3	1100	1950
4	805	1682
5	1356	2890

The 1500-barn value in Table 5-III is an experimental result for the effective absorption above 0.15 ev in a reactor cavity with 10 to 15% resonance power.* Referring to Table 5-II, the D_2O core at 530°R (Run 60) yields an average value near 1500 barns for groups 14, 15, and 16 alone.

The extreme cases listed in Table 5-I show that above the last group containing accelerating cross sections—i.e., group 14—the average fuel cross sections are practically independent of the reflector material. However, the 0.297 resonance value produces a large spectral effect in the three high thermal groups (groups 14, 15, and 16). These cover the range from 0.25

*R. W. Stoughton and J. Halperin, "Heavy Nuclide Cross Sections of Particular Interest to Thermal Reactor Operation: Conventions, Measurements and Preferred Values," Nuclear Science and Engineering, Vol 6, No. 2, August 1959, pp 100-118.

to 1.1256 ev which becomes the low energy resonance range of the 5-group, with a lower limit for the entire slowing-down range at 0.25 ev. By incorporating the peak into the effective resonance absorption, the effective value of σ_a for the collapsed group 2 should vary with reflector material or scattering cross section per plutonium atom. However, it is preferable to have a common fuel for all cases, and to accomplish this, some intermediate effective value of σ_a must be selected. A value of 1500 barns for group 2 was used since it also has some basis for measured data as mentioned previously.

15-Group

The average of groups 14, 15, and 16 of the 24-group set can be used as a single group in the high energy end of the thermal range. Also, since all isotopes considered have constant properties per unit lethargy through groups 11, 12, and 13, these groups can also be reduced to one. Combining these with the same three thermal groups used in the 5-group cross sections and groups 1 through 10 of the 24-group cross sections gives a 15-group structure with four thermal and five resonance groups.

Group 12, the high-energy thermal group which contains the plutonium 0.297 resonance, has an average cross section obtained directly from the 24-group runs (see Table 5-II). The group 12 value chosen for the BeO reflectors is 450 barns; for the BeO-D_2O combinations, the value increased to 1000 barns. This differs from the "effective" value obtained independently for the resonance range of the 5-group. In keeping the same thermal characteristics in this range, the flux can also be expected to reproduce. This is not the case for group 2 of the 5-group where groups 14, 15, and 16 of the 24-group cross section were converted to a slowing-down region as explained subsequently. The average value of groups 11, 12, and 13 is used for group 11 of the 15-group. This is the same as the effective value since it appears invariant to spectral shifts.

5-Group

A check-run comparison of the 5-group plutonium and carbon with the multigroups at 530°R was made and the normalized neutron balances are compared in Table 5-VI. The overall correspondence in neutron distribution and fuel worth is quite good considering the approximations necessary. The resonance absorption appears to be at least 25% too high using the 1500-barn value. This is mainly compensated for by a 20% reduction in the absorptions of group 4. The 1500-barn value is a compromise, since 5-group plutonium must also be used in a D_2O spectrum or D_2O-BeO and D_2O-carbon combination reflectors. The results in Table 5-VI are a good illustration of a common feature of the 5-group cross section—group 2

Table 5-VI.

Comparison of 24- with 5-group plutonium for a 48-in. radius cavity with 24 in. of carbon at 530°R.

Groups	Run 15, $\epsilon = 0.0001$, $N = 10^{-5}$, $k_{eff} = 1.005$, 24-group: Plutonium $\phi(u)\Delta u$	Fission neutrons	Plutonium absorption	Carbon $\phi(u)\Delta u$	Carbon absorption
1 through 6	196	0.017	0.0064	107.6	0
7 through 13	(188.8)	(0.089)	(0.0517)	(147.2)	(0)
14, 15, and 16	(10.2)	(0.104)	(0.0567)	(22.1)	(0.0014)
7 through 16	199.0	0.193	0.1084	169.3	0.0014
17, 18, and 19	11.8	0.192	0.109	82.6	0.0104
20, 21, and 22	25.0	0.415	0.198	197.5	0.0552
23 and 24	6.7	0.188	0.088	86	0.0404
Totals		1.005	0.5098		0.1074

Normalized leakage neutrons = 0.386 net

Groups	Run 51, $\epsilon = 0.0001$, $N = 10^{-5}$, $k_{eff} = 0.9964$, 5-group: Plutonium $\phi(u)\Delta u$	Fission neutrons	Plutonium absorption	Carbon $\phi(u)\Delta u$	Carbon absorption
1	292	0.0160	0.0060	128.6	0
2	8.78	0.2370	0.1317	19.9	0.0012
3	13.4	0.2090	0.1181	82.4	0.0131
4	21.0	0.3404	0.1628	151.0	0.0431
5	6.74	0.1940	0.0910	80.4	0.0385
		0.996	0.5096		0.0959

Normalized leakage neutrons = 0.393 net

is a slowing-down region only and no correspondence with 24-group fluxes is sought in this range. In other words, the absorption cross section is part of the total macroscopic slowing-down cross section which, together with volume leakage, reduces the slowing-down density passing through group 2 (groups 7 through 13 of the 24-group cross section).

DEUTERIUM OXIDE

For the first 16 groups, the terms are obtained directly from LAMS 2941 by adding the free atom values:

$$\sigma_{D_2O} = 2\sigma_D + \sigma_O \tag{5-8}$$

The upscattering and absorptions are contained in the remaining eight groups—17 through 24. For these groups, various modifications and approximations have been used, including a gas model calculation outlined in the appendix.

Downscattering

Using the D_2O low-energy scattering data from BNL 325, the bound D contribution is separated by subtracting the free oxygen value at each energy interval. The correction factor used to approximate the effects of binding is

$$(\xi_{bound}/\xi_{free}) \left[\sigma_s(E)_{bound}/\sigma_s(E)_{free}\right] \tag{5-9}$$

where ξ_{bound} is based on an effective mass for D of 3.2 amu. The resultant constant ratio, ξ_{bound}/ξ_{free}, equals 0.69 and the factor is plotted vs energy in Figure 5-1. Actually, the value of ξ_{bound} should reduce with energy, while $\overline{\xi\sigma_s}$ tends to remain constant. However, the single mean value is sufficient to show that binding effects are probably negligible on downscattering cross sections of D_2O. Since the oxygen downscattering terms vary quite slowly with temperature, the D_2O values have been assumed invariant with temperature up to 1000°R. Therefore, with these modifications, Equation (5-8) is used for downscattering in the thermal groups with the oxygen contribution taken from LAMS 2941.

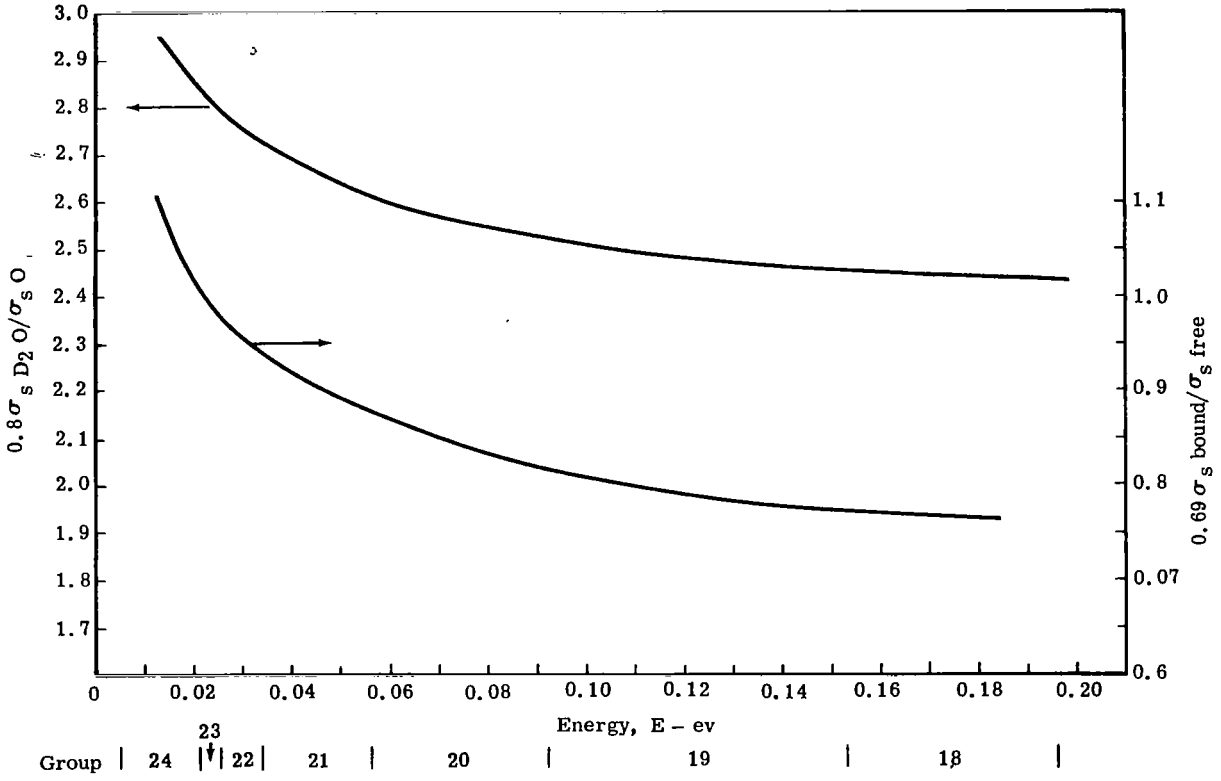

Figure 5-1. Factors in 24-group D_2O cross section calculations.

Upscattering

The 24-group LAMS 2941 oxygen upscattering cross sections were plotted vs temperature and values interpolated at 650, 800, and 1000°R. Assuming an inverse mass relationship and a direct ratio increase in scattering, the D_2O upscattering terms are approximately

$$\sigma_{g\rightarrow g'\ D_2O} = 0.8\ \sigma_{g\rightarrow g'\ O}\left[\sigma_s(E)_{D_2O}/\sigma_s(E)_O\right] \tag{5-10}$$

Using BNL 325 scattering cross sections for D_2O and oxygen, the thermal spectrum produced by these terms (and the downscattering cross sections previously described) is reasonably correct compared to a 530°R Maxwellian distribution. The approximation, therefore, tends to show that the heavy molecule as a whole does the accelerating with the additional (2D) atoms exerting influence mainly through the collision probability. Over the temperature range considered, it is sufficient to include upscattering in the groups below group 16. The correction factor discussed previously is plotted in Figure 5-1.

Transport Cross Sections

Since D_2O is a very low thermal absorber, care must be taken to maintain the thermal diffusion length through the transport cross sections. These are the most sensitive terms in the thermal groups. The 2D + O "free" atom values were modified slightly as shown in Table 5-VII.

Table 5-VII.
Modified free atom values.

Group	2D + O	Estimate
17	9.18 barns	8.6 barns
18	8.27	8.88
19	9.15	9.00
20	9.87	9.50
21	10.43	10.00
22	11.17	10.50
23	11.76	11.00
24	—	13.00

The group 24 value must be obtained experimentally. The data curve* of λ_{tr} (E) used yields an average value for this energy interval of 2.30 cm at 540°R. Over the 960°R D_2O temperature range of this study, the transport terms were considered constant with temperature.

Absorption

These values are based on a 110-cm diffusion length for 0.0331 density in an infinite D_2O medium. Setting group 24 at 2.5×10^{-3} barns, the other σ_a values are obtained by scaling inversely with group velocities.

Gas Model

The transfer cross sections at 530°R for groups 17 through 24 were calculated using the formulation of the appendix. The upscattering does not differ substantially from the approximate set, but the downscattering values are larger in many instances by a factor of at least 1.5. Incorporating these transfer values with the same transport and absorption cross sections of the approximate method produces the spectrum shown in Figure 5-2. The continuous $\phi(u)$ curve has a Maxwellian shape. Both methods show the typical flux buildup at the low energy end due to the scattering properties of the liquid in this energy range. Figure 5-3 compares the spectrum of this theoretical model with a measured result† through 100 cm, 530°R, D_2O.

A typical run made with the gas model set yielded a k_{eff} value approximately 2% higher than the alternate method actually used. This was apparently due to the higher downscattering terms, particularly $\sigma_{23\rightarrow24}$.

Check Runs

The 24-in. radius, 36-in. reflector core with D_2O at 530°R has the minimum load of the entire series of cores in the study. The two runs comparing cross section sets yielded the following data:

Run	M_c (kg)	L (cm)
60 (approximate)	1.17	131
61 (gas model)	0.98	123

The thermal spectra are plotted in Figure 5-2.

*R. Ramana et al., "On the Spectrum of Neutrons Emerging from Moderators," Proceedings of the Second United Nations International Conference on the Peaceful Uses of Atomic Energy (1-13 September 1958), Volume 16—Nuclear Data and Reactor Theory, Geneva, 1959, Figure 5.

†Ibid., Figure 4.

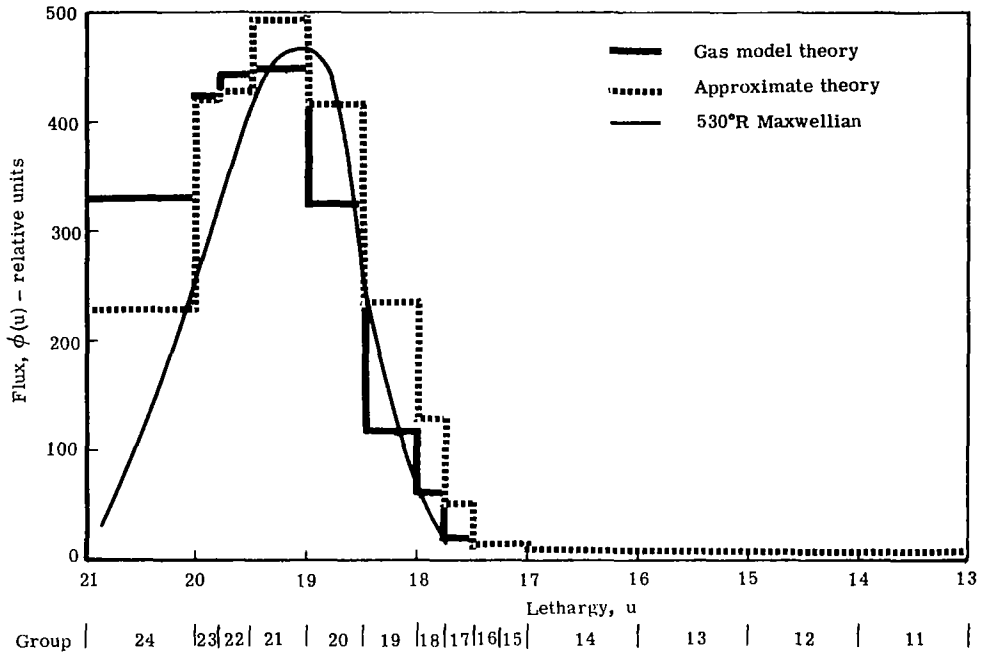

Figure 5-2. Thermal spectrum in 530°R D_2O for a 24-in. radius cavity with a 36-in. reflector.

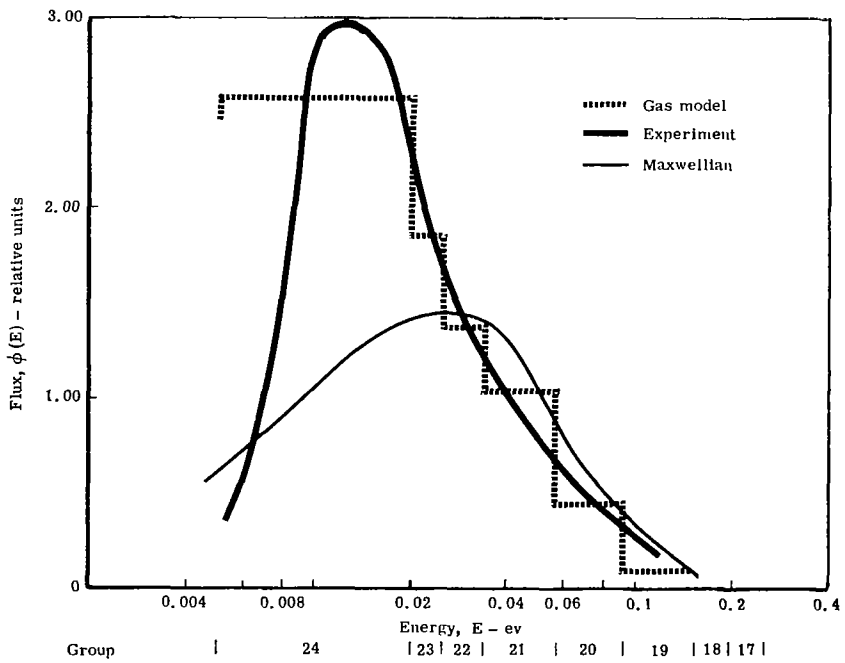

Figure 5-3. Comparison of spectrums for D_2O at 530°R through 100 cm.

At 1000°R, the same core gives a critical mass of 3.55 kg. Most of the additional fuel requirement over the 530°R case is due to the reduced D_2O density. However, the spectral effect, plus higher plutonium density, changes the fuel worth somewhat. The average plutonium thermal absorption cross section decreases from 987 to 930 barns. The thermal spectrum compares well with the 1000°R Maxwellian distribution of Figure 5-4. At the higher temperature the pileup in group 24 is relatively much less.

15-Group

The flux lethargy plot of Figure 5-5 compares 24- and 15-group D_2O at 1000°R. The latter set was found by the method outlined in the introduction. The 15-group fuel used had an absorption cross section in group 12 characteristic of the D_2O shielded value.

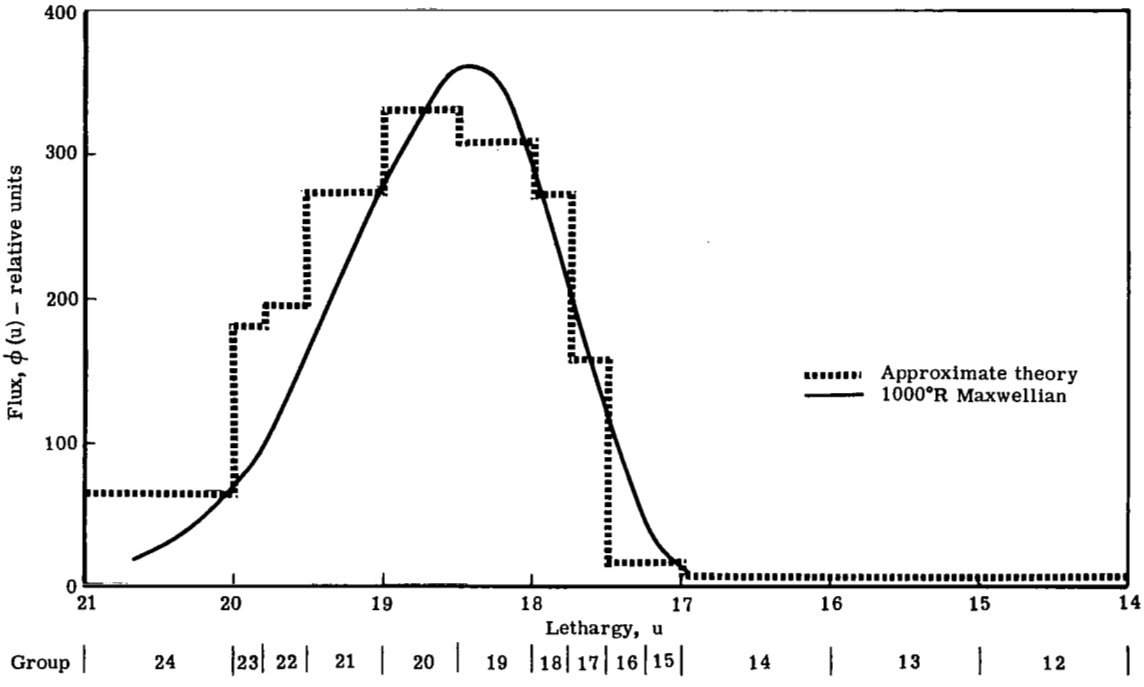

Figure 5-4. Thermal spectrum in 1000°R D_2O for a 24-in. radius cavity with a 36-in. reflector (approximate theory).

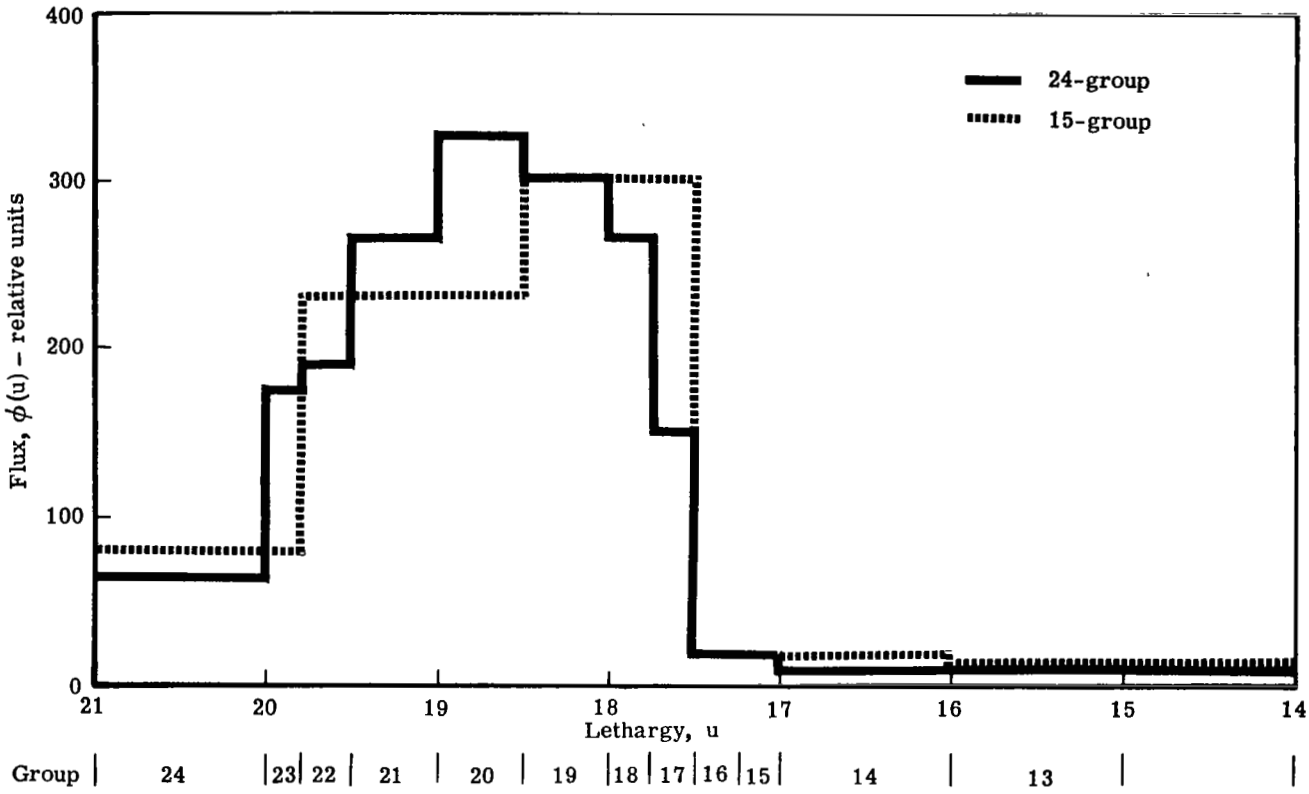

Figure 5-5. Comparison of 24- and 15-group D_2O thermal spectrum at 1000°R.

5-Group at 1000°R

These cross sections are used in the two-dimensional cores in combination with either BeO or carbon. As in all the moderators with one fast group, the first removal cross section is very sensitive. The approximation for this is

$$\sigma_{1\rightarrow 2} = 1/3\rho^2\sigma_{tr_1}\tau \qquad (5\text{-}11)$$

where

σ_{tr_1} = transport cross section for group 1
ρ = D_2O density at 530°R
τ = age to thermal

For D_2O, using 530°R values,

$$\sigma_{1\to 2} = 1/(3)(0.033)^2 (120)(7.55) \qquad (5\text{-}12)$$

$$= 0.34 \text{ barn}$$

which holds for all temperatures, since $\rho^2\tau \simeq$ constant

The value can be estimated directly from the 24-group runs by the formula of Equation (5-13):

$$\sigma_{1\to 2} \cong 1/(0.033)(\text{total of flux groups 1 through 16}) \qquad (5\text{-}13)$$

which gives

$$\sigma_{1\to 2} = 1/(0.033)(96.5) \qquad (5\text{-}14)$$

$$= 0.31 \text{ barn}$$

The transport and removal cross sections of group 2 are 8.14 and 4.2 barns, respectively. These relatively high values produce a short slowing-down length in this group, necessary to keep resonance leakage in D_2O at a very small value relative to thermal leakage.

Check runs in 24- and 5-groups for a 5000°R carbon reflector with 12 cm of D_2O (see paragraph C of the contract) are listed in Table 5-VIII. Although the division of fast and thermal fluxes and thermal absorptions are duplicated in each material, the 5-group thermal spectrum is considerably softer than that of the 24-group. The D_2O thermal spectrum is softened by both reduced upscattering and fast removal cross sections. This type of mock-up results in a higher fuel efficiency, compensated, in turn, by extra leakage. A better duplication of spectrums cannot be accomplished without more thermal groups for carbon at 5000°R. However, any refinements would raise the reactivity worth of the fuel. As it is, the 24-group value of the reactivity constant, k_{eff}, is probably too high due to unknown shielded value of the plutonium in group 16 (see Figure 5-6). Therefore, with the correct total flux-energy distribution, geometric effects on fuel load can be determined with fewer groups.

Table 5-VIII.

Comparison of neutron balance tables for 48-in. radius cavity with 12 cm of D_2O and 24 in. of carbon at 5000°R.

5-group		24-group	
Fission neutrons in Pu-239			
Groups		Groups	
1	0.0023	1 through 6	0.0015
2	0.048	7 through 16	0.2057
3	0.211	17 through 19	0.412
4	0.363	20 through 22	0.2957
5	0.387	23 and 24	0.1325
Total thermal flux in Pu-239			
360.0			333.0
Total thermal flux in D_2O			
138.0			119.0
Total thermal flux in carbon			
587.0			589.0
Total flux in carbon			
675.0			669.0
Total flux in D_2O			
206.0			223.0
Total absorptions in carbon			
0.0687			0.06617
Total absorptions in D_2O			
3.132×10^{-3}			3.16×10^{-3}
Total leakage			
0.43			0.3585
Reactivity constant (k_{eff})			
1.0109			1.052
Plutonium number density			
1.35×10^{-6}			1.35×10^{-6}
Convergence factor (ϵ)			
0.0001			0.0001

CARBON

24-Group

The LAMS 2941 24-group carbon cross sections are tabulated for the following material temperatures (in ev equivalents):

0.025, 0.056, 0.0788, 0.10, 0.152, 0.194, and 0.280.

All sets have upscattering terms from groups 14 through 24 except the 0.152-ev table, which deletes upscattering into group 14.

The transfer and transport cross sections yield smooth plots vs temperature. Therefore, other sets may be formed by interpolation, and group 14 in the 0.152-ev set can be rebuilt in this manner. The set at 0.0788 ev corresponds to 1675°R and is used directly instead of 1500°R—i.e., only 3000 and 5000°R are actually interpolated.

The initial run at 530°R indicated too large a thermal diffusion length for graphite; therefore, the values of σ_a are increased by an additional amount—$(0.0015)(V_{24}/V_n)$ barns—for the nth group. The correction is scaled inversely by group velocities.

At 5000°R (0.236 ev) the multigroup representation is particularly important in groups 14, 15, and 16. Thus, the flux per unit lethargy should peak at 0.47 ev, or just within the lower limit of group 14. This might be distorted somewhat by the fuel absorption since group 16 contains the plutonium resonance peak. The acceleration cross sections starting at group 14 cause a very abrupt rise in the flux spectrum at this group. It appears that for use with plutonium, the 5000°R carbon cross sections become more crude since so much of the description depends on these three groups. It would be desirable to divide group 14 into smaller intervals. As it is, there is a question that the infinite dilution fuel worth in this range should probably be modified since the groups may not give the correct amount of self-shielding for carbon. At least 58% of the fissions occur in this range at 5000°R. Without other refinements, the only alternative is to check the actual sensitivity of the fuel and transfer cross sections in this range by variation.

A direct reduction of plutonium absorption cross section in group 16 from 5060 to 4000 barns, and maintaining the group fuel multiplication factor (η), decreases k_{eff} by 0.4%. An increase of 0.5 barns in the transfer cross section, $\sigma_{14\to15}$, increased k_{eff} by 0.3% at 5000°R.

The high temperature case requires 70% more fuel than at 530°R. Therefore, the temperature coefficient of carbon using plutonium fuel is negative. Mainly, this is due to the total η reducing from 1.96 to 1.86 with temperature. The increase in normalized net leakage is only 0.032 neutrons in going from cold to hot.

The conclusion is that temperature effects are almost completely dependent on spectral shift causing the fuel multiplication constant to be temperature dependent.

With carbon reflector thickness approximately equal to one diffusion length at 530°R, reducing the moderator absorptions by 33% at 5000°R causes the thermal diffusion length to increase 50% beyond the reflector thickness. Thermal leakage does not increase, however, since the spectrum is too hot to allow the flux buildup in the low thermal groups. Therefore, the leakage does not increase despite the increase in thermal diffusion length.

5-Group

The group 1 fast diffusion coefficient for carbon is

$$\begin{aligned} D_f &= 1/3\Sigma_{tr} \\ &= 1/(3)(1.84)(0.084) \\ &= 2.16 \text{ cm} \end{aligned} \tag{5-15}$$

Therefore, assuming an age down to 0.25 ev of 300 cm^2, the fast removal cross section is approximately

$$\begin{aligned} \sigma_{1\to 2} &= 2.16/(300)(0.084) \\ &= 0.086 \text{ barn} \end{aligned} \tag{5-16}$$

The removal cross section of the slowing-down region (group 2) is held at the same value obtained for groups 14, 15, and 16 of the 24-group cross section—i.e., the upper thermal value. Consequently, the transport cross section of group 2 is reduced to obtain a slowing-down length across the group comparable with the age to thermal. The numbers used are

$$\sigma_{2\to 3} = 0.45 \text{ barn}$$
$$\sigma_{tr_2} = 0.5507 \text{ barn}$$

The slowing-down length is, therefore,

$$L_2 = \left[1/(3)\,(0.5507)\,(0.45)\,(0.084)^2\right]^{0.5} \qquad (5\text{-}17)$$
$$= \sqrt{190}$$
$$= 13.9 \text{ cm}$$

A comparison of 24- and 5-group runs at 530°R is listed in Table 5-VI. The 5000°R case is shown in Table 5-IX. In the latter, the thermal flux distribution is shifted since these groups terminate at 0.251 ev in the 5-group set. The gross picture of reactivity can be seen in the comparison at consistent critical mass calculations shown in Table 5-IX.

Table 5-IX.
Reactivity comparison at consistent critical mass calculations.

Fission neutrons		24-Group	5-Group
Group	Energy range		
1 through 6	17 kev to 10 mev	0.0288	0.0270
7 through 19	0.0924 ev to 17 kev	0.921	0.8140
20 through 24	0.005 to 0.0924 ev	0.0382	0.1668
Total absorption in plutonium		0.5377	0.5437
Total absorption in carbon		0.0412	0.0388
Net core leakage		0.417	0.412
Calculated thermal diffusion length		92 cm	86 cm
k_{eff}		0.992	1.007

The 24-group flux energy plot, Figure 5-6, shows the large accumulation at the upper thermal range where the flux rises abruptly out of the slowing-down region to a large maximum. This pileup tends to make reactivity effects independent of the complete spectrum since the lower groups could vary by a factor of two or more without causing a significant change in fuel load. The 5-group peaks in a similar way in its top thermal group which is shifted down the energy scale from the 24-group cross section. However, the reflector diffusion coefficients associated with this flux are the same for both in this range. Taking advantage of this, and adjusting the absorption cross section of carbon in group 3 at 5000°R, the multigroup reactivity effects per kilogram of plutonium can be simulated.

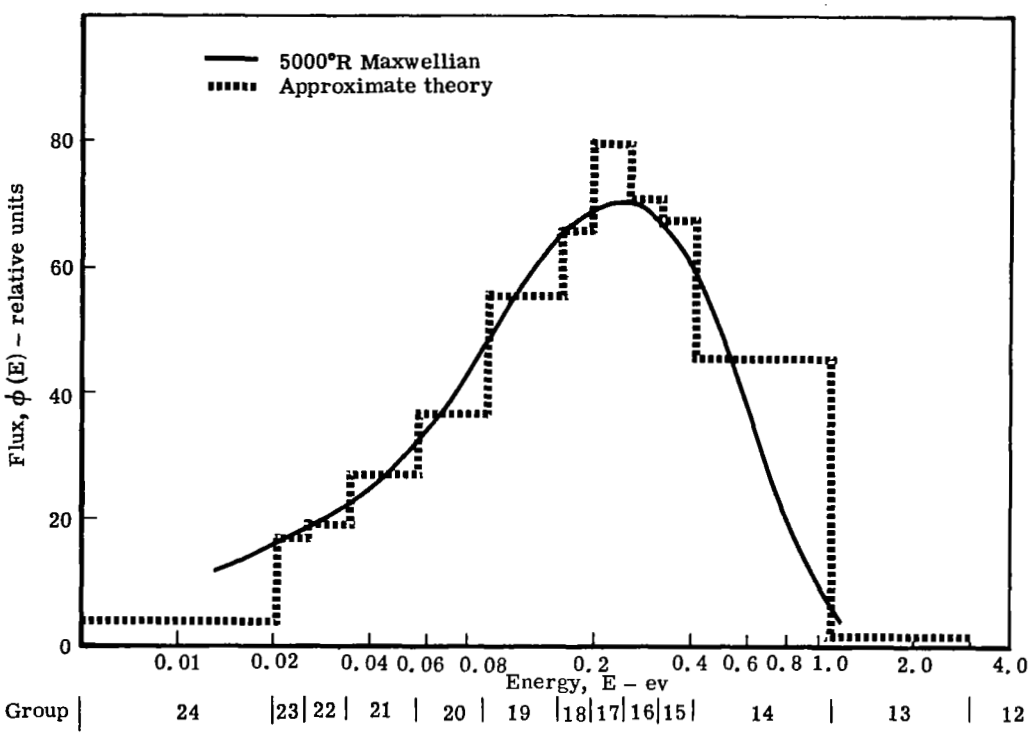

Figure 5-6. Thermal spectrum in carbon for a 48-in. radius cavity with a 24-in. carbon reflector—24-group.

BERYLLIUM OXIDE

15-Group

The LAMS 18-group BeO at 530°R has the same group specifications (down to group 14) as the 24-group. Since the thermal groups must be independently supplied for each temperature, it is convenient to work with the 15-group structure. Therefore groups 11, 12, and 13 of the 18-group set are collapsed into group 11 of the 15-group set and thermal groups 12, 13, 14, and 15 are added.

The first eleven groups of the 15-group set as described previously are divided by 2.00 to give the fast and resonance macroscopic cross sections per atom of BeO. The average amu value is 12.5; therefore, the 12-amu carbon thermal transfer numbers of the 15-group carbon are used with slight modification. The transport cross sections are obtained from λ_{tr} (E) data for

BeO, and the absorptions from 24-group Be. The resultant thermal diffusion length at 530°R acts as an overall check on the cross sections. Adjustments can be made if the spectrum demands it.

BeO has at least 30% more inelastic scattering in the epithermal range than carbon. Therefore, in using the 12-amu carbon transfer cross sections for an average atom model of BeO, the upscattering into group 12 (0.25 to 1.125 ev) has been reduced by a factor of 1.5.

5-Group

The fast group removal cross section is calculated in the same manner as carbon and D_2O:

$$\sigma_{1\to 2} = 1/(3)(1.769)(100)(0.1372)^2 \qquad (5\text{-}18)$$

$$= 0.10 \text{ barn}$$

where the numbers are

Transport cross section	= 1.769 barns/atom
Age in BeO	= 100 cm^2
Atom density of BeO	= 0.1372

An added problem in this isotope is that the fast flux content in the BeO must reproduce the same level of n, 2n reaction as the multigroup. The latter is added to group one as a negative absorption. The value, -8×10^{-3} barn, produces 85% of the 15-group (n, 2n) reaction.

The 5- and 15-group runs are compared in Tables 5-X and 5-XI. The correspondence of individual components of the balance appears fairly close. The higher k_{eff} of the 15-group is accounted for primarily by the reduced leakage in this case.

Spectrum plots at 530 and 3000°R are shown in Figures 5-7 and 5-8.

BERYLLIUM

The LAMS 2491 24-group cross sections for Beryllium are listed for 530, 2120, and 4240°R only. The four sets required are 530, 1000, 1500, and 2000°R. Therefore, the 1000 and 1500°R values must be interpolated. Both lie between given data points, (at 530 and 2120°R). The complete carbon plots of all cross sections vs temperature are an aid since the general shape of the curves for the two isotopes are similar. This helps estimate the degree of curvature between

Table 5-X.

Comparison of 15- with 5-group BeO for a 48-in. radius cavity with 24 in. of BeO at 530°R.

Run 89, $\epsilon = 0.0001$, $N = 1.6 \times 10^{-6}$, $k_{eff} = 1.0521$, 15-group

Groups	Plutonium $\phi(u)\Delta u$	Fission neutrons	Plutonium absorption	BeO $\phi(u)\Delta u$	BeO absorption
1 through 6	315.8	0.0028	0.0010	60.6	-0.1055
7 through 11	(228.0)	(0.0193)	(0.0109)	(91.0)	(0.0008)
12	(41.2)	(0.0519)	(0.0296)	(35.4)	(0.0049)
7 through 12	269.2	0.0712	0.0405	126.4	0.0057
13	89.7	0.225	0.127	158.8	0.0436
14	159.8	0.415	0.198	310.8	0.1577
15	73.6	0.339	0.159	167.6	0.138
Totals		1.053	0.5255		0.239

Normalized leakage neutrons = 0.230

Run 38, $\epsilon = 0.0001$, $N = 1.6 \times 10^{-6}$, $k_{eff} = 1.0042$, 5-group

Groups	Plutonium $\phi(u)\Delta u$	Fission neutrons	Plutonium absorption	BeO $\phi(u)\Delta u$	BeO absorption
1	293.6	0.0026	0.0010	78.6	-0.0863
2	23.7	0.1024	0.0569	16.4	0
3	65	0.1627	0.0920	115.2	0.0316
4	135	0.3507	0.1677	277.6	0.1409
5	83.8	0.3859	0.1809	201.4	0.1658
		1.0043	0.4985		0.2520

Normalized leakage neutrons = 0.246

Table 5-XI.

Comparison of 15- with 5-group BeO for a 48-in. radius cavity with 24 in. of BeO at 3000°R.

Run 53, $\epsilon = 0.0001$, $N = 1.7 \times 10^{-6}$, $k_{eff} = 1.016$, 15-group

Groups	Plutonium $\phi(u)\Delta u$	Fission neutrons	Plutonium absorption	BeO $\phi(u)\Delta u$	BeO absorption
1 through 6	315.7	0.00295	0.0011	60.6	-0.1056
7 through 11	(255.5)	(0.0272)	(0.0154)	(106.6)	(0.0012)
12	(152.3)	(0.2038)	(0.116)	(243.8)	(0.0335)
7 through 12	407.8	0.2310	0.1314	350.4	0.0347
13	185.3	0.493	0.279	367.2	0.101
14	91.4	0.252	0.121	184.5	0.0937
15	7.6	0.037	0.017	17.2	0.0142
Totals		1.01595	0.5495		0.1380

Normalized leakage neutrons = 0.306

Run 35, $\epsilon = 0.0001$, $N = 1.8 \times 10^{-6}$, $k_{eff} = 1.011$, 5-group

Groups	Plutonium $\phi(u)\Delta u$	Fission neutrons	Plutonium absorption	BeO $\phi(u)\Delta u$	BeO absorption
1	294	0.0029	0.00108	78.6	-0.0863
2	23	0.112	0.0624	16.3	0
3	201	0.565	0.3196	435	0.119
4	99	0.289	0.1383	218	0.1097
5	8.1	0.042	0.0198	20.4	0.0168
		1.0109	0.54118		0.1592

Normalized leakage neutrons = 0.293

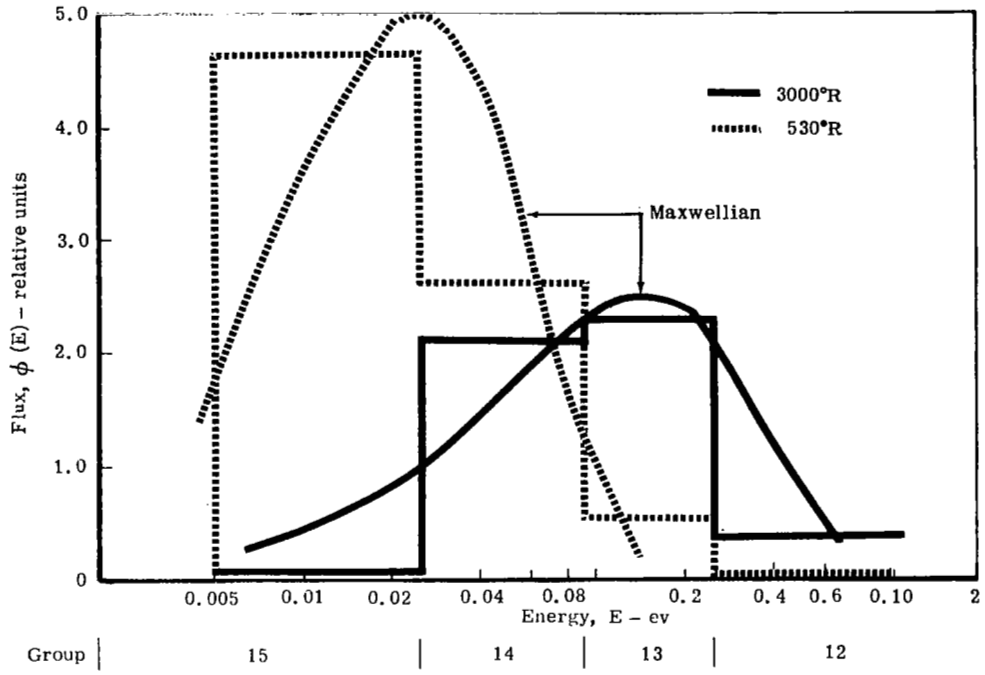

Figure 5-7. Four thermal group vs Maxwellian spectra—48-in. cavity radius and 24-in. BeO reflector.

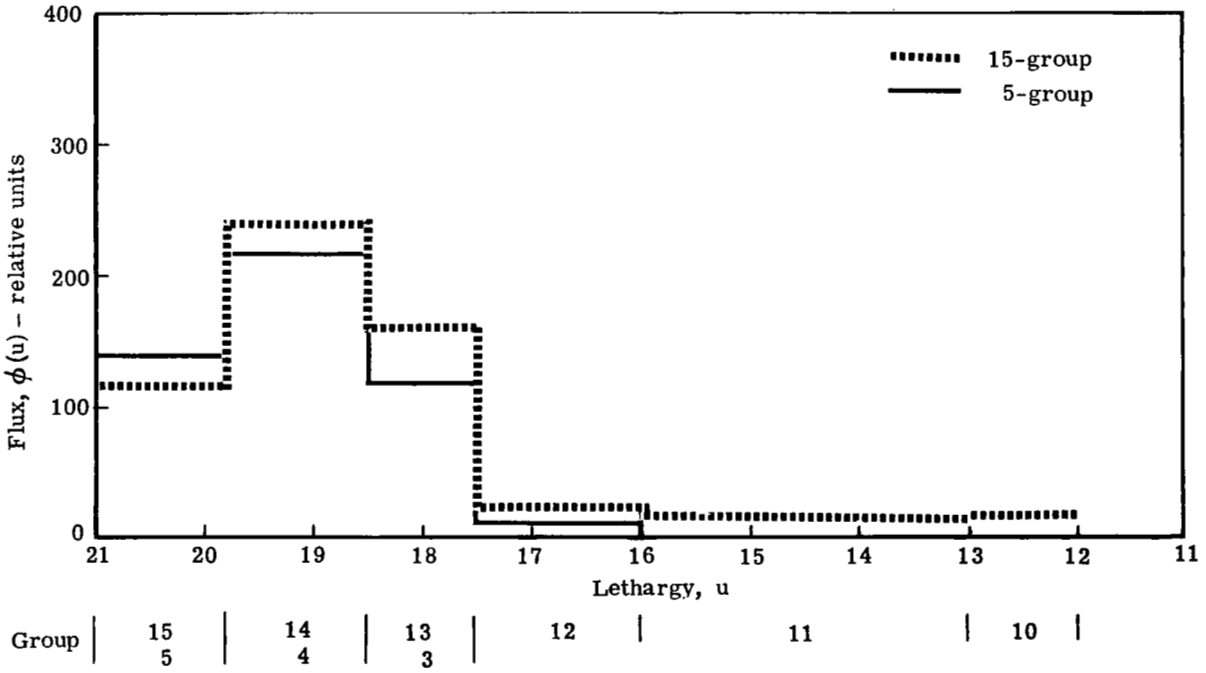

Figure 5-8. Thermal spectrum in 530°R BeO for a 48-in. radius cavity with a 24-in. reflector.

530 and 2120°R on the Beryllium plots. Since the temperature variation of the downscattering values vary slowly with temperature, the error in interpolation is further reduced. A cross check was made by plotting the resulting values of σ_{gg} vs temperature, since the latter characteristically produces smooth curves.

NIOBIUM

Niobium was chosen for an absorber since it is a reasonable construction material for the temperature considered and is available in 24-group cross sections from LAMS 2941. Since it is a heavy atom, it is reducible into fewer groups with little trouble.

The mean thermal absorption cross section at 530°R is equal to the value in group 23. For 1.58 cm of absorber thickness, the niobium number density required to produce a $\Sigma_a t$ of 0.066 is

$$N = 0.066/(1.16)(1.58) \qquad (5\text{-}19)$$
$$= 0,03597$$

The downscattering is constant for all groups at 0.014 barn. There is no upscattering, and the self-scattering (σ_{gg}) is also constant for this heavy isotope. The values of σ_a vary as 1/v.

The reduced groups are obtained by lethargy-weighting the absorption and transport numbers, then calculating new self-scattering terms from the total cross section balance.

HYDROGEN

The LAMS 24-group hydrogen at 1190°R (0.056 ev) is the basis the 5-group set used in this study. To test the reduced cross sections, the multigroup was used in combination with 1000°R D_2O in a 48-in. spherical cavity problem. The hydrogen is located in a 12-cm layer next to the plutonium, with 24 in. of D_2O added to make a total reflector thickness of 73 cm. By producing the same critical load, the neutron balances, etc, of the 5- and 24-group are available for comparison.

The result of this comparison, Table 5-XII, is a good example of the group collapsing method used. Although the 5-group reproduces the neutron balance and estimates the same flux levels as the 24-group, both spectra are shifted to the low energy side of 1190°R. This is caused by the 1000°R D_2O being too soft in both cases due to insufficient upscattering.

Table 5-XII.

Comparison of hydrogen spectrum in 24- and 5-group.

24-group			5-group		
Groups	Hydrogen $\phi(u)\Delta u$	Hydrogen absorption	Groups	Hydrogen $\phi(u)\Delta u$	Hydrogen absorption
1 through 13	76.50	0.0005	1	78.8	0
14 through 16	4.35	0.0002	2	3.7	0.0002
17 through 19	12.54	0.0012	3	14.2	0.0013
20 through 22	26.90	0.0045	4	28.5	0.0049
23 and 24	11.11	0.0031	5	10.8	0.0031

$N—3.45 \times 10^{-6}$
$k_{eff}—0.999$
Plutonium absorption—0.500
Leakage—0.477
$\epsilon—0.002$

$N—3.45 \times 10^{-6}$
$k_{eff}—1.008$
Plutonium absorption—0.502
Leakage—0.460
$\epsilon—0.002$

The first transfer cross section and fast transport—$\sigma_{1\to 2}$ and σ_{tr_1}—are obtained from the known fission group macroscopic cross sections of H_2O at 530°R.

The best values of the latter are

$\Sigma_R (H_2O) = 0.0656/cm$
$\Sigma_{tr} (H_2O) = 0.170/cm$
$\Sigma_s (H_2O) = 0.375/cm$

These are divided as follows:

$\Sigma_{tr} (H_2) = 0.103$ $\quad$ $\Sigma_{tr} (O) = 0.067$
$\Sigma_s (H_2) = 0.308$ $\quad$ $\Sigma_s (O) = 0.067$

At an H_2O density of 0.033, the microscopic cross sections for atomic hydrogen are, therefore,

$$\sigma_{tr} = (0.103)(0.5)/0.033 \quad (5\text{-}20)$$

$$= 1.56 \text{ barns}$$

$$\sigma_{1\to 2} = (0.308/0.375)(0.0656/0.033)(0.5) \quad (5\text{-}21)$$

$$= 0.81 \text{ barn}$$

The thermal transport numbers are obtained by the formula

$$1/\sigma_{tr} = (1/\Delta u)\int \left[du/\sigma_{tr}(u)\right] \quad (5\text{-}22)$$

and, similarly, for the absorptions,

$$\sigma_a = (1/\Delta u)\int \sigma_a(u)\, du \quad (5\text{-}23)$$

The transport cross section for group 2 is 6.66 barns—the value which covers most of the resonance range in the 24-group set.

DEVELOPMENT OF 3- AND 13-GROUP CROSS SECTIONS

A consistent set of cross sections with 15-, 13-, and 3-group structures was prepared for use with the calculations performed for Paragraph J in Section III. Specifications for 13- and 3-group structures are given in Table 5-XIII. These specifications are in addition to those given in Table 5-I. The basic 24-group cross sections for carbon and D_2O used for Paragraph A calculations were used as a standard for forming the cross sections as well as for rechecking existing 15-group sets. In particular, BeO 15-group fuel worth was rechecked and the original values were verified. However, for group 12, in a 3000°R BeO-D_2O, Paragraph C-type combination reflector, the fuel absorption cross section for BeO alone is 750 instead of 1000 barns as used previously. Thus, high-temperature BeO tends to lower the "effective" value of the Pu cross section even in the presence of 1000°R D_2O. Various Pu resonance absorption cross-section values for the reflector materials are listed in Table 5-XIV.

The 15-group, 1000°R D_2O values have been improved mainly by increasing the removal cross sections in the epithermal and thermal groups. The final changes were made by trial to force the 15-group, 1000°R spectrum close to the 24-group results. The formula in Equation (5-1b) is too approximate to give the necessary accuracy. Surprisingly, Equation (5-1a), the actual flux weighted formula, does not improve the results significantly.

Table 5-XIII.

13- and 3-group specifications.

13-group			3-group	
Group	V (cm/sec × 10^8)	u	Group	V (cm/sec × 10^8)
1	28.5	1.204		
2	19.9	1.966		
3	14.7	2.408	1	14.7
4	11.0	3.219		
5	6.7	4.605		
6	2.7	6.377		
7	1.237	8.0		
8	0.5071	10.0		
9	0.1866	12.0		
10	0.0854	13.0	2	0.1866
11	0.0372	16.0		
12	0.0106	17.5		
13 (thermal)	{ 0.00535 (3000°R) 0.00309 (1000°R) }	20.0	3 (thermal)	{ 0.00535 (3000°R) 0.00309 (1000°R) }

With the tabulated values of group 12 fuel worth and the revised 1000°R D_2O cross section, a Paragraph C-type run was made. The fuel concentration was the same as that used in the original calculations for Paragraph C, and k_{eff} changed from 1.011487 to 1.019082. From a criticality standpoint, this difference in k_{eff} is not significant, but the spectrum was improved substantially with respect to a Maxwellian and the 24-group structure.

The 24-group, 3000°R carbon cross sections were used to check fuel worth for the 15-group, 3000°R BeO. In particular, the fuel worth in group 12 for 15-group BeO was estimated from the 24-group carbon runs since group 12 includes the Pu resonance peak or groups 14, 15, and 16 of the 24-group structure. Although these are thermal groups, the different moderator materials and temperatures can require different group-12 values when it is attempted to approximate multigroup results with reduced groups. This is illustrated by the runs listed in Table 5-XV. The fuel density (Column 2) in the carbon (second run) is equal to that for the D_2O (first run), but the effective cross section (Column 6) is less by half. The third run tabulated using carbon (Column 6) shows the drastic self-shielding due to high fuel concentration.

Table 5-XIV.

Pu resonance absorption cross sections used for Paragraph J analysis.

Structure	Group number	σ_a (barns)
15-group		
D_2O	12	1000
D_2O-hydrogen	12	1000
D_2O-BeO	12	750
BeO	12	450
13-group		
D_2O	12	1000
D_2O-hydrogen	12	1000
D_2O-BeO	12	2000
BeO	12	1000
3-group		
D_2O	2	216
D_2O-hydrogen	2	216
D_2O-BeO	2	500
BeO	2	216

Table 5-XV.

Effect of materials and Pu concentrations on group-averaged cross sections.

	1	2	3	4	5	6	7	8	9
			← Groups 14, 15, and 16 →						
Criticality run	k_{eff}	$N_{Pu} \times 10^{-24}$	Absorption Pu	Flux in Pu, ϕ_{total}	Flux in reflector, ϕ_{total}	$\bar{\sigma}_{Pu}$ (barns)	$\bar{\sigma}_{Pu}\phi_{total}$ (absorptions/atom)	* $\phi_{14,15,16}/\phi_{13}$	Resonance, $\xi\Sigma_s$
1 D_2O, 1000°R, 48-36, 24-group	1.000	1.86×10^{-6}	0.0426	16.0	16.3	1470	0.237×10^5	1.56	0.1320
2 Carbon, 3000°R, 72-36, 24-group	1.015	1.82×10^{-6}	0.3090	236	589	722	1.7×10^5	24.7	0.0622
3 Carbon, 3000°R, 48-24, 24-group	0.998	1.91×10^{-5}	0.264	38	235	366	0.138×10^5	2.0	0.0622
4 D_2O, 1000°R 48-36, 24-group	1.000	3.65×10^{-6}	0.0574	12.5	15.8	1285	0.160×10^5	0.90	0.1320
5 BeO, 3000°R, 48-24, 15-group	1.025	1.7×10^{-6}	0.155	203	328	450	0.915×10^5	ϕ_{11}/ϕ_{12} 23.2	0.1170

*Ratio of flux levels in reflector = $\frac{\text{average flux level—groups 14, 15, and 16}}{\text{flux level—group 13}}$

The fourth run listed, using D_2O, which has a relatively flat flux in groups 13 to 16 (Column 8), shows in Column 6 what the group 12 cross section of the 15-group set should be. This case of pure slowing down gives the following core flux per unit slowing down density in the reflector.

$$\frac{\text{core flux, group 12}}{\xi\Sigma_s \times D_2O \text{ flux, group 12}} = \frac{12.5}{0.1320 \times 15.8} = 6.0$$

The fifth run, which used the 15-group, 3000°R BeO cross section with 450 barn Pu cross section value in group 12, has nearly the same fuel concentration as the carbon of the second run. The group 12 flux in the BeO is estimated by

$$\phi_{12}\,(\text{carbon}) \left(\frac{\xi\Sigma_s \text{ carbon}}{\xi\Sigma_s \text{ BeO}}\right) = 589 \times \frac{0.0622}{0.1170} = 313$$

The value 313 compares with the tabulated value of 329. The corresponding flux in the plutonium for this group is, therefore,

$$6.0 \times 0.117 \times 313 = 220$$

The value 220 compares with the tabulated value of 203. Referring to the second and fifth runs, the flux in the reflector drops from 589 to 329. The fuel absorptions are found by

$$\text{Pu absorptions, group 12 BeO} = 0.56 \times 0.309 = 0.173$$

The value 0.173 compares with the tabulated value of 0.155. From these approximations, the equivalent fuel cross section for thermal group 12 in the 15-group BeO core is

$$\frac{0.173}{220 \times 1.7 \times 10^{-6}} = 463 \text{ barns}$$

For the actual BeO-reflected cores of Paragraph A and for Paragraph J, the value of 450 barns was used as the absorption cross section of Pu in group 12. For the 15-group D_2O, 1000 barns was used. This value is 28% under the flat flux value of the fourth run (Column 6 in Table 5-XV). Note that at the same fuel density and temperature, BeO and carbon have the same shape spectrum at the high thermal end—i.e., the flux rises out of the resonance region by about the same ratio in both cases. This is shown in the second and fifth runs (Column 8 of Table 5-XV).

The resonance parameters, Column 9, for D_2O (runs one and four) at 1000°R and BeO (run five) at 3000°R are nearly equal. Also, the Pu atom densities are within a factor of 2.5, using each reflector in the same core geometry. It is possible to assume, therefore, that the fuel worth of group 12 when treated as a slowing down region in the BeO case is the same value as used for D_2O (1000°R)—i.e., 1000 barns. This is the value used in the 13-group fuel for BeO cores.

13-Group Cross Sections

As the first step in making the 13-group cross sections, the thermal cross sections are obtained as follows from 48-24, Paragraph A-type runs:

- 1000°R 24-group D_2O, 8 thermal groups averaged
  24-group Pu, 8 thermal groups averaged
- 3000°R 15-group BeO, 4 thermal groups averaged
  15-group Pu, 4 thermal groups averaged

This procedure automatically yields the correct thermal fuel cross section for each reflector temperature. The hydrogen thermal cross sections at 1000°R were obtained from Paragraph C-type criticality calculations that were made using both 24- and 15-group cross sections. Hydrogen was used in combination with 1000°R D_2O and Pu—i.e., 12 cm of hydrogen and 24 in. of D_2O. These were the same computations used to form the original 15-group hydrogen cross sections.

In the 13-group set, groups 1 through 11 are identical with those of the 15-group structure for each material. Using the thermal values obtained, the epithermal group between fast and thermal—i.e., group 12—is formed as follows.

1. The transport numbers are taken from thermal group 12 of the 15-group cross sections.

2. The removal cross section, $\sigma_{12\rightarrow 13}$, and σ_{gg} of group 12 are adjusted to reproduce 15- and 24-group results.

3. The group 12 value of Pu is taken as the slowing down value (Column 6 of Table 5-XV).

4. The material cross sections derived separately are used in Paragraph C-type runs using plutonium cross sections weighted by 1000°R D_2O to determine the effect of the materials on each other.

A comparison of the 13-group D_2O-BeO combination reflector with the equivalent 15-group solution shows that the epithermal group 12 fuel worth should increase by a factor of about two over that of the 1000°R D_2O weighted plutonium. This is similar to the situation with the 15-group value when that combination of materials is used, although in the latter case, group 12 is a thermal group.

A further comparison with 15-group results shows that the high-temperature BeO can reduce the average thermal fuel cross section by about 50 barns. However, the comparison between the 13- and 15-group criticality calculation appears to check well enough without this correction. See Table 5-XVII. Therefore, in D_2O-BeO combinations, the neutron temperature in the fuel is assumed equal to that in the D_2O.

3-Group Cross Sections

The one-thermal group cross sections used in the 13-group set are used for the 3-group set for all isotopes. The reduction of the remaining 12 groups of the 13-group set to two—one fast and one intermediate—requires the following steps.

1. The fuel cross sections for group 1 are obtained from the average of groups 1 through 8 of the 24-group set.

2. The fuel cross section for group 2 is obtained by lethargy scaling the group 12 value of the 13-group set—i.e., 1:4.

3. The groups 1 and 2 transport cross sections for D_2O (1000°R) and hydrogen (1190°R) are obtained from 24-group averages and the BeO (3000°R) values from the 15-group set.

4. The fast group removal cross sections for D_2O and BeO are estimated from the fast transport cross sections and the age to thermal. The value for hydrogen is the same as derived previously (page 5-27).

5. The removal cross section from group 2 to group 3 is estimated to be the reciprocal of the total flux in intermediate groups 9 through 12 of the 13-group criticality calculations.

The results of cross section check runs for Paragraph J are listed in Tables 5-XVI, 5-XVII, 5-XVIII and 5-XIX. In the cases where 3000°R BeO is present, the 13-group run is listed in an alternate form to compare it directly with 15-group results. This is done by adding the group 12 values to the thermal range to make the comparison.

Table 5-XVI.

Paragraph A-type cross section check calculations—D_2O relector.

	24	15	13	3
k_{eff}	1.000408	0.9949720	0.9991506	1.000610
ϵ	0.0001	0.0001	0.0001	0.0001
N	3.65×10^{-6}	3.65×10^{-6}	3.65×10^{-6}	3.65×10^{-6}
Leakage	0.4639	0.4731	0.4629	0.4637
Absorptions	0.5327	0.5252	0.5371	0.5363
$\bar{\eta}$	1.92	1.95	1.91	1.91
Fission neutrons				
Thermal	0.8710	0.8603	0.8853	0.8849
Resonance	0.1230	0.1294	0.1077	0.1102
Fast	0.0060	0.0054	0.0061	0.0056
Total flux				
Pu	462	474	469	492
D_2O	491	501	510	514
Thermal flux				
Pu	132	135	134	134
D_2O	362	364	378	360
Resonance flux				
Pu	77	86	82	78
D_2O	59	68	63	60
Fast flux				
Pu	253	253	253	280
D_2O	70	69	69	94
Absorptions				
Pu	0.5213	0.5132	0.5250	0.5248
D_2O	0.0114	0.0121	0.0121	0.0115

Table 5-XVII.

Paragraph A-type cross section check calculations—BeO reflector.

	3	13	13*	15
k_{eff}	1.024142	1.026613	1.026613	1.025307
ϵ	0.0001	0.0001	0.0001	0.0001
N	1.7×10^{-6}	1.7×10^{-6}	1.7×10^{-6}	1.7×10^{-6}
Leakage	0.3187	0.3121	0.3121	0.3222
Absorptions	0.6812	0.6879	0.6879	0.6844
$\bar{\eta}$	1.77	1.77	1.77	1.785
Fission neutrons				
Thermal	0.9405	0.9453	1.0036	1.0018
Resonance	0.0792	0.0768	0.0185	0.0188
Fast	0.0044	0.0045	0.0045	0.0045
Total flux				
Pu	1036	998	998	1013
BeO	991	989	989	1001
Thermal flux				
Pu	444	447	466	470
BeO	811	831	843	849
Resonance flux				
Pu	120	141	122	133
BeO	57	65	53	59
Fast flux				
Pu	472	410	410	410
BeO	123	93	93	93
Absorptions				
Pu	0.5633	0.5655	0.5655	0.5603
BeO	0.1179	0.1224	0.1224	0.1241

*Thermals include group 12.

Table 5-XVIII.

Paragraph C-type cross section check calculations—D_2O-BeO reflector.

	3	13	13*	15
k_{eff}	1.013869	1.015933	1.015933	1.019082
ϵ	0.0001	0.0001	0.0001	0.0001
N	8.5×10^{-7}	8.5×10^{-7}	8.5×10^{-7}	8.5×10^{-7}
Leakage	0.2567	0.2560	0.2560	0.2574
Absorptions	0.7433	0.7439	0.7439	0.7352
$\bar{\eta}$	1.89	1.88	1.88	1.91
Fission neutrons				
Thermal	0.9369	0.9425	1.0076	1.015
Resonance	0.0757	0.0720	0.0069	0.0070
Fast	0.0014	0.0015	0.0015	0.0015
Total flux				
Pu	998	989	989	1048
D_2O	309	309	309	323
BeO	881	880	880	875
Thermal flux				
Pu	608	612	634	691
D_2O	221	222	230	243
BeO	828	829	835	828
Resonance flux				
Pu	104	109	87	89
D_2O	33	35	27	28
BeO	31	28	22	24
Fast flux				
Pu	291	268	268	268
D_2O	57	52	52	52
BeO	26	23	23	23
Absorption				
Pu	0.5310	0.5326	0.5326	0.5237
D_2O	0.0071	0.0071	0.0071	0.0067
BeO	0.2052	0.2042	0.2042	0.2050

*Thermals include group 12.

Table 5-XIX.

Paragraph C-type cross section check calculations—hydrogen substituted for D_2O.

	3	13	15	24
k_{eff}	0.9991596	0.9963269	0.9875847	0.9887886
ϵ	0.0001	0.0001	0.0001	0.0001
N	4.25×10^{-6}	4.25×10^{-6}	4.25×10^{-6}	4.25×10^{-6}
Leakage	0.4562	0.4564	0.4696	0.4613
Absorption	0.5438	0.5436	0.5312	0.5351
$\overline{\eta}$	1.91	1.91	1.96	1.94
Fission neutrons				
Thermal	0.8933	0.8913	0.8673	0.8806
Resonance	0.1003	0.0992	0.1087	0.1023
Fast	0.0055	0.0058	0.0058	0.0058
Total flux				
Pu	414	394	399	390
H	133	126	127	125
D_2O	514	510	504	495
Thermal flux				
Pu	116	116	119	117
H	44	44	44	44
D_2O	366	384	373	373
Resonance flux				
Pu	61	67	69	62
H	21	23	24	22
D_2O	58	60	65	56
Fast flux				
Pu	237	211	211	211
H	68	59	59	59
D_2O	90	66	66	66
Absorption				
Pu	0.5237	0.5231	0.5103	0.5162
H	0.0084	0.0081	0.0085	0.0072
D_2O	0.0118	0.0123	0.0124	0.0117

Table 5-XX.

Index to cross-sections.

Table 5-XX (cont)

Pu		24-Group		Paragraph "A, B, & C"			
2.07	6.612	4.25	0.0	0.0	0.0	0.0	1.69
0.0	0.0	0.0	0.0				
2.15	6.026	4.5	0.0	0.0	0.0	0.0	1.42
.2	0.0	0.0	0.0				
2.05	5.472	4.8	0.0	0.0	0.0	0.0	2.09
.18	.27	0.0	0.0				
1.81	4.981	5.7	0.0	0.0	0.0	0.0	3.55
.3	.35	.31	0.0				
1.84	4.81	8.4	0.0	0.0	0.0	0.0	5.51
.29	.3	.35	.31				
2.53	5.83	12.	0.0	0.0	0.0	0.0	9.4
.05	.05	.06	.05				
4.99	8.7	15.	0.0	0.0	0.0	0.0	9.94
.07	0.0	0.0	0.0				
5.99	11.6	16.0	0.0	0.0	0.0	0.0	9.94
.07	0.0	0.0	0.0				
23.99	43.5	34.	0.0	0.0	0.0	0.0	9.94
.07	0.0	0.0	0.0				
15.99	29.	26.	0.0	0.0	0.0	0.0	9.94
.07	0.0	0.0	0.0				
152.	252.	162.01	0.0	0.0	0.0	0.0	9.94
.07	0.0	0.0	0.0				
65.99	95.7	76.	0.0	0.0	0.0	0.0	9.94
.07	0.0	0.0	0.0				
24.99	62.64	35.	0.0	0.0	0.0	0.0	9.94
.07	0.0	0.0	0.0				
221.	420.5	231.01	0.0	0.0	0.0	0.0	9.94
.07	0.0	0.0	0.0				
1650.0	3025.0	1660.02	0.0	0.0	0.0	0.0	9.95
0.07	0.0	0.0	0.0				
5060.0	8870.0	5070.02	0.0	0.0	0.0	0.0	9.95
0.07	0.0	0.0	0.0				
1775.0	2960.0	1785.02	0.0	0.0	0.0	0.0	9.95
0.07	0.0	0.0	0.0				
1082.0	1750.0	1092.02	0.0	0.0	0.0	0.0	9.95
0.07	0.0	0.0	0.0				
773.0	1415.0	783.02	0.0	0.0	0.0	0.0	9.95
0.07	0.0	0.0	0.0				
703.0	1455.0	713.02	0.0	0.0	0.0	0.0	9.95
0.07	0.0	0.0	0.0				
815.0	1715.0	825.02	0.0	0.0	0.0	0.0	9.95
0.07	0.0	0.0	0.0				
963.0	2040.0	973.02	0.0	0.0	0.0	0.0	9.95
0.07	0.0	0.0	0.0				
1072.0	2270.0	1082.02	0.0	0.0	0.0	0.0	9.95
0.07	0.0	0.0	0.0				
1405.0	3000.0	1415.00	0.0	0.0	0.0	0.0	10.0
0.07	0.0	0.0	0.0				

Table 5-XX (cont)

Pu	σResonance	450[b]	15-Group	Paragraph "A & B"	BeO only		
2.07	6.612	4.25	0.0	1.09	0.0	0.0	0.0
0.0							
2.15	6.026	4.5	0.0	1.42	.2	0.0	0.0
0.0							
2.05	5.472	4.8	0.0	2.09	.16	.27	0.0
0.0							
1.81	4.981	5.7	0.0	3.55	.3	.35	.31
0.0							
1.64	4.81	8.4	0.0	6.51	.29	.3	.35
.31							
2.53	5.83	12.	0.0	9.4	.05	.05	.06
.05							
4.99	8.7	15.	0.0	9.94	.07	0.0	0.0
0.0							
5.99	11.6	16.	0.0	9.94	.07	0.0	0.0
0.0							
23.99	43.5	34.	0.0	9.94	.07	0.0	0.0
0.0							
15.99	29.	26.	0.0	9.94	.07	0.0	0.0
0.0							
81.	142.0	91.01	0.0	9.94	.07	0.0	0.0
0.0							
450.0	787.5	460.01	0.0	9.94	.07	0.0	0.0
0.0							
884.9	1565.	894.9	0.0	9.93	.07	0.0	0.0
0.0							
775.9	1622.	785.9	0.0	9.93	.07	0.0	0.0
0.0							
1349.	2878.	1359.	0.0	10.	.07	0.0	0.0
0.0							

Table 5-XX (cont)

Pu	σ Resonance	1000[b]	15-Group	Paragraph "C"			
2.07	6.612	4.25	0.0	1.09	0.0	0.0	0.0
0.0							
2.15	6.026	4.5	0.0	1.42	.2	0.0	0.0
0.0							
2.05	5.472	4.8	0.0	2.09	.18	.27	0.0
0.0							
1.81	4.981	5.7	0.0	3.55	.3	.35	.31
0.0							
1.84	4.81	8.4	0.0	6.51	.29	.3	.35
.31							
2.53	5.83	12.	0.0	9.4	.05	.05	.06
.05							
4.99	8.7	15.	0.0	9.94	.07	0.0	0.0
0.0							
5.99	11.6	16.	0.0	9.94	.07	0.0	0.0
0.0							
23.99	43.5	34.	0.0	9.94	.07	0.0	0.0
0.0							
15.99	29.	26.	0.0	9.94	.07	0.0	0.0
0.0							
81.	142.0	91.01	0.0	9.94	.07	0.0	0.0
0.0							
750.0	1327.0	760.01	0.0	9.94	.07	0.0	0.0
0.0							
884.9	1565.	894.9	0.0	9.93	.07	0.0	0.0
0.0							
775.9	1622.	785.9	0.0	9.93	.07	0.0	0.0
0.0							
1349.	2878.	1359.	0.0	10.	.07	0.0	0.0
0.0							

Table 5-XX (cont)

Pu	σ Resonance	750[b]	15-Group	Paragraph "J"			
2.07	6.612	4.25	0.0	1.09	0.0	0.0	0.0
0.0							
2.15	6.026	4.5	0.0	1.42	.2	0.0	0.0
0.0							
2.05	5.472	4.8	0.0	2.09	.18	.27	0.0
0.0							
1.81	4.981	5.7	0.0	3.55	.3	.35	.31
0.0							
1.84	4.81	8.4	0.0	5.51	.29	.3	.35
.31							
2.53	5.83	12.	0.0	9.4	.05	.05	.06
.05							
4.99	8.7	15.	0.0	9.94	.07	0.0	0.0
0.0							
5.99	11.6	16.	0.0	9.94	.07	0.0	0.0
0.0							
23.99	43.5	34.	0.0	9.94	.07	0.0	0.0
0.0							
15.99	29.	26.	0.0	9.94	.07	0.0	0.0
0.0							
81.	142.0	91.01	0.0	9.94	.07	0.0	0.0
0.0							
750.0	1327.0	760.01	0.0	9.94	.07	0.0	0.0
0.0							
884.9	1565.	894.9	0.0	9.93	.07	0.0	0.0
0.0							
775.9	1622.	785.9	0.0	9.93	.07	0.0	0.0
0.0							
1349.	2878.	1359.	0.0	10.	.07	0.0	0.0
0.0							

Table 5-XX (cont)

Pu σResonance 1000[b] 13-Group Paragraph "A"

2.07	6.612	4.25	0.0	1.09	0.0	0.0	0.0
0.0							
2.15	6.026	4.5	0.0	1.42	.2	0.0	0.0
0.0							
2.05	5.472	4.8	0.0	2.09	.18	.27	0.0
0.0							
1.81	4.981	5.7	0.0	3.55	.3	.35	.31
0.0							
1.84	4.81	8.4	0.0	6.51	.29	.3	.35
.31							
2.53	5.83	12.	0.0	9.4	.05	.05	.06
.05							
4.99	8.7	15.	0.0	9.94	.07	0.0	0.0
0.0							
5.99	11.6	16.	0.0	9.94	.07	0.0	0.0
0.0							
23.99	43.5	34.	0.0	9.94	.07	0.0	0.0
0.0							
15.99	29.	26.	0.0	9.94	.07	0.0	0.0
0.0							
81.0	142.0	91.01	0.0	9.94	.07	0.0	0.0
0.0							
1000.0	1770.0	1010.01	0.0	9.94	.07	0.0	0.0
0.0							
945.0	1813.0	955.0	0.0	10.0	.07	0.0	0.0
0.0							

Pu σResonance 2000[b] 13-Group Paragraph "J"

2.07	6.612	4.25	0.0	1.09	0.0	0.0	0.0
0.0							
2.15	6.026	4.5	0.0	1.42	.2	0.0	0.0
0.0							
2.05	5.472	4.8	0.0	2.09	.18	.27	0.0
0.0							
1.81	4.981	5.7	0.0	3.55	.3	.35	.31
0.0							
1.84	4.81	8.4	0.0	6.51	.29	.3	.35
.31							
2.53	5.83	12.	0.0	9.4	.05	.05	.06
.05							
4.99	8.7	15.	0.0	9.94	.07	0.0	0.0
0.0							
5.99	11.6	16.	0.0	9.94	.07	0.0	0.0
0.0							
23.99	43.5	34.	0.0	9.94	.07	0.0	0.0
0.0							
15.99	29.	26.	0.0	9.94	.07	0.0	0.0
0.0							
81.0	142.0	91.01	0.0	9.94	.07	0.0	0.0
0.0							
2000.0	3540.0	2010.01	0.0	9.94	.07	0.0	0.0
0.0							
945.0	1813.0	955.0	0.0	10.0	.07	0.0	0.0
0.0							

Table 5-XX (cont)

Pu 5-Group Paragraph "D, E, & F"

2.05	5.472	4.8	0.0	2.68	0.0
1500.	2700.	1510.	0.0	9.93	.07
884.9	1565.0	894.9	0.0	9.93	.07
775.9	1622.0	785.9	0.0	9.93	.07
1349.0	2878.0	1359.0	0.0	10.	.07

Pu 3-Group Paragraph "J"

2.05	5.472	4.8	0.0	2.68	0.0
500.0	897.0	510.0	0.0	9.98	.07
945.0	1813.0	955.0	0.0	10.0	.02

Pu 3-Group Paragraph "A" Type BeO only

2.05	5.472	4.8	0.0	2.68	0.0
216.0	387.0	226.0	0.0	9.98	.07
685.0	1245.0	695.0	0.0	10.0	.02

Pu 3-Group Paragraph "A" Type D_2O

2.05	5.472	4.8	0.0	2.68	0.0
216.0	387.0	226.0	0.0	9.98	.07
945.0	1813.0	955.0	0.0	10.0	.02

Table 5-XX (cont)

Nb 24-Group Paragraph "B"

* CO

0.0	0.0	.87	0.0	0.0	0.0	0.0	.852
0.0	0.0	0.0	0.0				
0.0	0.0	3.5	0.0	0.0	0.0	0.0	3.486
.018	0.0	0.0	0.0				
0.0	0.0	4.2	0.0	0.0	0.0	0.0	4.186
.014	0.0	0.0	0.0				
0.0	0.0	5.1	0.0	0.0	0.0	0.0	5.086
.014	0.0	0.0	0.0				
0.0	0.0	8.0	0.0	0.0	0.0	0.0	7.986
.014	0.0	0.0	0.0				
0.0	0.0	9.1	0.0	0.0	0.0	0.0	9.086
.014	0.0	0.0	0.0				
.2	0.0	9.1	0.0	0.0	0.0	0.0	8.886
.014	0.0	0.0	0.0				
.5	0.0	8.8	0.0	0.0	0.0	0.0	8.286
.014	0.0	0.0	0.0				
1.9	0.0	9.8	0.0	0.0	0.0	0.0	7.886
.014	0.0	0.0	0.0				
.39	0.0	7.19	0.0	0.0	0.0	0.0	6.786
.014	0.0	0.0	0.0				
.05	0.0	6.45	0.0	0.0	0.0	0.0	6.386
.014	0.0	0.0	0.0				
.08	0.0	6.48	0.0	0.0	0.0	0.0	6.386
.014	0.0	0.0	0.0				
.14	0.0	6.54	0.0	0.0	0.0	0.0	6.386
.014	0.0	0.0	0.0				
.22	0.0	6.62	0.0	0.0	0.0	0.0	6.386
.014	0.0	0.0	0.0				
.31	0.0	6.71	0.0	0.0	0.0	0.0	6.386
.014	0.0	0.0	0.0				
.34	0.0	6.74	0.0	0.0	0.0	0.0	6.386
.014	0.0	0.0	0.0				
.38	0.0	6.78	0.0	0.0	0.0	0.0	6.386
.014	0.0	0.0	0.0				
.44	0.0	6.84	0.0	0.0	0.0	0.0	6.386
.014	0.0	0.0	0.0				
.53	0.0	6.93	0.0	0.0	0.0	0.0	6.386
.014	0.0	0.0	0.0				
.68	0.0	7.08	0.0	0.0	0.0	0.0	6.386
.014	0.0	0.0	0.0				
.88	0.0	7.28	0.0	0.0	0.0	0.0	6.386
.014	0.0	0.0	0.0				
1.07	0.0	7.47	0.0	0.0	0.0	0.0	6.386
.014	0.0	0.0	0.0				
1.21	0.0	7.61	0.0	0.0	0.0	0.0	6.386
.014	0.0	0.0	0.0				
1.44	0.0	7.84	0.0	0.0	0.0	0.0	6.400
.014	0.0	0.0	0.0				

Table 5-XX (cont)

Nb		15-Group		Paragraph "B"			
0.0	0.0	.87	0.0	.852	0.0	0.0	0.0
0.0							
0.0	0.0	3.5	0.0	3.486	.018	0.0	0.0
0.0							
0.0	0.0	4.2	0.0	4.186	.014	0.0	0.0
0.0							
0.0	0.0	5.1	0.0	5.086	.014	0.0	0.0
0.0							
0.0	0.0	8.0	0.0	7.986	.014	0.0	0.0
0.0							
0.0	0.0	9.1	0.0	9.086	.014	0.0	0.0
0.0							
.2	0.0	9.1	0.0	8.886	.014	0.0	0.0
0.0							
.5	0.0	8.8	0.0	8.286	.014	0.0	0.0
0.0							
1.9	0.0	9.8	0.0	7.886	.014	0.0	0.0
0.0							
.39	0.0	7.19	0.0	6.736	.014	0.0	0.0
0.0							
.09	0.0	6.48	0.0	6.376	.014	0.0	0.0
0.0							
.256	0.0	6.7	0.0	6.43	.014	0.0	0.0
0.0							
.47	0.0	6.85	0.0	6.366	.014	0.0	0.0
0.0							
.848	0.0	7.28	0.0	6.418	.014	0.0	0.0
0.0							
1.405	0.0	7.7	0.0	6.295	.014	0.0	0.0
0.0							

N_b		5-Group		Paragraph "D"	
0.0	0.0	4.2	0.0	4.186	0.0
.346	0.0	5.000	0.0	4.64	.014
.47	0.0	6.85	0.0	6.366	.014
.848	0.0	7.28	0.0	6.418	.014
1.405	0.0	7.7	0.0	6.295	.014

Table 5-XX (cont)

Hydrogen 1190°R 15-Group Paragraph "J"

0.0	0.0	.6	0.0	-.89	0.0	0.0	0.0
0.0							
0.0	0.0	.93	0.0	-1.3	.8	0.0	0.0
0.0							
0.0	0.0	1.33	0.0	-1.93	.8	.25	0.0
0.0							
0.0	0.0	1.83	0.0	-1.94	1.8	.8	.25
0.0							
0.0	0.0	3.0	0.0	-1.87	2.83	1.1	.48
.19							
0.0	0.0	5.19	0.0	-2.11	4.04	.78	.3
.15							
0.0	0.0	8.33	0.0	-1.01	5.87	.67	.13
.06							
.0022	0.0	8.6622	0.0	.07	8.08	1.24	.14
.03							
.004	0.0	8.664	0.0	.503	7.48	1.1	.17
.02							
.159	0.0	8.669	0.0	-5.05	5.47	.74	.11
.02							
.026	0.0	6.66	0.0	2.384	12.01	3.12	.37
.05							
.1065	0.0	7.1	0.0	-4.5265	3.31	1.55	.573
0.0							
.1475	0.0	14.4	5.4039	8.4644	10.17	.94	0.0
0.0							
.294	0.0	19.4	28.91	10.4723	5.1721	1.35	0.0
0.0							
.407	0.0	42.6	0.0	13.283	3.2298	.616	0.0
0.0							

Table 5-XX (cont)

Hydrogen 1190°R 13-Group Paragraph "J"

0.0	0.0	.6	0.0	-.89	0.0	0.0	0.0
0.0							
0.0	0.0	.93	0.0	-1.3	.8	0.0	0.0
0.0							
0.0	0.0	1.33	0.0	-1.93	.8	.25	0.0
0.0							
0.0	0.0	1.83	0.0	-1.94	1.8	.8	.25
0.0							
0.0	0.0	3.0	0.0	-1.87	2.83	1.1	.48
.19							
0.0	0.0	5.19	0.0	-2.11	4.04	.78	.3
.15							
0.0	0.0	8.33	0.0	-1.01	5.87	.67	.13
.06							
.0022	0.0	8.6622	0.0	.07	8.08	1.24	.14
.03							
.004	0.0	8.664	0.0	-.503	7.48	1.1	.17
.02							
.159	0.0	8.669	0.0	-5.05	5.47	.74	.11
.02							
.026	0.0	6.66	0.0	3.324	12.01	3.12	.37
.05							
.1065	0.0	7.1	0.0	-4.1665	3.31	1.55	.573
0.0							
.238	0.0	19.1	0.0	18.862	11.16	0.0	0.0
0.0							

Hydrogen 1190°R 5-Group Paragraph "D, E & F"

0.0	0.0	1.56	0.0	.75	0.0
.07	0.0	6.66	0.0	-4.57	.81
.136	0.0	14.4	5.46	7.867	11.16
.244	0.0	19.4	28.95	10.461	6.397
.407	0.0	42.6	0.0	13.243	3.235

Hydrogen 1190°R 3-Group Paragraph "J"

0.0	0.0	1.56	0.0	.75	0.0
.07	0.0	6.66	0.0	3.79	.81
.238	0.0	19.1	0.0	18.862	2.80

Table 5-XX (cont)

D_2O	530°R	24-Group		Paragraph "A, B & C"			
0.0	0.0	3.33	0.0	0.0	0.0	0.0	.328
0.0	0.0	0.0	0.0				
0.0	0.0	5.45	0.0	0.0	0.0	0.0	1.319
2.13	0.0	0.0	0.0				
0.0	0.0	9.55	0.0	0.0	0.0	0.0	4.668
2.091	.52	0.0	0.0				
0.0	0.0	8.47	0.0	0.0	0.0	0.0	3.894
3.462	1.5	.352	0.0				
0.0	0.0	8.14	0.0	0.0	0.0	0.0	4.543
4.156	1.42	.54	0.0				
0.0	0.0	8.14	0.0	0.0	0.0	0.0	5.3
3.597	.42	0.0	0.0				
0.0	0.0	8.14	0.0	0.0	0.0	0.0	5.08
2.84	0.0	0.0	0.0				
0.0	0.0	8.14	0.0	0.0	0.0	0.0	5.35
3.06	0.0	0.0	0.0				
0.0	0.0	8.14	0.0	0.0	0.0	0.0	5.33
2.79	0.0	0.0	0.0				
0.0	0.0	8.14	0.0	0.0	0.0	0.0	3.52
2.41	0.0	0.0	0.0				
0.0	0.0	8.14	0.0	0.0	0.0	0.0	3.52
3.64	.40	0.0	0.0				
0.0	0.0	8.14	0.0	0.0	0.0	0.0	3.52
3.64	.98	0.0	0.0				
0.0	0.0	8.14	0.0	0.0	0.0	0.0	3.4
3.64	.98	0.0	0.0				
0.0	0.0	8.14	0.0	0.0	0.0	0.0	3.28
3.74	.98	0.0	0.0				
0.0	0.0	8.14	0.0	0.0	0.0	0.0	1.44
3.82	1.0	0.0	0.0				
0.0	0.0	8.58	0.0	0.0	0.0	0.0	1.48
5.6	1.04	0.0	0.0				
.0005	0.0	8.6	0.0	0.0	.081	1.23	3.06924
6.0	1.1	0.0	0.0				
.00055	0.0	8.88	0.0	.0005	.0187	.878	3.64735
4.249	1.1	0.0	0.0				
.000805	0.0	9.0	.0045	.0143	.122	1.58	5.057895
2.763	1.273	0.0	0.0				
.0011	0.0	9.5	.05	.246	.546	2.33	5.1135
1.8376	.6968	.00826	0.0				
.0015	0.0	10.0	0.0	.597	2.14	3.58	5.0327
1.7072	.5528	.2923	0.0				
.0019	0.0	10.5	0.0	0.0	1.095	2.98	3.0129
1.1587	.3823	.3097	.25				
.0021	0.0	11.0	0.0	0.0	0.0	1.15	2.6134
1.4399	.4343	.305	.2822				
.0025	0.0	13.0	0.0	0.0	0.0	0.0	10.1055
3.014	1.905	.9203	.3922				

Table 5-XX (cont)

D_2O	650°R	24-Group		Paragraph "A, B & C"			
0.0	0.0	8.33	0.0	0.0	0.0	0.0	.328
0.0	0.0	0.0	0.0				
0.0	0.0	8.45	0.0	0.0	0.0	0.0	1.319
2.13	0.0	0.0	0.0				
0.0	0.0	8.55	0.0	0.0	0.0	0.0	4.668
2.091	.52	0.0	0.0				
0.0	0.0	8.47	0.0	0.0	0.0	0.0	3.894
3.462	1.5	.352	0.0				
0.0	0.0	8.14	0.0	0.0	0.0	0.0	4.543
4.156	1.42	.54	0.0				
0.0	0.0	8.14	0.0	0.0	0.0	0.0	5.3
3.597	.42	0.0	0.0				
0.0	0.0	8.14	0.0	0.0	0.0	0.0	5.08
2.84	0.0	0.0	0.0				
0.0	0.0	8.14	0.0	0.0	0.0	0.0	5.35
3.06	0.0	0.0	0.0				
0.0	0.0	8.14	0.0	0.0	0.0	0.0	5.33
2.79	0.0	0.0	0.0				
0.0	0.0	8.14	0.0	0.0	0.0	0.0	3.52
2.41	0.0	0.0	0.0				
0.0	0.0	8.14	0.0	0.0	0.0	0.0	3.52
3.64	.40	0.0	0.0				
0.0	0.0	8.14	0.0	0.0	0.0	0.0	3.52
3.64	.98	0.0	0.0				
0.0	0.0	8.14	0.0	0.0	0.0	0.0	3.4
3.64	.98	0.0	0.0				
0.0	0.0	8.14	0.0	0.0	0.0	0.0	3.28
3.74	.98	0.0	0.0				
0.0	0.0	8.14	0.0	0.0	0.0	0.0	1.44
3.82	1.0	0.0	0.0				
0.0	0.0	8.58	0.0	0.0	0.0	0.0	1.48
5.6	1.04	0.0	0.0				
.0005	0.0	8.6	.00005	.0025	.15	1.45	3.06969
6.0	1.1	0.0	0.0				
.00055	0.0	8.68	.00012	.0016	.0394	1.03	3.42735
4.249	1.1	0.0	0.0				
.000805	0.0	9.0	.014	.035	.224	1.86	4.836895
2.763	1.273	0.0	0.0				
.0011	0.0	9.5	.112	.414	.788	2.55	4.8103
1.8376	.6968	.00826	0.0				
.0015	0.0	10.0	0.0	.856	2.38	3.72	4.70955
1.7072	.5528	.2923	0.0				
.0019	0.0	10.5	0.0	0.0	1.29	2.91	3.08298
1.1587	.3823	.3097	.25				
.0021	0.0	11.0	0.0	0.0	0.0	1.24	2.2659
.967	.4343	.305	.2622				
.0025	0.0	13.0	0.0	0.0	0.0	0.0	9.4995
3.014	1.905	.9203	.3922				

Table 5-XX (cont)

D_2O	800°R	24-Group		Paragraph "A, B & C"			
0.0	0.0	3.33	0.0	0.0	0.0	0.0	.328
0.0	0.0	0.0	0.0				
0.0	0.0	5.45	0.0	0.0	0.0	0.0	1.319
2.13	0.0	0.0	0.0				
0.0	0.0	9.55	0.0	0.0	0.0	0.0	4.668
2.091	.52	0.0	0.0				
0.0	0.0	8.47	0.0	0.0	0.0	0.0	3.894
3.462	1.5	.352	0.0				
0.0	0.0	8.14	0.0	0.0	0.0	0.0	4.543
4.156	1.42	.54	0.0				
0.0	0.0	8.14	0.0	0.0	0.0	0.0	5.3
3.597	.42	0.0	0.0				
0.0	0.0	8.14	0.0	0.0	0.0	0.0	5.08
2.54	0.0	0.0	0.0				
0.0	0.0	8.14	0.0	0.0	0.0	0.0	5.35
3.08	0.0	0.0	0.0				
0.0	0.0	8.14	0.0	.0	0.0	0.0	5.33
2.79	0.0	0.0	0.0				
0.0	0.0	8.14	0.0	.0	0.0	0.0	3.52
2.41	0.0	0.0	0.0				
0.0	0.0	8.14	0.0	0.0	0.0	0.0	3.52
3.64	.40	0.0	0.0				
0.0	0.0	8.14	0.0	0.0	0.0	0.0	3.52
3.64	.98	0.0	0.0				
0.0	0.0	8.14	0.0	0.0	0.0	0.0	3.4
3.64	.98	0.0	0.0				
0.0	0.0	8.14	0.0	0.0	0.0	0.0	3.28
3.74	.98	0.0	0.0				
0.0	0.0	8.14	0.0	0.0	0.0	0.0	1.44
3.82	1.0	0.0	0.0				
0.0	0.0	8.58	0.0	0.0	0.0	0.0	1.48
3.8	1.04	0.0	0.0				
.0005	0.0	8.6	.0003	.0082	.236	1.67	3.06924
0.0	1.1	0.0	0.0				
.00055	0.0	8.88	.0008	.0056	.077	1.185	3.20735
4.249	1.1	0.0	0.0				
.000805	0.0	9.0	.041	.078	.372	2.11	4.595895
2.763	1.273	0.0	0.0				
.0011	0.0	9.5	.23	.635	1.07	2.8	4.5170
1.8376	.6968	.00826	0.0				
.0015	0.0	10.0	0.0	1.175	2.65	3.8	4.3073
1.7072	.5528	.2923	0.0				
.0019	0.0	10.5	0.0	0.0	1.475	2.82	2.6773
1.1587	.3823	.2097	.25				
.0021	0.0	11.0	0.0	0.0	0.0	1.325	1.8379
.967	.4343	.305	.2822				
.0025	0.0	13.0	0.0	0.0	0.0	0.0	8.7925
3.014	1.905	.9203	.3922				

Table 5-XX (cont)

D_2O	1000°R	24-Group	Paragraph "A, B & C"				
0.0	0.0	3.33	0.0	0.0	0.0	0.0	.328
0.0	0.0	0.0	0.0				
0.0	0.0	5.45	0.0	0.0	0.0	0.0	1.319
2.13	0.0	0.0	0.0				
0.0	0.0	7.53	0.0	0.0	0.0	0.0	4.668
2.091	.52	0.0	0.0				
0.0	0.0	8.47	0.0	0.0	0.0	0.0	3.894
3.462	1.5	.352	0.0				
0.0	0.0	8.14	0.0	0.0	0.0	0.0	4.343
4.155	1.42	.54	0.0				
0.0	0.0	8.14	0.0	0.0	0.0	0.0	5.3
3.597	.42	0.0	0.0				
0.0	0.0	8.14	0.0	0.0	0.0	0.0	5.08
2.84	0.0	0.0	0.0				
0.0	0.0	8.14	0.0	0.0	0.0	0.0	5.35
3.06	0.0	0.0	0.0				
0.0	0.0	8.14	0.0	0.0	0.0	0.0	5.33
2.79	0.0	0.0	0.0				
0.0	0.0	8.14	0.0	0.0	0.0	0.0	3.52
2.41	0.0	0.0	0.0				
0.0	0.0	8.14	0.0	0.0	0.0	0.0	3.52
3.64	.40	0.0	0.0				
0.0	0.0	8.14	0.0	0.0	0.0	0.0	3.52
3.64	.98	0.0	0.0				
0.0	0.0	8.14	0.0	0.0	0.0	0.0	3.4
3.64	.98	0.0	0.0				
0.0	0.0	8.14	0.0	0.0	0.0	0.0	3.28
3.74	.98	0.0	0.0				
0.0	0.0	8.14	0.0	0.0	0.0	0.0	1.44
3.82	1.0	0.0	0.0				
0.0	0.0	8.58	0.0	0.0	0.0	0.0	1.48
5.0	1.04	0.0	0.0				
.0003	0.0	8.6	.0019	.025	.348	1.87	3.06924
6.0	1.1	0.0	0.0				
.00055	0.0	8.88	.0042	.018	.147	1.34	3.00735
4.249	1.1	0.0	0.0				
.000805	0.0	9.0	.104	.177	.572	2.39	4.328895
2.763	1.273	0.0	0.0				
.0011	0.0	9.5	.437	.930	1.41	3.06	4.1502
1.8376	.6968	.00826	0.0				
.0015	0.0	10.0	0.0	1.58	2.91	3.88	3.8333
1.7072	.5528	.2923	0.0				
.0019	0.0	10.5	0.0	0.0	1.71	2.68	1.882
1.1587	.3823	.3097	.25				
.0021	0.0	11.0	0.0	0.0	0.0	1.42	1.3599
1.4399	.4343	.305	.2822				
.0025	0.0	13.0	0.0	0.0	0.0	0.0	7.8505
3.014	1.905	.9203	.3922				

Table 5-XX (cont)

D_2O	1000°R	15-Group		Paragraph "C"			
0.0	0.0	3.33	0.0	.328	0.0	0.0	0.0
0.0							
0.0	0.0	5.45	0.0	1.319	2.13	0.0	0.0
0.0							
0.0	0.0	9.55	0.0	4.668	2.091	.52	0.0
0.0							
0.0	0.0	8.47	0.0	3.894	3.462	1.5	.352
0.0							
0.0	0.0	8.14	0.0	4.543	4.156	1.42	.54
0.0							
0.0	0.0	8.14	0.0	5.3	3.597	.42	0.0
0.0							
0.0	0.0	8.14	0.0	5.08	2.84	0.0	0.0
0.0							
0.0	0.0	8.14	0.0	5.35	3.06	0.0	0.0
0.0							
0.0	0.0	8.14	0.0	5.33	2.79	0.0	0.0
0.0							
0.0	0.0	8.14	0.0	4.5	2.41	0.0	0.0
0.0							
0.0	0.0	8.14	0.0	6.93	3.64	.4	0.0
0.0							
0.0	0.0	8.2102	0.0	6.8436	1.21	0.0	0.0
0.0							
.0008	0.0	8.8574	1.6313	7.1947	1.3666	0.0	0.0
0.0							
.00144	0.0	9.9085	4.12	6.71466	1.6619	0.0	0.0
0.0							
.0024	0.0	12.6786	0.0	8.5562	1.5611	0.0	0.0
0.0							

Table 5-XX (cont)

D_2O		1000°R	15-Group		Paragraph "J"			
0.0	0.0	3.33	0.0	.328	0.0	0.0	0.0	0.0
0.0	0.0	5.45	0.0	1.319	2.13	0.0	0.0	0.0
0.0	0.0	9.55	0.0	4.668	2.091	.52	0.0	0.0
0.0	0.0	8.47	0.0	3.894	3.462	1.5	.352	0.0
0.0	0.0	8.14	0.0	4.543	4.156	1.42	.54	0.0
0.0	0.0	8.14	0.0	5.3	3.597	.42	0.0	0.0
0.0	0.0	8.14	0.0	5.08	2.84	0.0	0.0	0.0
0.0	0.0	8.14	0.0	5.35	3.06	0.0	0.0	0.0
0.0	0.0	8.14	0.0	5.33	2.79	0.0	0.0	0.0
0.0	0.0	8.14	0.0	3.52	2.41	0.0	0.0	0.0
0.0	0.0	8.14	0.0	6.60	4.62	.4	0.0	0.0
0.0	0.0	8.2102	0.0	6.4102	1.54	0.0	0.0	0.0
.0008	0.0	8.8574	1.6313	6.7566	1.8	0.0	0.0	0.0
.00144	0.0	9.9085	4.5	6.71466	2.1	0.0	0.0	0.0
.0024	0.0	12.6786	0.0	8.1762	1.5611	0.0	0.0	0.0

Table 5-XX (cont)

D_2O	1000°R	13-Group		Paragraph "J"			
0.0	0.0	3.33	0.0	.328	0.0	0.0	0.0
0.0							
0.0	0.0	5.45	0.0	1.319	2.13	0.0	0.0
0.0							
0.0	0.0	9.55	0.0	4.668	2.091	.52	0.0
0.0							
0.0	0.0	8.47	0.0	3.894	3.462	1.5	.352
0.0							
0.0	0.0	8.14	0.0	4.543	4.156	1.42	.54
0.0							
0.0	0.0	8.14	0.0	5.3	3.597	.42	0.0
0.0							
0.0	0.0	8.14	0.0	5.08	2.84	0.0	0.0
0.0							
0.0	0.0	8.14	0.0	5.35	3.06	0.0	0.0
0.0							
0.0	0.0	8.14	0.0	5.33	2.79	0.0	0.0
0.0							
0.0	0.0	8.14	0.0	3.52	2.41	0.0	0.0
0.0							
0.0	0.0	8.14	0.0	6.60	4.62	.4	0.0
0.0							
0.0	0.0	8.2102	0.0	5.8102	1.54	0.0	0.0
0.0							
.0013	0.0	10.45	0.0	10.4487	2.4	0.0	0.0
0.0							

D_2O	1000°R	5-Group		Paragraph "D, E & F"	
0.0	0.0	7.55	0.0	7.25	0.0
0.0	0.0	8.14	0.0	3.94	.3
0.0	0.0	8.80	.482	6.856	4.2
.001	0.0	10.0	1.628	8.065	1.94
.002	0.0	12.66	0.0	11.03	1.452

D_2O	1000°R	3-Group		Paragraph "J"	
0.0	0.0	7.6	0.0	7.18	0.0
0.0	0.0	8.14	0.0	7.54	.42
.0013	0.0	10.45	0.0	10.4487	.6

Table 5-XX (cont)

Carbon	530°R	24-Group		Paragraph "A, B & C"			
0.0	0.0	1.23	0.0	0.0	0.0	0.0	.715
0.0	0.0	0.0	0.0				
0.0	0.0	1.42	0.0	0.0	0.0	0.0	1.106
.515	0.0	0.0	0.0				
0.0	0.0	2.26	0.0	0.0	0.0	0.0	1.404
.314	0.0	0.0	0.0				
0.0	0.0	2.93	0.0	0.0	0.0	0.0	2.326
.856	0.0	0.0	0.0				
0.0	0.0	3.59	0.0	0.0	0.0	0.0	3.157
.604	0.0	0.0	0.0				
0.0	0.0	4.25	0.0	0.0	0.0	0.0	3.849
.433	0.0	0.0	0.0				
0.0	0.0	4.44	0.0	0.0	0.0	0.0	4.01
.401	0.0	0.0	0.0				
0.0	0.0	4.34	0.0	0.0	0.0	0.0	3.97
.43	0.0	0.0	0.0				
0.0	0.0	4.34	0.0	0.0	0.0	0.0	3.97
.37	0.0	0.0	0.0				
0.0	0.0	4.34	0.0	0.0	0.0	0.0	3.61
.37	0.0	0.0	0.0				
0.0	0.0	4.34	0.0	0.0	0.0	0.0	3.61
.73	0.0	0.0	0.0				
0.0	0.0	4.34	0.0	0.0	0.0	0.0	3.61
.73	0.0	0.0	0.0				
0.0	0.0	4.34	0.0	0.0	0.0	0.0	3.61
0.73	0.0	0.0	0.0				
.0008	0.0	4.947	0.0	.00008	.0043	.2273	4.4851
.73	0.0	0.0	0.0				
.0012	0.0	4.581	.00001	.0004	.0111	.2953	2.2024
.3721	0.0	0.0	0.0				
.0014	0.0	4.5643	.00001	.0014	.0259	.3786	2.1614
1.616	.0785	0.0	0.0				
.0016	0.0	4.5436	.00002	.0009	.0478	.5514	2.18472
1.579	.4603	.0098	0.0				
.0017	0.0	4.542	.00006	.0007	.0145	.399	1.9058
1.313	.4085	.0643	.0007				
.0022	0.0	4.5951	.0006	.0148	.0816	.7259	2.91172
1.862	.6224	.1121	.0095				
.00271	0.0	4.6135	.0424	.1593	.3065	1.033	2.63898
1.076	.1836	.0311	.0023				
.00351	0.0	4.6509	0.0	.3272	.9231	1.4838	2.32307
1.0053	.1403	.0106	.001				
.00431	0.0	4.6996	0.0	0.0	.4954	1.1375	1.37403
.6899	.1462	.01227	.0006				
.00486	0.0	4.744	0.0	0.0	0.0	.4765	.87374
.5963	.2251	.0395	.0044				
.0058	0.0	5.688	0.0	0.0	0.0	0.0	4.34070
1.6395	.9198	.294	.0395				

Table 5-XX (cont)

Carbon	3000°R	24-Group		Paragraph "A, B & C"			
0.0	0.0	1.23	0.0	0.0	0.0	0.0	.715
0.0	0.0	0.0	0.0				
0.0	0.0	1.42	0.0	0.0	0.0	0.0	1.106
.515	0.0	0.0	0.0				
0.0	0.0	2.26	0.0	0.0	0.0	0.0	1.404
.314	0.0	0.0	0.0				
0.0	0.0	2.93	0.0	0.0	0.0	0.0	2.326
.856	0.0	0.0	0.0				
0.0	0.0	3.59	0.0	0.0	0.0	0.0	3.157
.604	0.0	0.0	0.0				
0.0	0.0	4.25	0.0	0.0	0.0	0.0	3.849
.433	0.0	0.0	0.0				
0.0	0.0	4.44	0.0	0.0	0.0	0.0	4.01
.401	0.0	0.0	0.0				
0.0	0.0	4.34	0.0	0.0	0.0	0.0	3.97
.43	0.0	0.0	0.0				
0.0	0.0	4.34	0.0	0.0	0.0	0.0	3.97
.37	0.0	0.0	0.0				
0.0	0.0	4.34	0.0	0.0	0.0	0.0	3.61
.37	0.0	0.0	0.0				
0.0	0.0	4.34	0.0	0.0	0.0	0.0	3.61
.73	0.0	0.0	0.0				
0.0	0.0	4.34	0.0	0.0	0.0	0.0	3.61
.73	0.0	0.0	0.0				
0.0	0.0	4.34	0.0	0.0	0.0	0.0	3.61
0.73	0.0	0.0	0.0				
.0008	0.0	4.375	.077	.19	.46	1.27	3.8311
.73	0.0	0.0	0.0				
.0012	0.0	4.65	.14	.237	.457	.955	1.5758
.3314	0.0	0.0	0.0				
.0014	0.0	4.63	.148	.275	.54	.955	1.4631
.985	.1332	0.0	0.0				
.0016	0.0	4.63	.22	.275	.585	1.005	1.3894
.95	.484	.0517	0.0				
.0017	0.0	4.58	.34	.257	.425	.785	1.057
.765	.405	.184	.0268				
.0022	0.0	4.74	1.08	.82	1.02	1.455	1.8133
1.193	.654	.308	.15				
.00271	0.0	4.89	2.62	1.195	1.255	1.425	1.53499
.768	.334	.16	.0875				
.00351	0.0	5.15	0.0	1.76	1.307	1.315	1.27849
.66	.244	.0938	.058				
.00431	0.0	5.44	0.0	0.0	.984	.702	.92569
.40	.17	.0583	.0415				
.00486	0.0	5.7	0.0	0.0	0.0	.597	.39614
.302	.16	.0703	.069				
.0058	0.0	9.03	0.0	0.0	0.0	0.0	3.9632
1.015	.478	.386	.149				

Table 5-XX (cont)

Carbon	5000°R	24-Group		Paragraph "A, B & C"			
0.0	0.0	1.23	0.0	0.0	0.0	0.0	.715
0.0	0.0	0.0	0.0				
0.0	0.0	1.42	0.0	0.0	0.0	0.0	1.106
.515	0.0	0.0	0.0				
0.0	0.0	2.26	0.0	0.0	0.0	0.0	1.404
.314	0.0	0.0	0.0				
0.0	0.0	2.93	0.0	0.0	0.0	0.0	2.326
.856	0.0	0.0	0.0				
0.0	0.0	3.59	0.0	0.0	0.0	0.0	3.157
.604	0.0	0.0	0.0				
0.0	0.0	4.25	0.0	0.0	0.0	0.0	3.849
.433	0.0	0.0	0.0				
0.0	0.0	4.44	0.0	0.0	0.0	0.0	4.01
.401	0.0	0.0	0.0				
0.0	0.0	4.34	0.0	0.0	0.0	0.0	3.97
.43	0.0	0.0	0.0				
0.0	0.0	4.34	0.0	0.0	0.0	0.0	3.97
.37	0.0	0.0	0.0				
0.0	0.0	4.34	0.0	0.0	0.0	0.0	3.61
.37	0.0	0.0	0.0				
0.0	0.0	4.34	0.0	0.0	0.0	0.0	3.61
.73	0.0	0.0	0.0				
0.0	0.0	4.34	0.0	0.0	0.0	0.0	3.61
.73	0.0	0.0	0.0				
0.0	0.0	4.34	0.0	0.0	0.0	0.0	3.61
0.73	0.0	0.0	0.0				
.0008	0.0	4.7	.305	.52	.895	1.645	4.1243
.73	0.0	0.0	0.0				
.0012	0.0	4.65	.42	.43	.622	.98	1.3453
.3194	0.0	0.0	0.0				
.0014	0.0	4.68	.55	.475	.668	.942	1.1746
.8	.1415	0.0	0.0				
.0016	0.0	4.72	.745	.48	.704	.985	1.2796
.796	.445	.066	0.0				
.0017	0.0	4.79	1.08	.455	.557	.76	.8963
.635	.37	.1945	.048				
.0022	0.0	4.92	2.4	1.18	1.25	1.427	1.5303
.995	.605	.326	.219				
.00271	0.0	5.13	5.3	1.38	1.305	1.31	1.13929
.658	.33	.0188	.137				
.00351	0.0	5.45	0.0	1.88	1.17	1.13	.87049
.56	.24	.1125	.096				
.00431	0.0	6.035	0.0	0.0	.93	.562	.73069
.32	.156	.0645	.0665				
.00486	0.0	6.43	0.0	0.0	0.0	.53	.13914
.236	.142	.091	.066				
.0058	0.0	10.96	0.0	0.0	0.0	0.0	2.3142
.824	.369	.354	.167				

Table 5-XX (cont)

Carbon	5000°R	5-Group		Paragraph "F"	
0.0	0.0	1.84	0.0	1.754	0.0
.00072	0.0	.55072	0.0	.1	.086
.00072	0.0	4.78932	2.412	4.109	.450
.0034	0.0	5.45	7.412	2.6816	.6796
.0057	0.0	9.9717	0.0	2.554	.353

BeO	530°R	15-Group		Paragraph "A, B & C"			
-.134	0.0	1.086	0.0	.424	0.0	0.0	0.0
0.0							
-.044	0.0	1.2275	0.0	.8615	.621	0.0	0.0
0.0							
0.0	0.0	2.805	0.0	1.7505	.35	.175	0.0
0.0							
0.0	0.0	3.47	0.0	2.5625	1.0545	.06	0.0
0.0							
0.0	0.0	3.825	0.0	3.3395	.9075	0.0	0.0
0.0							
0.0	0.0	4.22	0.0	3.7795	.4855	0.0	0.0
0.0							
0.0	0.0	4.415	0.0	3.9475	.4405	0.0	0.0
0.0							
0.0	0.0	4.505	0.0	3.975	.4675	0.0	0.0
0.0							
0.0	0.0	4.53	0.0	4.0	.53	0.0	0.0
0.0							
0.0	0.0	4.56	0.0	4.02	.53	0.0	0.0
0.0							
.0002	0.0	4.55	0.0	4.2698	.53	0.0	0.0
0.0							
.001	0.0	4.55	.052	4.099	.28	0.0	0.0
0.0							
.002	0.0	4.55	.323	3.826	.45	0.0	0.0
0.0							
.0037	0.0	4.55	1.06	3.6433	.67	0.0	0.0
0.0							
.006	0.0	5.55	0.0	4.484	.58	0.0	0.0
0.0							

Table 5-XX (cont)

BeO		1500°R	15-Group		Paragraph "A, B & C"			
-.134	0.0	1.086	0.0	.424	0.0	0.0	0.0	0.0
-.044	0.0	1.2275	0.0	.8615	.621	0.0	0.0	0.0
0.0	0.0	2.805	0.0	1.7505	.35	.175	0.0	0.0
0.0	0.0	3.47	0.0	2.5625	1.0545	.06	0.0	0.0
0.0	0.0	3.825	0.0	3.3395	.9075	0.0	0.0	0.0
0.0	0.0	4.22	0.0	3.7795	.4855	0.0	0.0	0.0
0.0	0.0	4.415	0.0	3.9475	.4405	0.0	0.0	0.0
0.0	0.0	4.505	0.0	3.975	.4675	0.0	0.0	0.0
0.0	0.0	4.53	0.0	4.0	.53	0.0	0.0	0.0
0.0	0.0	4.55	0.0	3.71	.53	0.0	0.0	0.0
.00015	0.0	4.55	0.0	4.27	.84	0.0	0.0	0.0
8.75		-4[illegible] 0.0	4.575	.3886	4.119	.28	0.0	0.0
2.05	0.0	-3[illegible] 0.0	4.567	.9422	3.467	.4547	0.0	0.0
3.67	0.0	-3[illegible] 0.0	4.72	2.915	3.201	.7098	0.0	0.0
6.15	0.0	-3[illegible] 0.0	5.44	0.0	2.519	.5736	0.0	0.0

Table 5-XX (cont)

BeO	2000°R	15-Group		Paragraph "A, B & C"			
-.134	0.0	1.086	0.0	.424	0.0	0.0	0.0
0.0							
-.044	0.0	1.2275	0.0	.8615	.621	0.0	0.0
0.0							
0.0	0.0	2.805	0.0	1.7505	.35	.175	0.0
0.0							
0.0	0.0	3.47	0.0	2.5625	1.0545	.06	0.0
0.0							
0.0	0.0	3.825	0.0	3.3395	.9075	0.0	0.0
0.0							
0.0	0.0	4.22	0.0	3.7795	.4855	0.0	0.0
0.0							
0.0	0.0	4.415	0.0	3.9475	.4405	0.0	0.0
0.0							
0.0	0.0	4.505	0.0	3.975	.4675	0.0	0.0
0.0							
0.0	0.0	4.53	0.0	4.0	.53	0.0	0.0
0.0							
0.0	0.0	4.55	0.0	4.02	.53	0.0	0.0
0.0							
.0002	0.0	4.55	0.0	4.2698	.53	0.0	0.0
0.0							
.001	0.0	4.59	.28	4.0455	.28	0.0	0.0
0.0							
.002	0.0	4.578	1.209	3.583	.5435	0.0	0.0
0.0							
.0037	0.0	4.83	3.774	3.0525	.713	0.0	0.0
0.0							
.006	0.0	5.92	0.0	2.14	.5648	0.0	0.0
0.0							

Table 5-XX (cont)

BeO	3000°R	15-Group		Paragraph "A, B & C"			
-.134	0.0	1.086	0.0	.424	0.0	0.0	0.0
0.0							
-.044	0.0	1.2275	0.0	.8615	.621	0.0	0.0
0.0							
0.0	0.0	2.805	0.0	1.7505	.35	.175	0.0
0.0							
0.0	0.0	3.47	0.0	2.5625	1.0545	.06	0.0
0.0							
0.0	0.0	3.825	0.0	3.3395	.9075	0.0	0.0
0.0	0.0	4.22	0.0	3.7795	.4855	0.0	0.0
0.0							
0.0	0.0	4.415	0.0	3.9475	.4405	0.0	0.0
0.0							
0.0	0.0	4.505	0.0	3.975	.4675	0.0	0.0
0.0							
0.0	0.0	4.53	0.0	4.0	.53	0.0	0.0
0.0							
0.0	0.0	4.55	0.0	4.02	.53	0.0	0.0
0.0							
.0002	0.0	4.55	0.0	4.2698	.53	0.0	0.0
0.0							
.001	0.0	4.62	.408	4.1533	.28	0.0	0.0
0.0							
.002	0.0	4.6	1.674	3.5185	.4657	0.0	0.0
0.0							
.0037	0.0	5.021	5.06	2.869	.6715	0.0	0.0
0.0							
.006	0.0	6.85	0.0	1.784	.4743	0.0	0.0
0.0							

Table 5-XX (cont)

BeO	3000°R	15-Group		Paragraph "J"			
-.134	0.0	1.086	0.0	.424	0.0	0.0	0.0
0.0							
-.044	0.0	1.2275	0.0	.8615	.621	0.0	0.0
0.0							
0.0	0.0	2.805	0.0	1.7505	.35	.175	0.0
0.0							
0.0	0.0	3.47	0.0	2.5625	1.0545	.06	0.0
0.0							
0.0	0.0	3.825	0.0	3.3395	.9075	0.0	0.0
0.0							
0.0	0.0	4.22	0.0	3.7795	.4855	0.0	0.0
0.0							
0.0	0.0	4.415	0.0	3.9475	.4405	0.0	0.0
0.0							
0.0	0.0	4.505	0.0	3.975	.4675	0.0	0.0
0.0							
0.0	0.0	4.53	0.0	4.0	.53	0.0	0.0
0.0							
0.0	0.0	4.55	0.0	3.71	.53	0.0	0.0
0.0							
.0002	0.0	4.55	0.0	4.2698	.84	0.0	0.0
0.0							
.001	0.0	4.62	.408	4.1533	.28	0.0	0.0
0.0							
.002	0.0	4.6	1.674	3.5185	.4657	0.0	0.0
0.0							
.0037	0.0	5.021	5.06	2.869	.6715	0.0	0.0
0.0							
.006	0.0	6.85	0.0	1.784	.4743	0.0	0.0
0.0							

Table 5-XX (cont)

BeO 3000°R 13-Group Paragraph "J"

-.134	0.0	1.086	0.0	.424	0.0	0.0	0.0
0.0							
-.044	0.0	1.2275	0.0	.8615	.621	0.0	0.0
0.0							
0.0	0.0	2.805	0.0	1.7505	.35	.175	0.0
0.0							
0.0	0.0	3.47	0.0	2.5625	1.0545	.06	0.0
0.0							
0.0	0.0	3.825	0.0	3.3395	.9075	0.0	0.0
0.0							
0.0	0.0	4.22	0.0	3.7795	.4855	0.0	0.0
0.0							
0.0	0.0	4.415	0.0	3.9475	.4405	0.0	0.0
0.0							
0.0	0.0	4.505	0.0	3.975	.4675	0.0	0.0
0.0							
0.0	0.0	4.53	0.0	4.0	.53	0.0	0.0
0.0							
0.0	0.0	4.55	0.0	3.71	.53	0.0	0.0
0.0							
0.0	0.0	4.55	0.0	4.27	.84	0.0	0.0
0.0							
0.0	0.0	4.62	0.0	3.992	.28	0.0	0.0
0.0							
.002	0.0	4.78	0.0	4.778	.628	0.0	0.0
0.0							

BeO 3000°R 5-Group Paragraph "D & E"

-.008	0.0	1.769	0.0	1.677	0.0	
1.0	0.0	-3E 0.0	.55	0.0	.100	.1
2.00	0.0	-3E 0.0	4.6	1.324	3.928	.450
3.67	0.0	-3E 0.0	5.021	5.06	3.219	.6700
6.00	0.0	-3E 0.0	6.85	0.0	1.784	.4743

BeO 3000°R 3-Group Paragraph "A" Type Only

-.0062	0.0	3.02	0.0	2.9612	0.0
0.0	0.0	4.5	0.0	4.365	.065
.002	0.0	4.78	0.0	4.778	.135

BeO 3000°R 3-Group Paragraph "J"

-.0062	0.0	3.02	0.0	2.9062	0.0
0.0	0.0	4.5	0.0	4.365	.12
.002	0.0	4.78	0.0	4.778	.135

Table 5-XX (cont)

Be 530°R 24-Group Paragraph "A, B & C"

-.308	0.0	.842	0.0	0.0	0.0	0.0	-.018
0.0	0.0	0.0	0.0				
-.088	0.0	1.275	0.0	0.0	0.0	0.0	.734
.818	0.0	0.0	0.0				
0.0	0.0	2.38	0.0	0.0	0.0	0.0	1.173
.509	.35	0.0	0.0				
0.0	0.0	3.31	0.0	0.0	0.0	0.0	2.397
1.207	.12	0.0	0.0				
0.0	0.0	3.94	0.0	0.0	0.0	0.0	3.306
.913	0.0	0.0	0.0				
0.0	0.0	5.18	0.0	0.0	0.0	0.0	4.525
.634	0.0	0.0	0.0				
0.0	0.0	5.28	0.0	0.0	0.0	0.0	4.6
.655	0.0	0.0	0.0				
0.0	0.0	5.37	0.0	0.0	0.0	0.0	4.54
.68	0.0	0.0	0.0				
0.0	0.0	5.42	0.0	0.0	0.0	0.0	4.59
.83	0.0	0.0	0.0				
0.0	0.0	5.46	0.0	0.0	0.0	0.0	4.24
.83	0.0	0.0	0.0				
.0003	0.0	5.46	0.0	0.0	0.0	0.0	4.2397
1.22	0.0	0.0	0.0				
.0004	0.0	5.46	0.0	0.0	0.0	0.0	4.2396
1.22	0.0	0.0	0.0				
.0007	0.0	5.46	0.0	0.0	0.0	0.0	4.2396
1.22	0.0	0.0	0.0				
.0012	0.0	5.9633	0.0	.0002	.0063	.2457	4.7985
1.22	0.0	0.0	0.0				
.0027	0.0	5.6121	0.0	.001	.0166	.3303	2.3334
.5505	0.0	0.0	0.0				
.003	0.0	5.5988	0.0	.0030	.0391	.4341	2.3196
1.9948	.1641	0.0	0.0				
.0034	0.0	5.576	0.0	.0025	.0707	.6416	2.3787
1.954	.8043	.0343	0.0				
.0038	0.0	5.5782	.0004	.0023	.0278	.4804	2.0849
1.6082	.6808	.1821	.0048				
.0046	0.0	5.6447	.0187	.0375	.1449	.9178	3.3182
2.3887	1.0287	.2898	.0491				
.0059	0.0	5.6807	.1037	.2867	.4807	1.3078	3.0211
1.45	.3758	.099	.015				
.0076	0.0	5.7461	0.0	.5561	1.2314	1.8142	2.6614
1.305	.2675	.0392	.0071				
.0093	0.0	5.8304	0.0	0.0	.7139	1.3295	1.5515
.8485	.2355	.0334	.0041				
.0105	0.0	5.9048	0.0	0.0	0.0	.6349	.9812
.6971	.3023	.0732	.0167				
.0126	0.0	7.3418	0.0	0.0	0.0	0.0	5.3206
2.0468	1.2397	.4713	.0919				

Table 5-XX (cont)

Be 1000°R 24-Group Paragraph "A, B & C"

-.308	0.0	.842	0.0	0.0	0.0	0.0	-.018
0.0	0.0	0.0	0.0				
-.088	0.0	1.275	0.0	0.0	0.0	0.0	.734
.818	0.0	0.0	0.0				
0.0	0.0	2.38	0.0	0.0	0.0	0.0	1.173
.509	.35	0.0	0.0				
0.0	0.0	3.31	0.0	0.0	0.0	0.0	2.397
1.207	.12	0.0	0.0				
0.0	0.0	3.94	0.0	0.0	0.0	0.0	3.306
.913	0.0	0.0	0.0				
0.0	0.0	5.18	0.0	0.0	0.0	0.0	4.525
.634	0.0	0.0	0.0				
0.0	0.0	5.28	0.0	0.0	0.0	0.0	4.6
.655	0.0	0.0	0.0				
0.0	0.0	5.37	0.0	0.0	0.0	0.0	4.54
.68	0.0	0.0	0.0				
0.0	0.0	5.42	0.0	0.0	0.0	0.0	4.59
.83	0.0	0.0	0.0				
0.0	0.0	5.46	0.0	0.0	0.0	0.0	4.24
.83	0.0	0.0	0.0				
.0003	0.0	5.46	0.0	0.0	0.0	0.0	4.2397
1.22	0.0	0.0	0.0				
.0004	0.0	5.46	0.0	0.0	0.0	0.0	4.2396
1.22	0.0	0.0	0.0				
.0007	0.0	5.46	0.0	0.0	0.0	0.0	4.2393
1.22	0.0	0.0	0.0				
.0012	0.0	5.84	.00425	.015	.055	.665	5.0758
1.22	0.0	0.0	0.0				
.0027	0.0	5.6	.0075	.054	.137	.784	2.1473
.519	0.0	0.0	0.0				
.0027	0.0	5.6	.0095	.085	.252	.825	2.1633
1.65	.179	0.0	0.0				
.0034	0.0	5.6	.021	.076	.237	.965	2.1035
1.595	.763	.952	0.0				
.0038	0.0	5.6	.035	.065	.178	.75	1.79725
1.335	.636	.232	.013				
.0046	0.0	5.7	.285	.34	.65	1.395	2.9749
1.995	.992	.36	.135				
.0059	0.0	5.77	.765	.99	1.15	1.595	2.5366
1.25	.434	.169	.061				
.0076	0.0	5.8	0.0	1.63	1.459	1.78	1.9834
1.12	.3	.0815	.02				
.0093	0.0	6.05	0.0	0.0	1.005	1.155	1.0427
.712	.236	.0565	.0132				
.0105	0.0	6.2	0.0	0.0	0.0	.705	.5825
.563	.266	.083	.0345				
.0126	0.0	8.55	0.0	0.0	0.0	0.0	4.4324
1.718	1.13	.5	.13				

Table 5-XX (cont)

Be 1500°R 24-Group Paragraph "A, B & C"

-.308	0.0	.842	0.0	0.0	0.0	0.0	-.018
0.0	0.0	0.0	0.0				
-.088	0.0	1.275	0.0	0.0	0.0	0.0	.734
.818	0.0	0.0	0.0				
0.0	0.0	2.38	0.0	0.0	0.0	0.0	1.173
.509	.35	0.0	0.0				
0.0	0.0	3.31	0.0	0.0	0.0	0.0	2.397
1.207	.12	0.0	0.0				
0.0	0.0	3.94	0.0	0.0	0.0	0.0	3.306
.913	0.0	0.0	0.0				
0.0	0.0	5.18	0.0	0.0	0.0	0.0	4.525
.634	0.0	0.0	0.0				
0.0	0.0	5.28	0.0	0.0	0.0	0.0	4.6
.655	0.0	0.0	0.0				
0.0	0.0	5.37	0.0	0.0	0.0	0.0	4.54
.68	0.0	0.0	0.0				
0.0	0.0	5.42	0.0	0.0	0.0	0.0	4.59
.83	0.0	0.0	0.0				
0.0	0.0	5.46	0.0	0.0	0.0	0.0	4.24
.83	0.0	0.0	0.0				
.0003	0.0	5.46	0.0	0.0	0.0	0.0	4.2397
1.22	0.0	0.0	0.0				
.0004	0.0	5.46	0.0	0.0	0.0	0.0	4.2396
1.22	0.0	0.0	0.0				
.0007	0.0	5.46	0.0	0.0	0.0	0.0	4.2393
1.22	0.0	0.0	0.0				
.0012	0.0	5.72	.0188	.063	.17	.923	4.9413
1.22	0.0	0.0	0.0				
.0027	0.0	5.65	.034	.115	.28	.94	2.0793
.498	0.0	0.0	0.0				
.0027	0.0	5.65	.0425	.162	.405	.97	2.0163
1.475	.189	0.0	0.0				
.0034	0.0	5.65	.085	.17	.435	1.12	1.9906
1.42	.728	.066	0.0				
.0038	0.0	5.65	.116	.14	.315	.86	1.6224
1.155	.598	.256	.0245				
.0046	0.0	5.75	.66	.62	.91	1.61	2.6694
1.77	.94	.408	.186				
.0059	0.0	5.87	1.55	1.215	1.34	1.707	2.2391
1.135	.453	.204	.095				
.0076	0.0	6.05	0.0	1.89	1.572	1.745	1.8284
.995	.32	.111	.044				
.0093	0.0	6.3	0.0	0.0	1.138	1.028	.9497
.615	.234	.0695	.031				
.0105	0.0	6.52	0.0	0.0	0.0	.744	.5145
.477	.242	.0895	.0603				
.0126	0.0	9.6	0.0	0.0	0.0	0.0	4.2654
1.52	1.043	.515	.169				

Table 5-XX (cont)

Be 2000°R 24-Group Paragraph "A, B & C"

-.308	0.0	.842	0.0	0.0	0.0	0.0	-.018
0.0	0.0	0.0	0.0				
-.088	0.0	1.275	0.0	0.0	0.0	0.0	.734
.818	0.0	0.0	0.0				
0.0	0.0	2.38	0.0	0.0	0.0	0.0	1.173
.509	.35	0.0	0.0				
0.0	0.0	3.31	0.0	0.0	0.0	0.0	2.397
1.207	.12	0.0	0.0				
0.0	0.0	3.94	0.0	0.0	0.0	0.0	3.306
.913	0.0	0.0	0.0				
0.0	0.0	5.18	0.0	0.0	0.0	0.0	4.525
.634	0.0	0.0	0.0				
0.0	0.0	5.28	0.0	0.0	0.0	0.0	4.6
.655	0.0	0.0	0.0				
0.0	0.0	5.37	0.0	0.0	0.0	0.0	4.54
.68	0.0	0.0	0.0				
0.0	0.0	5.42	0.0	0.0	0.0	0.0	4.59
.83	0.0	0.0	0.0				
0.0	0.0	5.46	0.0	0.0	0.0	0.0	4.24
.83	0.0	0.0	0.0				
.0003	0.0	5.46	0.0	0.0	0.0	0.0	4.2397
1.22	0.0	0.0	0.0				
.0004	0.0	5.46	0.0	0.0	0.0	0.0	4.2396
1.22	0.0	0.0	0.0				
.0007	0.0	5.46	0.0	0.0	0.0	0.0	4.2393
1.22	0.0	0.0	0.0				
.0012	0.0	5.6	.047	.126	.35	1.15	4.8028
1.22	0.0	0.0	0.0				
.0027	0.0	5.65	.085	.182	.415	1.035	1.9713
.481	0.0	0.0	0.0				
.0027	0.0	5.67	.106	.24	.53	1.075	1.8463
1.345	.197	0.0	0.0				
.0034	0.0	5.67	.175	.255	.595	1.21	1.7946
1.3	.686	.077	0.0				
.0038	0.0	5.7	.27	.212	.43	.92	1.4682
1.04	.568	.268	.041				
.0046	0.0	5.82	1.02	.85	1.11	1.733	2.4277
1.612	.908	.444	.225				
.0059	0.0	5.97	2.56	1.38	1.475	1.762	2.0156
1.045	.461	.229	.124				
.0076	0.0	6.23	0.0	2.07	1.623	1.7	1.7064
.9	.333	.13	.079				
.0093	0.0	6.55	0.0	0.0	1.22	.93	.8687
.52	.23	.0787	.056				
.0105	0.0	6.85	0.0	0.0	0.0	.76	.5135
.407	.22	.0925	.091				
.0126	0.0	10.6	0.0	0.0	0.0	0.0	3.9774
1.373	.97	.517	.202				

APPENDIX - PROCEDURE FOR COMPUTING 24-GROUP D_2O CROSS SECTIONS FOR THE DTK AND DSN NEUTRON TRANSPORT CODE

INTRODUCTION

This appendix presents a fundamental method of calculating D_2O microscopic neutron cross sections to be used as input to 24 energy group DTK or DSN neutron transport problems. Comparisons have been run over a limited range with an alternate method for generating the cross sections actually used for calculations presented in this report (reference Section V, subsection titled Gas Model). All group cross sections are in barns/molecule. The temperature of the moderator is a variable. For each energy group, 12 cross sections, defined as follows, are evaluated:

- σ_c —the absorption cross section. The only absorptive reactions in deuterium are the high energy (n, 2n) reaction and the low energy (n,γ) reaction. In oxygen, (n, p) and (n,α) reactions occur at high energies and (n,γ) and (n,α) reactions occur at low energies.
- $\nu\sigma_f$ —the fission cross section times the number of neutrons per fission. No true fission reactions, of course, occur in deuterium or oxygen. There is, however, a high energy (n, 2n) reaction in deuterium which is equivalent to fission with a $\nu = 2$. This reaction gives an effective $\nu\sigma_f$ to deuterium.
- σ_{tr} —the transport cross section = $\sigma_s(1 - \bar{\mu}_o) + \sigma_c$ where σ_s is the elastic scattering cross section, and $\bar{\mu}_o$ is the average of the cosine of the scattering angle in the laboratory system.
- $\sigma_{g'g}$—the transfer cross section from group g' to group g. Transfer is the result of elastic and inelastic scattering. Nine values of g' ranging from g + 4 to g - 4 are considered.

The total cross section for the D_2O molecule in the neutron energy range greater than 1 ev is the sum of the cross sections of the individual atoms:[1]*

$$\sigma_{D_2O} = 2\sigma_D + \sigma_O \quad (E>1 \text{ ev}) \qquad \text{(A-1)}$$

Below this energy, molecular binding effects become important and the molecule can no longer be considered as simply three free atoms. Thus, 1 ev constitutes a convenient cutoff point between "fast" and "slow" cross sections. Since the lower bound of energy group 13 is at approximately this energy (1.1256 ev), groups 1 through 13 are treated as fast groups and groups 14 through 24 as slow groups. Distinction between fast and slow groups will be made in the procedures used in the computation of the respective cross sections. The energy which separates fast and slow groups is called E_c, the cutoff energy:

$$E_c = 1.1256 \text{ ev} \qquad \text{(A-2)}$$

*Superscript numbers refer to references at the end of this appendix.

Other notation used throughout this appendix includes:

E	—the neutron energy—ev or Mev
u	—the neutron lethargy = $\ln [10^7/E(\text{ev})]$
v	—the neutron velocity—cm/sec
$\phi(E)$	—the neutron flux per unit energy interval—neutrons/cm^2-sec/ev or Mev
$\phi(u)$	—the neutron flux per unit lethargy interval—neutrons/cm^2-sec; thus, $\phi(u) = E\phi(E)$
T	—the temperature of the moderator—°K
k	—Boltzmann's constant
$f(E)$	—the normalized Watt fission spectrum $f(E) = 0.484\, e^{-E} \sinh\sqrt{2E}$, where E is in Mev
$f_n^L(E)$	—the nth coefficient in the Legendre polynomial expansion of the differential elastic scattering cross section in the laboratory frame
$f_n^c(E)$	—the nth coefficient in the Legendre polynomial expansion of the differential elastic scattering cross section in the center of mass frame
$\sigma_s(E)$	—the elastic scattering cross section at energy E
$\sigma_{in}(E)$	—the inelastic scattering cross section at energy E
μ	—the cosine of the scattering angle in the lab system
μ_c	—the cosine of the scattering angle in the center of mass system
$E_{\ell g}$	—the lower energy bound of group g
E_{ug}	—the upper energy bound of group g
$N(E)$	—the energy spectrum of neutron flux in the slow neutron region
$N(v)$	—the speed spectrum of neutron flux in the slow neutron region
$M(V)$	—the speed spectrum of deuterium or oxygen atoms
$\bar{\mu}(E)$	—the experimentally determined average cosine for neutrons of energy E scattering in D_2O at 300°K
$P(v', v)dv$	—the probability that a neutron of initial speed v' will be scattered into speed range dv about v in collision with a Maxwellian distribution of atoms

The lower limit of the energy range of each of the 24 energy groups is listed in Table A-I with the lethargy width of each group.[5]

Table A-I.
24-group specifications.

Fast groups			Slow groups		
g	$E_{\ell g}$	Δu_g	g	$E_{\ell g}$	Δu_g
1	3 Mev	1.204	14	0.414 ev	1.0
2	1.4	0.762	15	0.3224	0.25
3	0.9	0.442	16	0.2511	0.25
4	0.4	0.811	17	0.1965	0.25
5	0.1	1.386	18	0.1535	0.25
6	17 kev	1.772	19	0.0924	0.5
7	3.35	1.623	20	0.0560	0.5
8	454 ev	2.0	21	0.0340	0.5
9	61.44	2.0	22	0.0252	0.3
10	22.60	1.0	23	0.0206	0.2
11	8.315	1.0	24	0.005	1.22
12	3.059	1.0			
13	1.1256	1.0			

FAST CROSS SECTIONS ($E \geq 1.1256$ ev)

To obtain accurate group average cross sections, it is necessary to weight point cross sections in energy by an assumed (or known) neutron energy spectrum within the group. Because the actual spectrum is not known, the natural assumption is made that the neutron energy spectrum above E_c has the usual 1/E shape with a very high energy fission spectrum tail. The energy at which the spectrum changes from 1/E to a fission spectrum can be estimated from infinite medium calculations to be slightly below the peak in the fission spectrum. Since the peak in f(E) occurs at 0.7 Mev, it is assumed that cross sections in groups 1 through 4 (which contain neutrons with energies ranging from 10 Mev to 0.4 Mev) must be fission spectrum weighted. Cross sections in groups 5 through 13 will be 1/E weighted.

σ_c for Groups 1 through 13

Oxygen has an (n, p) reaction above 10.9 Mev and an (n, α) reaction above 3.82 Mev.[2] The (n, p) threshold is greater than the maximum neutron energy considered in the DTK and DSN codes; nevertheless, it should rigorously be taken into account since it does contribute slightly

to absorption of group 1 neutrons. Oxygen exhibits no other absorptive interactions in groups 1 through 13, and deuterium exhibits only the (n, 2n) absorptive reaction in group 1.[2] Thus σ_c^g will be zero for g = 2 through 13. In group 1, σ_c^g will be given by

$$\sigma_c^1 = \int_{3.82}^{18\ \text{Mev}} \sigma_{co}(E)\, f(E)\, dE \Big/ \int_{3}^{18\ \text{Mev}} f(E)\, dE + \frac{(\nu\sigma_f)^1}{\nu} \qquad \text{(A-3)}$$

where

$\sigma_{co}(E)$ is the sum of the oxygen (n, p) and (n,α) cross sections expressed in barns (see reference 2)

f(E) is the fission spectrum

$\nu\sigma_f$ is given in subsequent paragraphs

The integral in the numerator can be evaluated numerically or graphically. The integral in the demoninator can be readily shown to be given by

$$F(E_1) = 1 + f(E_1) - (1/2)\left[\text{erf}\left(\sqrt{E_1} - \sqrt{1/2}\right) + \text{erf}\left(\sqrt{E_1} + \sqrt{1/2}\right)\right] \qquad \text{(A-4)}$$

where E_1 = 3.0 Mev.

$\nu\sigma_f$ for Groups 1 through 13

At energies greater than 3.46 Mev, deuterium has a very small (but finite) cross section for "fissioning" in the reaction

$$H^2 + n \rightarrow H^1 + n + n \qquad \text{(A-5)}$$

The cross section for this (n, 2n) reaction increases monotonically from 0.005 barns at 3.46 Mev to 0.23 barns at 18 Mev.[2] Since two neutrons are emitted per "fission," ν = 2, and since there are two deuterium atoms per molecule of D_2O,

$$(\nu\sigma_f)^1 = 4 \int_{3.46}^{18\ \text{Mev}} \sigma_{2n}(E)\, f(E)\, dE \Big/ \int_{3}^{18\ \text{Mev}} f(E)\, dE \qquad \text{(A-6)}$$

where $\sigma_{2n}(E)$ is the deuterium (n, 2n) cross section expressed in barns.[2]

Once again the numerator can be evaluated numerically or graphically, and the denominator is given by Equation (A-4).

It should be noted that the code will not give the correct distribution in energy of the "fission" neutrons released by deuterium unless the fission spectrum is collapsed into one group. It will, however, give the correct number in either case.

σ_{tr} for Groups 1 through 13

The transport cross section is defined as*

$$\sigma_{tr} = 2\pi \int_{-1}^{1} (1 - \mu)\sigma_s(\mu)\, d\mu + \sigma_c \qquad \text{(A-7)}$$

where μ is the cosine of the scattering angle in the laboratory system.

If the differential elastic scattering cross section were expressed by a expansion in Legendre polynomials in μ,

$$\sigma_s(\mu) = \frac{\sigma_s}{4\pi} \sum_{n=0}^{N} (2n + 1)\, f_n^L(E)\, P_n(\mu) \qquad \text{(A-8)}$$

Substitution of Equation (A-8) into Equation (A-7) then yields

$$\sigma_{tr} = \sigma_s \left[1 - f_1^L(E)\right] + \sigma_c \qquad \text{(A-9)}$$

where use has been made of the fact that $f_0 = 1$, $P_0 = 1$, $P_1 = \mu$, and the orthonormality relations

$$\int_{-1}^{+1} P_n(\mu)\, P_m(\mu)\, d\mu = \frac{2}{2n + 1} \delta_{mn} \qquad \text{(A-10)}$$

where δ_{mn} is the Kronecker delta $\qquad \delta_{mn} = \begin{cases} 1 \text{ if } m = n \\ 0 \text{ if } m \neq n \end{cases}$

Thus, only the first expansion coefficient $f_1^L(E)$ need be known to obtain the transport cross section. Most compilations of differential cross sections, however (including those in reference 2), list the expansion coefficients in the center of mass system, not the laboratory system. The relationship between the laboratory coefficients and the center of mass coefficients is given in references 3 and 4. After modification to account for the slightly different normalization of these coefficients,

* N. B. If inelastic scattering is to be included in σ_{tr} and if the natural assumption of isotropic (in c/m) inelastic scattering is made, then a term $\sigma_{in}(1-2/3A)$ must be added to the right side of Equations (A-7) and (A-9), and a term σ_{in}^{g} (1-2/3A) must be added to the right side of Equation (A-12).

$$(2n + 1)\, f_n^L(E) = \sum_{m = 0} T_{nm}(2m + 1) f_m^c(E)$$

and, for n = 1,

$$f_1^L(E) = \sum_{m = 0} \frac{T_{1m}}{3} (2m + 1) f_m^c(E) \qquad \text{(A-11)}$$

In this equation, f_m^c is the mth expansion coefficient in the c/m system and T_{1m} is the second row of the transformation matrix.

The second column of Table A-II lists the approximate general forms for the transformation vector T_{1m}.[3] These approximate equations are reasonably accurate if A, the atomic weight of the target nucleus, is greater than 2. In the third and fourth columns of Table A-II, the first six of the exact transformation vector components are listed.[4] Six or fewer components are required because both the higher order Legendre expansion coefficients and the transformation components decrease rapidly with order.

Table A-II.
Transformation vector.

	T_{1m}		
m	Approximate general expression	Deuterium (exact)	Oxygen (exact)
0	2/A	1.000	0.125
1	$1-(3/5A^2)$	0.8500	0.9977
2	-2/5A	-0.1571	-0.0249
3	$9/35A^2$	0.0493	0.00099
4	0	-0.0187	-0.00005
5	0	0.0063	-0.00001

Upon combining Equations (A-1), (A-9), and (A-11), and taking account of spectrum weighting, the transport cross section in groups 1 through 4 takes the form

$$\sigma_{tr}^{g} = \int_{E_{\ell g}}^{E_{ug}} \left\{ 2\sigma_{s,D}(E) \left[1 - \frac{1}{3} \sum_{m=0} T_{1m}^{D} (2m+1) f_{m,D}^{c}(E) \right] + \right.$$

$$\left. \sigma_{s,O}(E) \left[1 - \frac{1}{3} \sum_{m=0} T_{1m}^{O} (2m+1) f_{m,O}^{c}(E) \right] \right\} f(E)\, dE \div \left[\int_{E_{\ell g}}^{E_{ug}} f(E)\, dE \right] + \sigma_{c}^{g} \quad (g = 1, 4) \quad \text{(A-12)}$$

where

$E_{\ell g}$ is the lower energy bound of group g

E_{ug} is the upper energy bound of group g

$\sigma_{s,D}(E)$ is the total elastic scattering cross section of deuterium at energy E (from reference 2)

$\sigma_{s,O}(E)$ is the total elastic scattering cross section of oxygen at energy E (from reference 2)

$f_{m,D}^{c}(E)$ and $f_{m,O}^{c}(E)$ are the Legendre expansion coefficients for deuterium and oxygen, respectively, at energy E (from reference 2)

T_{1m}^{D} and T_{1m}^{O} are the transformation vectors for deuterium and oxygen respectively (from Table A-II)

f(E) is the fission spectrum

The energy spectrum in groups 5 through 13 is assumed to be inversely proportional to energy. Since a flux per unit energy which is inversely proportional to energy is identical with a constant flux per unit lethargy, it is much easier to carry out group averages over lethargy rather than over energy. Thus, the transport cross sections for groups 5 through 13 take the form:

$$\sigma_{tr}^{g} = \frac{1}{\Delta u_g} \int_{u_{\ell g}}^{u_{ug}} \left\{ 2\sigma_{s,D}(u) \left[1 - \frac{1}{3} \sum_{m=0} T_{1m}^{D} (2m+1) f_{m,D}^{c}(u) \right] + \right.$$

$$\left. \sigma_{s,O}(u) \left[1 - \frac{1}{3} \sum_{m=0} T_{1m}^{O} (2m+1) f_{m,O}^{c}(u) \right] \right\} du$$

where

$u_{\ell g}$ is the lower lethargy bound of group g

u_{ug} is the upper lethargy bound of group g

$\Delta u_g = u_{ug} - u_{\ell g}$, which is the lethargy width of group g

Since the tabulated scattering cross sections and Legendre coefficients in reference 2 are equal increments apart in lethargy, the integral above may be replaced by a simple summation and the Δu_g replaced by the number of terms summed.

Below 0.1 Mev—i.e., in groups 6 through 13—scattering from both deuterium and oxygen is isotropic in the center of mass system, the scattering cross sections are constant, and there is no absorption so the transport cross section is constant:

$$\sigma_{tr}^{g} = 2\sigma_{s,D}\left(1 - \frac{2}{3A_D}\right) + \sigma_{s,O}\left(1 - \frac{2}{3A_O}\right) \qquad \text{(A-14)}$$

$$= 2\,(3.35\text{b})\left(1 - \frac{1}{3}\right) + (3.80\text{b})\left(1 - \frac{1}{24}\right)$$

$$= 8.10 \text{ barns/molecule} \qquad (g = 6, 7, \ldots 13)$$

In summary, transport cross sections are obtained from Equation (A-12) for groups 1 through 4, from Equation (A-13) for group 5, and from Equation (A-14) for groups 6 through 13. These transport cross sections include effects of both anisotropic scattering and flux weighting.

$\sigma_{g'g}$ for Groups 1 through 13

The transfer cross section from group g' to group g is designated $\sigma_{g'g}$. Transfer between groups results from elastic scattering and, at very high energies, inelastic scattering. Above E_c—i.e., in groups 1 through 13—there is no mechanism which will produce upscattering in energy. Thus, the first four of the nine transfer cross sections are zero.

$$\sigma_{g'g} = 0 \qquad g' = g + 1,\ g + 2,\ g + 3,\ g + 4 \ (g = 1 \text{ through } 13) \qquad \text{(A-15)}$$

The general downscattering expression for $\sigma_{g'g}$ in groups 1 through 13 is

$$\sigma_{g'g} = \int_{g'} \phi(E') \int_{g} \sigma(E', E)\, dE dE' \Big/ \int_{g'} \phi(E') dE' \qquad \text{(A-16)}$$

where $\sigma(E', E)\, dE$ is the cross section for a neutron with initial energy E' scattering so that its final energy lies in the energy range dE about E. The g and g' indicate that these integrals are to extend over the energy ranges of groups g and g' respectively.

Elastic Scattering

In the event of elastic scattering, a neutron with initial energy E' which scatters through a center of mass angle $\cos^{-1}\mu_c$ will emerge with energy E given by

$$E = E' \frac{A^2 + 1 + 2A\mu_c}{(A+1)^2} \qquad \text{(A-17)}$$

where A is the mass of the scatterer in neutron mass units—for deuterium A = 2, for oxygen A = 16.

Differential cross sections for elastic scattering are listed in terms of μ_c, not E. An expression relating the two can be readily obtained, however, since

$$\sigma_s(E', E)\, dE = \sigma_s(E', \mu_c)\, 2\pi d\mu_c \qquad \text{(A-18)}$$

An expression for $d\mu_c$ in terms of known quantities is readily obtained by differentiating Equation (A-17),

$$d\mu_c = \frac{(A+1)^2}{2AE'}\, dE$$

Thus,

$$\sigma_s(E', E) = \frac{\pi}{E'} \frac{(A+1)^2}{A} \sigma_s(E', \mu_c)$$

We note that for the special case of isotropic scattering in the center of mass system, $\sigma_s(E', \mu_c) = \frac{1}{4\pi}$ barns/steradian and $\sigma_s(E', E) = \frac{(A+1)^2}{4A} \frac{1}{E'}$, the usual result.

Upon substituting Equation (A-18) into Equation (A-16), the following results:

$$(\sigma_{g'g})_{el} = 2\pi \int_{g'} \phi(E') \int_{\mu_1}^{\mu_2} \sigma_s(E', \mu_c) d\mu_c dE' \Big/ \int_{g'} \phi(E') dE' \qquad \text{(A-19)}$$

The limits on the integral over μ_c are set by consideration of the scattering law, Equation (A-17). Since the minimum possible value of E, corresponding to $\mu_c = -1$, is, from Equation (A-17),

$$E_{min} = E' \left(\frac{A - 1}{A + 1}\right)^2 \tag{A-20}$$

several cases must be distinguished. If, for a given E',

- Group g has an upper energy bound less than E_{min}, then the inner integral is zero
- Group g has an upper energy bound greater than E_{min} but a lower energy bound smaller than E_{min}, then

  - $\mu_1 = \frac{E_{ug}}{E'} \frac{(A + 1)^2}{2A} - \frac{A^2 + 1}{2A}$ (A-21a)

  - $\mu_2 = -1$ (A-21b)

  where E_{ug} is the upper energy limit of group g.

- Group g has both upper and lower bounds greater than E_{min}, then

$$\mu_1 = \frac{E_{ug}}{E'} \frac{(A + 1)^2}{2A} - \frac{A^2 + 1}{2A} \tag{A-22a}$$

$$\mu_2 = \frac{E_{\ell g}}{E'} \frac{(A + 1)^2}{2A} - \frac{A^2 + 1}{2A} \tag{A-22b}$$

The elastic scattering transfer cross sections for oxygen and deuterium are found individually from numerical or graphical evaluation of the integrals in Equation (A-19). In groups g' = 1 through 4, the flux is assumed to have the fission spectrum shape—$\phi(E') = f(E')$. In groups $g' \geq 5$, the outer integration is evaluated over lethargy with the following result:

$$(\sigma_{g'g})_{el} = \frac{2\pi}{\Delta u'_{g'}} \int_{g'} \int_{\mu_1}^{\mu_2} \sigma_s(u', \mu_c)\, d\mu_c\, du' \tag{A-23}$$

where u' is the lethargy corresponding to E'.

Below 0.1 Mev ($g' \geq 6$), the scattering in both oxygen and deuterium is isotropic in the center of mass system—that is,

$$\sigma_s(u', \mu_c) = \sigma_s(u')/4\pi$$

where σ_s is the total elastic scattering cross section (tabulated as σ_n in reference 2), and so Equation (A-23) becomes simply

$$(\sigma_{g'g})_{el} = \frac{1}{2}\left[\sigma_s\,(\mu_2 - \mu_1)\right]_{g'} \qquad g' = 6,\ 7,\ \ldots 13) \tag{A-24}$$

where $\left[\sigma_s\,(\mu_2 - \mu_1)\right]_{g'}$ is the average value of the product of $\sigma_s(u')$ and $\mu_2(u') - \mu_1(u')$, averaged over the lethargy interval of group g'. The cross sections in reference 2 are tabulated in equal lethargy increments. Thus, the averaging process becomes one of simple addition followed by division by the number of items added.

After computing the elastic transfer cross sections from each group, g', it is advisable to check them by applying the condition that their sum must equal the average (flux-weighted) elastic scattering cross section in the group from which they came. That is,

$$\sum_{g=g'}^{g=g'+4} \sigma_{g'g} = \int_{g'} \sigma_s(E')\,\phi(E')\,dE' \Big/ \int_{g'} \phi(E')\,dE' \tag{A-25}$$

If the sum differs greatly from the flux weighted average, an error has been made; if it differs slightly due to the approximations inherent in numerical integrations, then each of the $\sigma_{g'g}$ should be scaled up or down by the ratio of the right side to the left side of Equation (A-25) to obtain agreement.

Inelastic Scattering

Transfer between groups in D_2O by inelastic scattering occurs only for neutrons with initial energies above 6.63 Mev, the energy of the first excited state in oxygen. (Deuterium has no bound excited states.) Since the lower limit of group 1 is 3 Mev, inelastic scattering occurs only from group 1. The inelastic neutrons must go into groups 1 through 5 because the Los Alamos 24-group cross sections allow no transfer to lower groups than the (g' + 4)th. Actually, only a completely insignificant fraction of neutrons will inelastically scatter down to an energy lower than 0.1 Mev, the lower limit of the fifth group, so the restriction to four lower groups is not deleterious.

For initial neutron energies above 10 Mev, a continuous spectrum of inelastic neutrons is produced; for initial neutron energies between 10 Mev and 6.63 Mev, only the 7.0- and 6.63-Mev levels are excited. (See Tables 2 and 4 of reference 2.)

Thus, for inelastic transfer, the general downscattering expression [Equation (A-16)] becomes:

$$(\sigma_{1g})_{inel} = \left\{ \int_{10\ Mev}^{18\ Mev} f(E') \left[\int_{E_{\ell g}}^{E_{ug}} \sigma_{in}(E', E)dE \right] dE' + \int_{E_1}^{E_2} f(E')\,\sigma_{6.1}(E')dE' + \int_{E_3}^{E_4} f(E')\,\sigma_{7.0}(E')dE' \right\} \div \int_{3.0}^{18\ Mev} f(E')dE' \qquad \text{(A-26)}$$

where

$\sigma_{in}(E', E)dE$ is the cross section for inelastic scattering from neutron energy E' to energy range dE about E (it is listed in Table 2 of reference 2, where the E and E' have the reverse of the definitions given here)

and

$\sigma_{6.1}(E')$ and $\sigma_{7.0}(E')$ are the cross sections for inelastic scattering from neutron energy E' to energy (E'-6.1 Mev) and (E'-7.0 Mev), respectively (these are listed in Table 4 of reference 2)

The limits on the integrals of Equation (A-26) depend on the lower and upper energy bounds of the groups into which the neutrons are scattering; thus:

$$\left.\begin{aligned} E_1 &= E_{\ell g} + 6.1\ Mev \\ E_2 &= E_{ug} + 6.1\ Mev \\ E_3 &= E_{\ell g} + 7.0\ Mev \\ E_4 &= E_{ug} + 7.0\ Mev \end{aligned}\right\} \quad (g = 1\text{ -}5) \qquad \text{(A-27)}$$

where $E_{\ell g}$ and E_{ug} are the lower and upper energy bounds of group g.

In the case of scattering from group 1 into group 1, the E_{ug} which appears as an upper limit in the inner integral in Equation (A-26) must be replaced by E'.

The integral of the fission spectrum from 3 to 18 Mev, which appears in the denominator of Equation (A-26), has a numerical value of 0.213.

Since inelastic scattering occurs only from group 1 and into groups 1 through 5,

$$(\sigma_{g'g})_{inel} = 0 \text{ for all } g' > 1 \text{ and all } g > 5 \tag{A-28}$$

The elastic transfer cross sections for deuterium and oxygen, and the inelastic transfer cross sections for oxygen are added to obtain the D_2O transfer cross sections.

$$(\sigma_{gg'})^{D_2O} = 2(\sigma_{gg'})^{D}_{el} + (\sigma_{gg'})^{O}_{el} + (\sigma_{gg'})^{O}_{inel} \tag{A-29}$$

SLOW CROSS SECTIONS (E' < 1.1256 ev)

Three new considerations complicate the calculation of cross sections for neutrons with energies below 1 ev:

- The neutron does not collide with individual free atoms but rather with the entire D_2O molecule.
- The molecules are moving translationally and the deuterium atoms are vibrating toward and rotating about the center of mass of the molecule with velocities comparable to the neutron velocity, so that energy can be transferred from the molecule to the neutron as well as vice versa.
- The neutrons have a spectrum which is no longer simply 1/E but a combination of 1/E and a Maxwellian distribution.

To find the group cross sections it is necessary to specify:

- The velocity (or energy) distribution of the moderator atoms
- The velocity (or energy) distribution of the neutrons
- The microscopic scattering and capture cross sections as a function of relative velocity
- The scattering kernel

The first two items are discussed herein; the last two are discussed in subsequent sections.

Velocity Distribution of Moderator Atoms

Following the procedure of Brown and St. John,[7] the deuterium atoms in liquid heavy water are seen to have a velocity which is primarily due to the rotation of the molecules, with a smaller translational component. The actual distribution of velocities of the deuterium atoms in liquid heavy water can be calculated and an effective mass assigned to the deuteron so that the Maxwellian velocity distribution

$$M_j(V) = \frac{4}{\sqrt{\pi}} \left(\frac{m_j}{2kT}\right)^{3/2} V^2 \exp\left[-m_j V^2/2kT\right]$$

gives the correct values. The atoms in the D_2O molecule form a triangular array. If a neutron collides with a deuterium atom in a direction perpendicular to the plane of the molecule (hence, the interatomic bonds), the deuterium nucleus will be effectively free and will have an effective mass of 2. If the neutron strikes the deuterium nucleus along the line between the deuterium nucleus and the center of gravity of the molecule, the molecule will recoil as a whole, in which case the effective mass of the deuterium nucleus is 20. The effective mass at other angles of approach will vary from 2 to 20. Using a bond angle of 106°, Brown and St. John[7] calculate effective mass of 3.595 and 17.607 amu for deuterium and oxygen in D_2O. Their calculation follows the mass tensor procedure of Sachs and Teller.[8]

In the procedure of Brown and St. John,[7] oxygen scattering is completely ignored. This approximation may be rationalized by noting that a neutron can lose no more than 20% of its initial energy in scattering off a particle of mass 17.607, whereas a neutron can lose as much as 68% in scattering off a particle of mass 3.596. Furthermore, there are twice as many deuterium atoms as oxygen atoms, and since the scattering cross sections of D and O are approximately equal, approximately twice as many deuterium as oxygen interactions will occur.

The practice by Brown and St. John[7] of ignoring oxygen scattering is not followed herein. Instead, it is assumed that oxygen scattering also contributes to the transfer cross sections. Thus, two atomic velocity distributions are considered:

$$M_j(V) = \left[\frac{4}{\sqrt{\pi}} \left(\frac{m_j}{2kT}\right)^{3/2} V^2 \exp(-m_j V^2/2kT)\right] \quad (j = 1, 2) \qquad \text{(A-30)}$$

where

$M_1(V)dV$ and $M_2(V)dV$ are, respectively, the fraction of deuterium and oxygen atoms having speeds in the interval dV about V

m_1 and m_2 are the effective masses of the deuterium and the oxygen atoms in D_2O

$$m_1 = 3.595 \times 1.67 \times 10^{-24} \text{ gm}$$
$$m_2 = 17.607 \times 1.67 \times 10^{-24} \text{ gm}$$

T is the temperature of the moderator—°K
k is Boltzmann's constant = 1.3805×10^{-16} erg/°K
V is the speed of atoms—cm/sec

Velocity Distribution of Neutrons

The distribution of neutron velocities, N(v), enters the calculation of effective group cross sections as a factor which weights the cross sections within each group. Because there is no information on the actual neutron spectrum which will be obtained in the finite D_2O regions, it is assumed that the spectrum will be that of an infinite medium of D_2O at temperature T. Any deviations from this spectrum because of the finiteness of the D_2O regions and the nearness of the D_2O region to highly absorbing regions may be expected to have but second order effect on the multigroup cross sections. Only a second order effect occurs because neither the cross sections nor the spectrum vary rapidly within any single group in the 24-group formulation. This is, of course, one distinct advantage of using a multigroup rather than a few-group formulation of the neutron transport equation.

A convenient expression for the thermal and near-epithermal neutron distribution function was derived by Carl Westcott[9] on the assumption that the thermal spectrum would have a Maxwellian shape and the epithermal flux a 1/E shape. Westcott derives, as the fraction of neutrons flux in the energy range dE about E, the expression

$$N(E)dE = \left[\left(\frac{E}{kT}\right)^2 e^{-E/kT} + \beta\right]\frac{dE}{E} \qquad (A\text{-}31)$$

where β is the epithermal flux per unit lethargy interval, per unit true thermal flux.

β is constant, for $E > 5$ kT
$\beta = 0$ for $E \leq 5$ kT

Strictly speaking, N(E)dE is not the "fraction" of neutrons in energy range dE about E because it has not been normalized. It need not be normalized, however, in the subsequent development.

Hughes[10] suggests that β is approximately 0.0625 for a D_2O reactor, but Westcott[9] believed β to be between 0.028 and 0.056 depending on position in a D_2O-metal lattice.

For an infinite, pure D_2O moderator, a rather elementary estimate of β can be made. The number of neutrons slowing down past lethargy u (in the epithermal region) must equal the number of neutrons absorbed as thermal neutrons. Thus,

$$\frac{\xi \Sigma_{s,\,epi}\, \phi_{epi}(u)}{\int \phi_{th}(E)\, dE} = \frac{\int \Sigma_c (E)\, \phi_{th}(E)\, dE}{\int \phi_{th}(E)\, dE} \tag{A-32}$$

where $\phi_{th}(E)$ is the Maxwell-Boltzmann distribution of thermal neutrons. For a 1/v absorber such as D_2O, the right side is simply $\left(\frac{\pi T_0}{4T}\right)^{1/2} \cdot \Sigma_c(2200\ m/sec)$, where $T_0 = 273°K$.

Since the definition of β is

$$\beta = \frac{\phi_{epi}(u)}{\int \phi_{th}(E)dE} \tag{A-33}$$

Equation (A-32) can be written as

$$\beta = \left(\frac{\pi T_0}{4\,T}\right)^{1/2} \frac{\Sigma_a(2200\ m/sec)}{\xi \Sigma_s(epi)} = \left(\frac{\pi T_0}{4\,T}\right)^{1/2} \frac{\sigma_c(2200\ m/sec)}{\xi\, \sigma_s(epi)} \tag{A-34}$$

and since in D_2O

σ_c (2200 m/sec) = 0.0012 barns/molecule

$\xi \sigma_s$ (epi thermal) = (0.42) (2) (3.35) + (0.11) (3.80)

= 3.24 barns/molecule (the ξ's were calculated using effective deuterium and oxygen masses) (A-13)

therefore,

$$\beta = 0.00033 \left(\frac{T_0}{T}\right)^{1/2} \tag{A-35}$$

The ratio of epithermal flux per unit lethargy interval to total thermal flux for an infinite D_2O medium is seen to be two orders of magnitude smaller than those quoted by Westcott [9] and Hughes[10] for reactor lattices. This is not surprising, since D_2O has such a small absorption cross section that any metal diluent may be expected to greatly depress the thermal flux.

In D_2O regions which are small compared with the diffusion length in D_2O—100 centimeters—the value of β may be expected to be strongly influenced by the absorptive properties of neighboring regions. In such cases, the only practical means of obtaining β is by iteration. A reasonable guess is made for β, cross sections are calculated based on this guess, the transport codes are run, and their flux outputs are used to obtain a better figure for β. This better β value then is used to compute improved cross sections, and so on, until a converged figure for β is found. For a thin D_2O region (e.g., 10 to 60 cm) next to a highly absorbant region, a reasonable first guess for β might be in the range 0.5 to 0.05.

In terms of neutron velocity, the distribution equation, Equation (A-31), may be written, for future reference,

$$N(v)dv = \left[\frac{1}{2}\left(\frac{m}{kT}\right)^2 v^3 \exp(-mv^2/2kT)\right] dv + \frac{2\beta}{v} dv \qquad \text{(A-36)}$$

σ_c for Groups 14 through 24

The capture cross section per D_2O molecule is assumed to have the expected inverse velocity dependence

$$\sigma_c(v_r) = \sigma_0 \frac{v_0}{v_r} \text{ barns/molecule} \qquad \text{(A-37)}$$

where

σ_0 is the capture cross section per D_2O molecule at relative velocity of 2200 m/sec. The oxygen capture cross section at 2200 m/sec is not known exactly, but it is known to be less than 0.0002 barns/atom. The deuterium 2200-m/sec capture cross section is 0.00057 barns/atom. The total capture cross section, σ_0, is thus approximately 0.0012 barns/molecule and may be assumed to be entirely capture in deuterium.

v_0 is 2.2×10^5 cm/sec.

v_r is the relative velocity between neutron and deuterium atom—cm/sec.

Because the capture cross section varies as $\frac{1}{v_r}$, the average capture cross section of a neutron of velocity v_r interacting with any velocity distribution of nuclei is independent of the velocity distribution—i.e., by definition of the average

$$N v_r \overline{\sigma_c(v_r)} = N \int_0^\infty M(V) \frac{\sigma_0 v_0}{v_r} v_r \, dV \Big/ \int_0^\infty M(V) dV \tag{A-38}$$

and so,

$$\overline{\sigma_c(v_r)} = \frac{\sigma_0 v_0}{v_r} = \sigma_c(v_r) \tag{A-39}$$

as was asserted.

This convenient property of the 1/v cross section allows the velocity distribution of the atoms to be ignored. The cross sections must still be averaged over the neutron flux distribution, however. Thus,

$$\sigma_c^g = \int_{v_{\ell g}}^{v_{ug}} N(v) \frac{\sigma_0 v_0}{v} dv \Big/ \int_{v_{\ell g}}^{v_{ug}} N(v) \, dv \quad (g = 14 \text{ through } 24) \tag{A-40}$$

where N(v)dv is given by Equation (A-36), and $v_{\ell g}$ and E_{ug} are the lower and upper neutron velocities in group g,

$$v_{\ell g} = \left(\frac{2E_{\ell g}}{m}\right)^{1/2} \qquad v_{ug} = \left(\frac{2E_{ug}}{m}\right)^{1/2} \tag{A-41}$$

where $E_{\ell g}$ and E_{ug} are the upper and lower energy bounds of group g expressed in ergs, and m is the neutron mass expressed in grams.

The terms in the numerator and denominator of Equation (A-40) containing β can be integrated in closed form, since

$$\int \frac{2\beta}{v} dv = 2\beta \ln v$$

Integrals of the form

$$\int v^2 e^{-av^2} dv \text{ and } \int v^3 e^{-av^2} dv$$

must be evaluated numerically or graphically, however.

In evaluating σ_c^g, it should be borne in mind that $\beta = 0$ for neutron energies less than 5kT—that is, neutron velocities less than $(10 \, kT/m)^{1/2}$.

$\nu\sigma_f$ for Groups 14 through 24

There is no "fission" in D_2O at low energies; hence,

$$(\nu\sigma_f)^g = 0 \quad (g = 14 \text{ through } 24) \tag{A-42}$$

σ_{tr} for Groups 14 through 24

Ramanna and others[11] have conducted experiments on D_2O from which they have inferred λ_{tr} as a function of neutron energy in the energy range from 0.006 to 0.1 ev. Above 0.1 ev there was indication that λ_{tr} increased to the free atom value.

A "resonance" in λ_{tr} which was observed at about 0.012 ev was ascribed to "a coherent scattering phenomenon with perhaps small contributions from inelastic and incoherent scattering."[11]

From the same data, Ramanna et al[11] inferred the variation of $\bar{\mu}(E)$ by using the relationship

$$\lambda_{tr}(E) = \lambda_s(E)/\left[1 - \bar{\mu}(E)\right] \tag{A-43}$$

This experimentally determined $\bar{\mu}(E)$ is used herein to calculate σ_{tr}^g. Presumably, $\bar{\mu}(E)$ is a function of moderator temperature; unfortunately, these experiments were conducted only at T = 300°K, and no references have been found to experiments at higher temperatures. It must therefore be assumed that no variation of $\bar{\mu}(E)$ occurs with moderator temperature.

The transport cross section per D_2O molecule is defined, in terms of $\bar{\mu}(E)$, as

$$\sigma_{tr}(E) = \sigma_s(E) \quad \left[1 - \bar{\mu}(E)\right] + \sigma_c(E) \tag{A-44}$$

where $\sigma_s(E)$ is the scattering cross section per D_2O molecule, which can be rather accurately fitted by the expression[6]

$$\sigma_s(E) = 10.5 + 0.72/\sqrt{E} \qquad (0.005 \leq E \leq 10 \text{ ev}) \tag{A-45}$$

The group averaged cross section is then

$$\sigma_{tr}^g = \left[\int \sigma_{tr}(E)\, N(E)dE \;/ \int_g N(E)dE\right] + \sigma_c^g \tag{A-46}$$

where

$\sigma_{tr}(E)$ is given by Equations (A-44) and (A-45) with $\bar{\mu}(E)$ taken from Figure 6 of Reference 11
N(E) is the neutron energy distribution— Equation (A-31)
σ_c^g is the absorption cross section in group g, calculated previously

Equation (A-46) must be evaluated numerically or graphically because $\bar{\mu}(E)$ is known only graphically and has a shape not readily fit by a simple function which would be integrable when multiplied by $\sigma_s(E)$ and N(E).

Note that σ_{tr}^g is a function of temperature. The temperature is introduced through the neutron distribution, N(E), which is, of course, temperature dependent.

$\sigma_{g'g}$ for Groups 14 through 24

In calculating slow group transfer cross sections, some of the approximations of Brown and St. John[7] are used. In particular, it is assumed that:

- The neutrons collide with free atoms of deuterium and oxygen having effective masses of 3.595 and 17.607 amu, respectively
- The atoms have Maxwellian velocity distributions as given by Equation (A-30)
- Scattering is isotropic in the c/m system of neutron and atom

Oxygen scattering, however, is not ignored, but is explicitly taken into account. The deuterium and oxygen transfer cross sections are separately calculated, then added with proper weighting,

$$\sigma_{D_2O}(v', v) = 2\sigma_D(v', v) + \sigma_O(v', v) \qquad \text{(A-47)}$$

Slowing-down and Speeding-up Kernel, P (v',v)

Following Brown and St. John,[7] P(v', v)dv is defined as the probability per unit time that a neutron of speed v' will be scattered into the range dv about v. This probability is related to the transfer cross section from speed v' to v by the relationship

$$\sigma(v', v)dv = \frac{P(v', v)dv}{v'} \qquad \text{(A-48)}$$

which follows directly from $P = Nv'\sigma M$ when both the neutron and target number densities N and M are normalized to unity.

$P(v', v)$ is obtained by integrating the differential probability, $P(v', v; V, \mu')dVd\mu'$, which is the probability for the v' to v velocity change as a function of the speed, V, of the atom and the cosine of the angle between neutron and nucleus velocities, μ', weighted by the frequency of collision with nuclei in that state and the relative speed between nucleus and neutron. Thus,

$$P_j(v', v) = \int_{-1}^{+1} \int_0^{\infty} v_r \, \sigma_{sj} \, M_j(V) P(v', v; V, \mu')dV \frac{d\mu'}{2} \tag{A-49}$$

where

j = 1 refers to deuterium
j = 2 refers to oxygen

Brown and St. John[7] fit the scattering cross section, σ_s, in a form particularly amenable to calculation of the scattering kernel:

$$\sigma_{sj} = A_j + B_j e^{-K_j v_r^2} \tag{A-50}$$

For deuterium, j = 1, and $A_1 = 3.35$ barns/atom
$B_1 = 1.60$ barns/atom
$K_1 = 2.88$ amu/ev
For oxygen, j = 2, and $A_2 = 3.80$ barns/atom
$B_2 = 0.60$ barns/atom
$K_2 = 2.88$ amu/ev

This fit is in excellent agreement with the observed scattering cross sections of D_2O.

Upon integrating Equation (A-49), Brown and St. John obtained the following results.[7] (The subscript j is omitted for clarity.)

For energy decrease in a collision, $v' > v$,

$$P(v', v) = A \frac{(m+1)^2 v}{4mv'} \left\{ \left[\mathrm{Erf}(\psi\xi v' + \psi\theta v) + \mathrm{Erf}(\psi\theta v - \psi\xi v') \right] + e^{\frac{\psi^2(v'^2 - v^2)}{m}} \left[\mathrm{Erf}(\psi\theta v' - \psi\xi v) - \right.\right.$$

$$\left.\left. \mathrm{Erf}(\psi\theta v' + \psi\xi v) \right] \right\} + B \frac{(m+1)^2 \psi^3}{4m\sqrt{\psi^2 + K}} \left[\psi^2 + K(m+1) \right]^{-1} (v/v') \left\{ e^{\frac{-K\psi^2 v'^2}{\psi^2 + K}} \left[\mathrm{Erf}(\psi\xi' v' + \psi\theta' v) + \right. \right.$$

$$\mathrm{Erf}(\psi\theta' v - \psi\xi' v')\Big] + e^{\frac{\psi^2}{m}\left(v'^2 - \frac{\psi^2+K(m+1)v^2}{\psi^2+K}\right)}\Big[\mathrm{Erf}(\psi\theta' v' - \psi\xi' v) - \mathrm{Erf}(\psi\theta' v' + \psi\xi' v)\Big]\Bigg\} \qquad \text{(A-51)}$$

For energy increase in a collision, $v \geq v'$,

$$P(v', v) = A\frac{(m+1)^2 v}{4m\, v'}\Bigg\{e^{\frac{\psi^2}{m}(v'^2 - v^2)}\Big[\mathrm{Erf}(\psi\xi v + \psi\theta v') - \mathrm{Erf}(\psi\xi v - \psi\theta v')\Big] + \Big[\mathrm{Erf}(\psi\theta v - \psi\xi v')$$
$$-\mathrm{Erf}(\psi\theta v + \psi\xi v')\Big]\Bigg\} + B\frac{(m+1)^2\psi^3}{4m\sqrt{\psi^2+K}}\Big[\psi^2+K(m+1)\Big]^{-1}(v/v')\Bigg\{e^{\frac{-K\psi^2 v'^2}{\psi^2+K}}\Big[\mathrm{Erf}(\psi\theta' v - \psi\xi' v')$$
$$-\mathrm{Erf}(\psi\theta' v + \psi\xi' v')\Big] + e^{\frac{\psi^2}{m}\left(v'^2 - \frac{\psi^2+K(m+1)v^2}{\psi^2+K}\right)}\Big[\mathrm{Erf}(\psi\xi' v + \psi\theta' v') - \mathrm{Erf}(\psi\xi' v - \psi\theta' v')\Big]\Bigg\} \qquad \text{(A-52)}$$

The following definitions were used

$$\psi^2 = \frac{m}{2kT}, \qquad \psi\theta = \frac{m+1}{2m}\psi, \qquad \psi\xi = \frac{m-1}{2m}\psi$$

$$\psi\theta' = \frac{m+1}{2m}(\psi^2+K)^{1/2}, \qquad \psi\xi' = \frac{(m-1)\psi^2 - (m+1)K}{2m(\psi^2+K)^{1/2}} \qquad \text{(A-53)}$$

and, of course, $\mathrm{Erf}(x) = \frac{2}{\sqrt{\pi}}\int_0^x e^{-y^2}\,dy$

In these equations, m has dimensions of amu, kT has dimensions of ev, where $k = 8.6168 \times 10^{-5}$ ev/°K, K and ψ^2 have dimensions of (amu/ev), ψ and $\psi\xi$ have dimensions of $(\text{amu/ev})^{1/2}$, and all velocities have dimensions of $(\text{ev/amu})^{1/2}$, where

$$1(\text{ev/amu})^{1/2} = 0.98 \times 10^6 \text{ cm/sec}$$

Notice that $P(v', v)dv$ has dimensions of barns × velocity, so that $\sigma(v', v)dv$—which equals $P(v', v)dv/v'$—has the proper dimensions of barns. In making the final division of $P(v', v)$ by v' to obtain $\sigma(v', v)$, v' need not necessarily be in $(\text{ev/amu})^{1/2}$, but can be in cm/sec, in m/sec, or any other velocity units. Whatever the units used, these same units must be used in subsequent numerical integration over dv.

The masses in Equations (A-51) through (A-53) are the effective masses of deuterium and oxygen: $m_1 = 3.595$, $m_2 = 17.607$. Note further that A, B, K, and all the special functions defined by Equations (A-53) depend on whether the scattering atom is deuterium or oxygen. In other words, A, B, K, and m—and all functions which depend on them, including the scattering kernel, $P(v', v)$—must be imagined to be subscripted with a 1 for deuterium and a 2 for oxygen.

The matrices of numbers $\sigma_j(v', v) = P_j(v', v)/v'$ should be calculated at a number of equally spaced velocity points within each of the groups to facilitate the subsequent numerical integration to find the average group-to-group transfer cross sections. Both v' and v extend from the neutron velocity corresponding to 0.005 ev to the velocity corresponding to 1.1256 ev.

Let us designate the points in v' and v at which σ_1 and σ_2 are to be evaluated as v_1, v_2, v_3.... One possible procedure would consist of setting the following equalities.

v_1 = the neutron velocity corresponding to the lower bound of group 24
v_5 = the neutron velocity corresponding to the lower bound of group 23
v_9 = the neutron velocity corresponding to the lower bound of group 22
.
.
.
v_{41} = the neutron velocity corresponding to the lower bound of group 14
v_{45} = the neutron velocity corresponding to the upper bound of group 14

The points not lying on the group boundaries would be evenly spaced (in velocity) between the boundaries. Thus v_1, v_2, v_3, v_4, and v_5 would split the 24th group into four equal velocity increments; v_5, v_6, v_7, v_8, and v_9 would split the 23rd group into four equal velocity increments, etc. The velocity increments would, in general, differ from group to group, but would be the same within any one group.

By choosing an equal number of increments within each group, and by calculating at the end points, numerical integration (via, for example, Simpson's Rule) is facilitated. The number of increments chosen for each group depends, of course, on the precision desired; four was chosen here only as an example. Hopefully, however, four increments will prove sufficient, since with only four increments per group it is possible that $45 \times 45 = 2025$ values of $\sigma(v_m, v_n)$ might have to be calculated for deuterium alone. Undoubtedly, beyond a certain velocity difference, the values of the matrix elements will become so small as to be ignorable. If set up for digital computer calculation, the most efficient procedure would be to calculate $\sigma(v_m, v_m)$, $\sigma(v_{m,m+1})$, $\sigma(v_m, v_{m-1})$, etc, working toward larger velocity changes until the cross section

falls below some preset limit. This may be expected to happen after relatively few terms in oxygen, because of its large mass, so that almost all the matrix elements in $\sigma_2(v_m, v_n)$ are effectively zero. The cross sections of deuterium and oxygen are then summed.

$$\sigma(v_m, v_n) = 2\sigma_1(v_m, v_n) + \sigma_2(v_m, v_n) \tag{A-54}$$

Having evaluated $\sigma(v', v)$, the next step is the numerical integration over v, the final velocity, for each of the fourteen groups and for all velocity points.

$$\sigma_g(v') = \int_g \sigma(v', v)dv \qquad (g = 14 \text{ through } 24) \tag{A-55}$$

As an example, the cross section for scattering from velocity point v_m into group 23, assuming four increments per group, is given by Simpson's rule as

$$\sigma_{23}(v_m) = \frac{v_9 - v_5}{12}\left[\sigma(v_m, v_5) + 4\sigma(v_m, v_6) + 2\sigma(v_m, v_7) + 4\sigma(v_m, v_8) + \sigma(v_m, v_9)\right] \tag{A-56}$$

The final step consists of group averaging over v', the initial velocity, with weight given by the neutron flux spectrum in group g'.

$$\sigma_{g'g} = \int_{g'} \sigma_g(v')N(v')dv' \Big/ \int_{g'} N(v')dv' \tag{A-57}$$

As an example, the average cross section for scattering from group 21 into group 23, assuming four increments per group, is given by Simpson's rule as

$$\sigma_{21,23} = \left[\sigma_{23}(v_{13})N(v_{13}) + 4\sigma_{23}(v_{14})N(v_{14}) + 2\sigma_{23}(v_{15})N(v_{15}) + 4\sigma_{23}(v_{16})N(v_{16}) + \sigma_{23}(v_{17})N(v_{17})\right] \div \left[N(v_{13}) + 4N(v_{14}) + 2N(v_{15}) + 4N(v_{16}) + N(v_{17})\right] \tag{A-58}$$

Symmetry Requirement

For two velocities v_m and v_n within the pure Maxwellian distribution of neutrons, the principal of detailed balance requires that

$$N(v_m)\sigma(v_m, v_n) = N(v_n)\sigma(v_n, v_m) \tag{A-59}$$

This equation may be used either as a check on the computation of the transfer cross sections, or to determine $\sigma(v_n, v_m)$ from a calculated $\sigma(v_m, v_n)$. Notice that this equation is valid only within the pure Maxwellian distribution, $E < 5kT$, or

$$(v_m \text{ and } v_n) < (10kT/m)^{1/2}$$

where m is the mass of the neutron

Zero Cross Sections

Ten of the group-to-group transfer cross sections must be zero simply because there is no 25th group.

$$\sigma_{g+4,g} = \sigma_{g+3,g} = \sigma_{g+2,g} = \sigma_{g+1,g} = 0 \qquad (g = 24)$$
$$\sigma_{g+4,g} = \sigma_{g+3,g} = \sigma_{g+2,g} = 0 \qquad (g = 23)$$
$$\sigma_{g+4,g} = \sigma_{g+3,g} = 0 \qquad (g = 22)$$
$$\sigma_{g+4,g} = 0 \qquad (g = 21)$$

Temperature Dependence

It should be noted that all cross sections in groups 14 through 24 are, to varying degrees, temperature dependent. If these prove to be smoothly varying with temperature, as one might expect, they can be evaluated at a few temperatures covering the range of interest and plotted versus temperature to facilitate interpolation for any temperature within the range of interest.

Required Data

Finally, it should perhaps be pointed out that the only data required for the evaluation of the 24-group cross sections of D_2O which is not contained within these pages may be found in references 2 and 11. Reference 2 is United Nuclear Company report UNC-5038, which is also called NDL-TR-40, and reference 11 is the article by Ramanna, et al. in Volume 16 of the Second Geneva Conference.

REFERENCES

1. Hughes, D. J. and Schwartz; R. B. Neutron Cross Sections. BNL-325 (1958).

2. Kalos, M. H., Goldstein, H., and Ray, J. Revised Cross Sections for Neutron Interactions with Oxygen and Deuterium. UNC-5038 (1962).

3. Reactor Physics Constants. 2nd ed. ANL-5800 (1963), pp 50-51.

4. Lane, R. O., Miller, W. F., and Hillstrom, K. E. Matrices for Transforming Legendre Polynomial Coefficients between Laboratory and Center of Mass Systems. ANL-6039 (1959).

5. Los Alamos Group Averaged Cross Sections. LAMS-2941 (1963).

6. Amaldi, E. "The Production and Slowing Down of Neutrons." Handbuch der Physik. XXXVIII/2 (1959).

7. Brown, H. D. and St. John, D. S. Neutron Energy Spectrum in D_2O. DP-33 (1954).

8. Sachs, R. G. and Teller, E. "The Scattering of Slow Neutrons by Molecular Gases." Phys. Rev. 60, 18 (1941).

9. Westcott, Carl H. "The Specification of Neutron Flux and Nuclear Cross-Sections in Reactor Calculations." J. Nuc. Eng. 2, 59 (1955).

10. Hughes, D. J. Pile Neutron Research. Addison-Wesley (1953) and Nucleonics, 11 (1), 30 (1953).

11. Ramanna, R., Sarma, N., Somanathan, C. S., Usha, K., and Venkataraman, G. "On the Spectrum of Neutrons Emerging from Moderators." Proceedings of the Second Geneva Conference on Atomic Energy. Volume 16 (1958).

NASA-Langley, 1966 E-3371